Novel Molecular Mechanisms of Regulation of Enzyme Cytochrome P4503A via Pregnane X Receptor

A Dissertation Presented to the

Faculty of the Department of Pharmacological and Pharmaceutical Sciences

College of Pharmacy, University of Houston

In Partial Fulfillment of

the Requirements for the Degree of

Doctor of Philosophy

By

Guncha Taneja

July, 2017

Novel Molecular Mechanisms of Regulation of Enzyme Cytochrome P4503A via Pregnane X Receptor

By

_____
Guncha Taneja

Approved By:

_____
Romi Ghose, PhD (Advisor)

_____
Diana Chow, PhD

_____
Ming Hu, PhD

_____
Bhagavatula Moorthy, PhD

_____
Sundararajah Thevananther, PhD

_____

Lamar Pritchard, PhD

Dean, College of Pharmacy

July 2017

Dedicated to my parents

ACKNOWLEDGEMENTS

First and foremost, I would like to thank my advisor Dr. Romi Ghose for providing me immense support and encouragement throughout my Ph.D. I am extremely grateful I got an opportunity to work and hone my research and analytical skills with such an accomplished professor. Over the period of five years, I learnt the skill to critically analyze my own as well as published data, determine the correct model for a study and finally make concise and apt conclusions to make a project presentable for reviewers. While working with her, I not only learnt numerous technical skills but also gained expertise on presenting/ selling my work effectively.

My doctoral research would not have been possible without the support of Dr. Bhagavatula Moorthy, my committee member. Even though I was not a part of his lab, he always treated me as his own student and his constant advice and guidance encouraged me to pursue my best always. His jovial nature and pleasing personality provided a comfortable environment for me in the lab. I would especially like to thank all his lab members including Dr. Weiwu Jiang, Dr. Chun Chu and Dr. Paramahamsa Maturu for teaching me numerous important lab skills and the art of troubleshooting. I would also like to thank Dr. Sundararajah Thevenanther for his crucial and extremely valuable suggestions for my research project. His tough questions motivated me to think critically and widen my research scope in terms of understanding the big picture. My grateful thanks are also extended to Dr. Diana Chow and Dr. Ming Hu for being a part of my thesis committee and also sharing their knowledge with me through meticulously designed lectures and course materials. When I joined the

department, I was new to drug metabolism and pharmacokinetics field but rigorous coursework along with challenging discussions and assignments strengthened my basics tremendously. I would like to thank Dr. Chow further for instilling in me the qualities of a responsible researcher in pursuit of my goals. I would also like to extend my thanks to Dr. Cristian Coarfa for his guidance during analysis of my microarray data.

I would like to further thank my seniors- Dr. Pankajini Mallick and Dr. Pranav Shah for teaching me all laboratory techniques. Furthermore, I would also like to thank Dr. Pankajini for her constant support as well as the numerous random scientific and personal discussions, which provided a friendly atmosphere at work. I would also like to thank my current lab mate Pavan Chitalaya for helping me with my experimental studies and also finalizing my manuscripts. I am thankful to all my wonderful friends Yu Jin, Mahua, Nandita, Arshad, Alex, Grady and Srishti in Houston and abroad. I would also like to thank Tristan for her help during my committee meetings.

Last but not the least, I am extremely indebted to my parents who always supported me in my endeavors. Their love gave me strength to overcome all obstacles and encouraged me in my times of need. Although my late grandfather, Shri Ram Dev Chaudhary, is not here to see me graduate, he envisioned a successful career in research for me and I want to thank him for guiding me in this direction. I would also like to thank my brother Manik Taneja and my sister-in-law Cherrie Chow for being my support system in United States.

Guncha Taneja

University of Houston

TABLE OF CONTENTS

Abstract

Cytochrome P450 3A (CYP3A) is a family of Phase I drug metabolizing enzymes (DMEs) that metabolize up to 50% of currently clinically prescribed drugs. In humans, CYP3A family comprises of CYP3A4, 3A5, 3A7 and 3A43. Out of these enzymes, CYP3A4 is considered the most important contributor of hepatic drug metabolism in adults. Impairment in *CYP3A4* gene expression/ activity leads to unanticipated adverse reactions or therapeutic failures; culminating in early termination of drug development or withdrawal of drugs from the market. Induction of gene expression of CYP3A4 is mainly regulated by basal regulators such as transcription factors and nuclear receptors including (Pregnane X Receptor (PXR). PXR, upon activation by xenobiotics, induces *CYP3A4* gene and is largely considered responsible for its expression. On the other hand, gene expression and activity of CYP3A4 enzyme is down-regulated in many disorders such as hepatitis, diabetes, cancer, cardiovascular diseases etc. This alteration in CYP3A4 enzyme can cause harmful clinical consequences due to potentially dangerous drug-drug interactions. Therefore, a comprehensive understanding of the role of key regulators (i.e. transcription factors (TFs), epigenetic modulators, cell signaling pathways etc.) in transcriptional up or down-regulation of *CYP3A4* is required to prevent disorders due to impaired drug metabolism. *Hence, our **objective** was to identify key regulators and signaling pathways involved in PXR-mediated regulation of CYP3A4 enzyme in order to discover interventions for improved clinical therapy.*

To achieve this objective, we had the following specific aims:

Specific Aim 1: To determine the key regulators (transcription factors, epigenetic mechanisms, and signaling pathways) of Cyp3a enzyme *in vivo.* We used a combined approach of Cyp3a11 (mouse homolog of CYP3A4) induction by PXR ligand (PCN) and down-regulation by LPS in mice. High throughput technologies- DNA Microarray analysis and Reverse phase protein array (RPPA) were used to determine the changes in genes and proteins respectively which were altered in opposite directions by PCN and LPS.

Specific Aim 2: To determine the mechanism of PXR-mediated induction of CYP3A4 *in vitro.* Post-translational modifications such as phosphorylation, ubiquitination etc. modulate the activity of PXR and this alters the ability of PXR to induce CYP3A4. We determined the role of mitogen activated protein kinases, especially, JNK in PXR-mediated induction of CYP3A4 in human liver carcinoma cells.

Specific Aim 3: To study the effect of PXR ligand on Cyp3a-mediated drug metabolism *in vivo.* We will study the metabolism of Irinotecan, an important chemotherapeutic agent used for colorectal cancer treatment. In humans, irinotecan is metabolized via CYP3A4 (Phase I) to SN-38 and via UGT1A1 (Phase II) enzymes to SN-38G. Despite being highly effective, SN-38 accumulation (primary metabolite of irinotecan) *in vivo* leads to fatal diarrhea. Irinotecan also causes liver toxicity, although the role of metabolism in irinotecan hepatotoxicity is not known. We tested the hypothesis that PXR mediated induction of Cyp3a11 enzyme will alter the metabolism of irinotecan in mice and hence reduce in vivo accumulation and thereby toxicity of SN-38. We determined

the effect of specific PXR ligand- PCN on hepatic and intestinal disposition of irinotecan and its metabolites- SN38 and SN38 glucuronide in mice.

To conclude, understanding the mechanism of regulation of CYP3A enzymes is important as it will contribute to the development of novel safe and effective approaches to treat patients having disorders due to impaired CYP3A metabolism.

List of Tables

List of Figures

Chapter 1

General Introduction

1.1 Hepatic Drug Metabolism

In humans, multiple sites are involved with drug metabolism including the gut wall, lungs, kidney and plasma (Krishna et al, 1994). However, the liver is the most metabolically active tissue per unit weight and is thus responsible for the majority of xenobiotic metabolism. Moreover, it has a large size, is perfused by blood containing drugs absorbed from the gut (enterohepatic circulation) and has a very high concentration of most of the drug metabolizing enzymes relative to other organs (Williams et al, 1972). Strategically positioned to receive blood directly from the gut and small intestine, the liver is the first organ to encounter all absorbed compounds and is therefore equipped with enzymes and proteins capable of neutralizing potentially harmful insults. Apart from being the primary organ responsible for detoxification of both endogenous compounds such as ammonia, bile acids and exogenous compounds such as environmental toxins, drugs etc.; the liver performs important functional roles. It is also responsible for energy homeostasis and cholesterol metabolism, filtering blood and processing nutrients, producing bile and processing hemoglobin (Tompkins et al, 2011).

The human liver has evolved a pathway of metabolism and elimination for xenobiotics and endobiotics, which can be divided into three phases (Fig. 1). Phase 1 is made up of a mixed-function oxidase system responsible for oxidation, reduction, or hydrolysis of substrates in order to make them more polar, more water soluble and suitable substrates for phase 2 metabolism. The actual activity of a drug can be altered in one of 3 ways by phase 1 metabolism: the metabolite can have a similar or different activity to the parent compound,

it can be converted from an active to a relatively inactive compound or from an inactive to active compound. If the metabolites of phase 1 reactions are sufficiently water soluble in nature, they can be readily excreted at this point. Phase 1 metabolism occurs primarily through the cytochrome P450 family (CYP) of enzymes located in the hepatic endoplasmic reticulum (Nebert et al., 2002), but may also occur through non-CYP enzyme systems, such as Flavin mono-oxidase (FMO), monoamine oxidase (MAO) etc. (Nelson and Gordon, 1983; Guengerich, 2001; Parkinson, 2001).

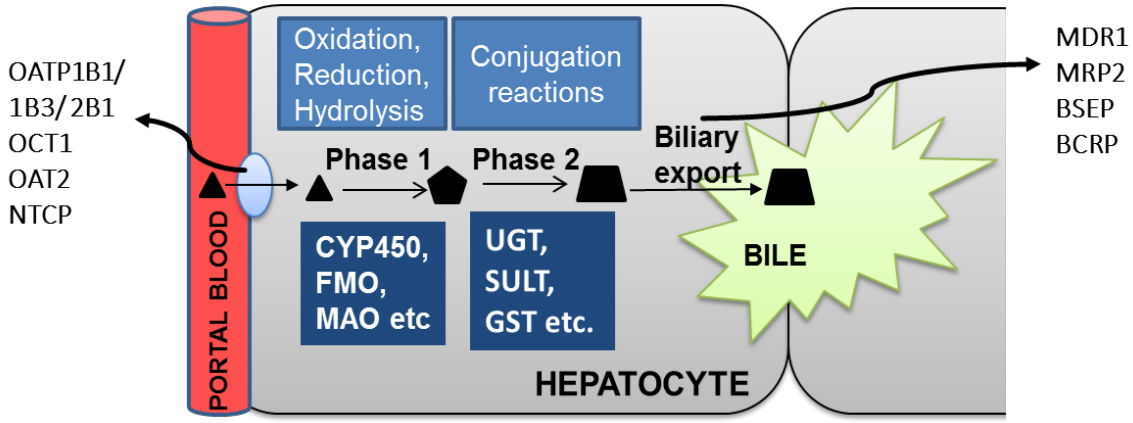

Fig. 1.1 Schematic pathway of hepatic drug metabolism

Phase 2 consists of conjugating enzymes which introduce endogenous hydrophilic moieties such as sugars, sulfates and amino acids to substrate compounds resulting in significant increases in polarity and hydrophilicity. Phase 2 usually involves three primary mechanisms- glucuronidation, sulfation and glutathione conjugation. All three reactions share two commonalities—a necessary cofactor, the concentration of which determines the

capacity of the pathway, and a catalyzing enzyme represented in a number of gene products which provides variety and redundancy to a critical metabolic process (Tompkins et al, 2011). Most phase 2 reactions inactivate drugs or the active metabolites formed from phase 1 reactions.

Lastly, phase III represents the efflux transporters responsible for removing conjugated and oxidized substrates to the blood or bile for excretion in urine or feces, respectively. Most drugs and/or their metabolites are excreted into the bile via efflux transporters such as-multidrug resistance 1 (MDR1), multidrug resistance associated protein 2 (MRP2), breast cancer resistance protein (BCRP) or bile salt export pump (BSEP). These transporters can also work in concert with metabolizing enzymes and play an important role in drug metabolism (Endou, 2000; Ito et al, 2005).

1.2 Cytochrome P450 family of enzymes

CYPs are heme containing pigments found in the microsomes of hepatocytes (Wheeler et al., 2001). CYP450s are the largest family of membrane-bound, nonspecific, mixed-function enzymes responsible for more than 75% of drug metabolism (Guengerich FP, 1999; 2008). They contain a heam-bound iron at the active site, responsible for binding with and metabolizing the drug, attached to a protein chain. It is so named because of its location (cyto= cell) and the fact that the heam moiety absorbs colored (chrome) light at a wavelength of 450nm. Although the liver represents the major site of CYP expression, P 450s are also expressed in extrahepatic tissues such as the small intestine, colon, kidney, lung, skin, placenta, heart, and the brain. About 57 human P450 enzymes have been

identified till now (Guengerich, 2008) and are classified according to their number of shared amino acid sequences (Nebert et al, 1989; Nelson et al, 1993). Families are given the nomenclature CYP1, CYP2 etc. and are further divided into sub-families CYP1A, CYP1B etc. Sub-families can be further divided into isoforms CYP1A1, CYP1A2 etc. Among all these CYP450s, CYP3A4 is notoriously known as the most abundantly expressed CYP protein in the human liver, accounting for as much as 40% of total CYP content (Guengerich, 1995; Leeder & Okey, 1996; Krishna & Klotz, 1994; Wilkinson, 2005). This also allows CYP3A4 to be responsible for the metabolism of more than 50% of currently marketed drugs (Guengerich, 1999; Veith et al, 2009; Zanger et al, 2013).

1.3 CYP3A Family

The human cytochrome P450 3A (CYP3A) gene family is considered to be a major family of drug metabolizing enzymes and comprises of 4 genes, CYP3A4, CYP3A5, CYP3A7 and CYP3A43, which are arranged in tandem at a locus on chromosome 7 (Gellner et al, 2001). The CYP3A subfamily is one of the most versatile of the biotransformation systems that facilitates the elimination of many drugs, other xenobiotic compounds and endogenous molecules from the body (Nelson, 2004; Guengerich, 2008; Zanger et al., 2008). Among adults, CYP3A4 is the dominant CYP3A enzyme in the liver and small intestine. CYP3A5 is also found in the adult liver and small intestine (and other organs), but its expression is clearly polymorphic, with individuals exhibiting a relatively high or low level of protein (Paine et al, 1997; Wrighton et al, 1990). CYP3A5 is also polymorphically expressed in fetal liver (Hakkola et al, 2001). CYP3A7 is the major fetal liver CYP3A enzyme, whereas

CYP3A4 is absent (De Wildt et al, 1999). In mice, Cyp3a cluster contains 7 full length genes but there are no orthologous pairs between mouse and human, suggesting that a single CYP3A gene present in the common ancestor existed, which independently expanded during the last 75 MY (Nelson et al., 2004). Expression of the three minor isoforms, CYP3A5, CYP3A7, and CYP3A43 is generally lower compared to CYP3A4. CYP3A7 is the major fetal liver CYP3A enzyme, whereas CYP3A4 is absent (De Wildt et al, 1999). Although the hepatic CYP3A7 expression appears to be significantly down-regulated after birth (De Wildt et al, 1999), protein has been detected in some adults (Tateishi et al, 1999), and it may contribute to drug/xenobiotic clearance. CYP3A43 is the most recent member of the human CYP3A gene locus to have been reported. Gene transcription was detected in liver, kidney, prostate and pancreas, but its mRNA level was much lower than that of CYP3A4, and it is unlikely to contribute much to the systemic clearance of drugs or other xenobiotics.

1.4 Alteration of CYP3A- Problems and Outcomes

As polypharmacy is commonplace in many patient populations, the risk of dangerous drug-drug interactions (DDIs) is high. A DDI may be defined as the modification of a patient's clinical response to the administered drug by co-administration of another drug. DDIs can take place through two mechanisms- pharmacodynamic interactions, when a pharmacological response is altered through either agonism or antagonism; or pharmacokinetic interactions, *i.e*. alterations of drug disposition occur mainly *via* inhibition or induction of metabolic enzymes or transporters involved in drug

absorption, distribution, metabolism, or excretion. Since CYP3A enzyme is responsible for the metabolism of majority of drugs in the market, most of the drug interactions are a result of an alteration of CYP3A metabolism. Metabolism based DDIs mediated via CYP3A enzyme can either be due to induction or inhibition of the enzyme. They are an important cause of serious adverse events that have often resulted in early termination of drug development or withdrawal of drugs from the market. The non-sedating antihistamines terfenadine (Seldane) and astemizole (Hismanal), and the gastrointestinal motility agent cisapride (Propulsid), were all withdrawn from the U.S. market because metabolic inhibition of CYP3A4 by other drugs led to life-threatening arrhythmias (Dresser et al, 2000). The calcium channel blocker mibefradil (Posicor) was withdrawn from the U.S. market in 1998 because it was a potent enzyme inhibitor that resulted in toxic levels of other cardiovascular drugs (Mullins et al, 1998).

The clinical consequences of CYP3A inhibition or induction depend on the pharmacological and toxic effects of both the parent drug and its metabolite(s) and may be particularly important if the victim drug has a narrow therapeutic index, since metabolism-based DDIs may cause up to 10-fold changes in the concentrations of the drug whose biotransformation is inhibited or induced. Following are some of the reported clinical drug -drug interactions with CYP3A enzyme.

1.4.1 Clinical Incidences of Induction of Cyp3a

Drug interactions involving enzyme induction are not as common as inhibition-based drug interactions but equally profound and clinically important. Exposure to environmental pollutants as well as the large number of lipophilic drugs can result in induction of CYP enzymes. The most common mechanism is transcriptional activation leading to increased synthesis of more CYP enzyme proteins (Gallelli et al, 2005). The effect of induction is simply to increase the amount of P450 present and speed up the oxidation and clearance of a drug (Markowitz et al, 1995).

The most common enzyme inducers are rifampicin, phenobarbital, phenytoin, carbamazepine and anti-tubercular drugs. Rifampicin induces CYP3A enzymes in the liver, although weak induction of other CYP enzymes, including, CYP2A6, CYP2C and CYP2B6, have also been noticed. Rifampicin increases the elimination of a large number of drugs, although most of them are substrates for CYP3A4, such as midazolam, quinidine, cyclosporine A and many steroids. The short half-life of rifampicin results in enzyme induction (CYP3A4, CYP2C), apparent within 24 h, whereas phenobarbital, which has a half-life of 3-5 days, requires approximately 1 week for induction (CYP3A4, CYP1A2, CYP2C) to become apparent.

A clinically relevant decrease was observed in faldaprevir (hepatitis C virus protease inhibitor) exposure when co-administered with an antiretroviral efavirenz (CYP3A inducer). Faldaprevir doses were thus doubled in order to manage the disease (Sabo et al, 2014). Therefore, in order to prevent these drug-drug interactions and/or adverse drug

reactions, it is crucial to gain an understanding of the complete molecular mechanism behind up-regulation of CYP3A enzyme.

1.4.2 Clinical Incidences of Down-regulation of Cyp3a

Inhibition-based DDIs constitute the major proportion of clinically relevant DDIs. In this process enzyme activity is reduced due to direct interaction with a drug, usually begins with the first dose of the inhibitor, while the extinction of inhibition is related to the drug half-lives (Murray et al, 1997). The metabolic inhibition may be reversible (competitive, metabolic-intermediate complex, non-competitive) or irreversible, and clinical effects are influenced by basic mechanisms.

The reversible competitive inhibition occurs when inhibitor and substrate compete for the same binding site on the enzyme. In this type of interaction, the inhibition mechanism is direct and is rapidly reversible. The drugs are converted through multiple CYP dependent steps to nitroso-derivatives that bind with high affinity to the reduced form of CYP enzymes. Thus CYP enzymes are unavailable for further oxidation and synthesis of new enzymes is therefore, the only means by, which activity can be restored and this may take several days (Murray et al, 1992). Some of the inhibitors of CYP3A4 that act by this mechanism of inhibition include azole antifungal agents, some HIV protease inhibitors such as nelfinavir mesylate (Lillibridge et al, 1998) and antihypertensives such as diltiazem (Sutton et al, 1997).

Similarly, HIV protease inhibitors (i.e., saquinavir and ritonavir) increase sildenafil serum concentrations up to 11-fold (Muirhead et al, 2000). It has been recently reported that azole

antifungal drugs (i.e., ketoconazole, itraconazole, voriconazole and posaconazole) are CYP3A inhibitors and are able to induce DDIs. For example, ketoconazole (a strong CYP3A inhibitor) treatment increased the AUC and Cmax of romidepsin by ~25% and 10% respectively in patients with advanced cancer (Laille et al, 2015). Romidepsin, a CYP3A substrate, is indicated for the treatment of cutaneous T-cell lymphoma and its increased plasma concentrations lead to thrombocytopenia. Similarly, treatment with an anti-fungal agent and a CYP3A4 inhibitor drug voriconazole enhanced the AUC for oxycodone, an opioid receptor agonist, resulting in increased toxicity of oxycodone in cancer patients (Watanabe et al, 2011). Apart from that, posaconazole exhibited inhibitory effects upon CYP3A and PGP and reduced the steady-state clearance of cyclosporine. Moreover, in an open-label study performed in 36 healthy volunteers, the treatment with posaconazole (400 mg twice daily) for 14 days increased the plasma concentrations of tacrolimus of 2.2-fold, the area under the curve (AUC) of 4.5-fold, and the half-life up to 7.5 h (Parsons et al, 2007). Therefore, the dosage of tacrolimus had to be reduced up to 66% of the original dose, in presence of posaconazole.

The production of metabolic-intermediate complexes is an unusual form of inibition where the inhibitor binds only to the enzyme-substrate complex. The formation of a metabolic-intermediate complexes results from inhibitors that have an N-alkyl substituent. After the binding of inhibitor, the latter is oxidized by 3A4 and the resultant oxidized species of the inhibitor remains complexed with the reduced heme group of CYP3A4 forming a complex slowly reversible.

In irreversible inhibition, the metabolite resulting from the oxidation of the substrate by CYP3A4 becomes irreversible and covalently bound to 3A4, thus leading to a permanent inhibition of the enzyme. In the case of irreversible inhibition the critical factor is represented by the total amount rather than the concentration of the inhibitor to which CYP isoenzyme is exposed. Lipophilic and large molecular size drugs are more likely to cause inhibition (Thummel et al, 1998). Two characteristics make a drug susceptible to inhibitory interactions: one metabolite must account for >30-40% metabolism of a drug and that metabolic pathway is catalyzed by a single isoenzyme.

Apart from DDIs, food-drug interactions also represent a major clinical problem. The effects of several fruit juices on CYP3A expression and activity have been studied extensively *in vitro* and in human participants. Specific inhibitory ingredients in some fruit juices have been identified and characterized. Juice prepared from grapefruit is one of the most exhaustively studied dietary substances shown to inhibit enteric metabolism of numerous CYP3A substrates. GFJ can enhance systemic drug exposure by inhibiting CYP3A-mediated pre-systemic (first-pass) metabolism in the intestine (Paine and Oberlies, 2007). The increase in systemic drug exposure can be sufficient to produce adverse events, such as muscle pain with some statins and severe hypotension with some calcium channel blockers (Saito et al., 2005). Compounds known as furanocoumarins (e.g., 6′, 7′-dihydroxybergamottin, bergamottin), in aggregate, have been established as major mediators of the ‘GFJ effect’ in humans (Paine et al., 2006).

1.5 Mechanism of regulation of CYP3A enzyme

1.5.1 Basal regulation

The CYP3A4 5'-flanking region is 35.8 kb and only 13 kb has been analyzed for hepatic or intestinal regulation. The first, the proximal *CYP3A4* promoter (bases -362 to +53), is an everted repeat of the AG(G/T)TCA hexamer separated by six nucleotides (ER-6), and works as a minimal promoter (prPXRE). The second is a distal enhancer module (XREM) located between -7.8 and -7.2 kb upstream of the *CYP3A4* transcription start site that, in conjunction with elements in the proximal promoter region, directs the pregnane X receptor (PXR) and the constitutive androstane receptor (CAR)- mediated transactivation of *CYP3A4*. For the constitutive activation of the *CYP3A4* gene, a region from -11.4 to -10.5 kb designated the constitutive liver enhancer module of *CYP3A4* (CLEM4), has been characterized. CLEM4 consists of an array of *cis*-acting elements encompassing 900 bp. Several transcription factors, including HNF1α, HNF4α, USF1 and AP1 interact with CLEM4 and appear to activate the enhancer cooperatively. Another functional HNF4α binding site has been identified within the distal enhancer module (XREM). It has been suggested that this HNF4α site is involved in the induction of *CYP3A4* by cooperatively interacting with the adjacent PXR sites. The transcription factor C/EBPβ can also play an important role in CYP3A4 basal expression and variability. In a recent study the existence of a distal enhancer site at -5.95 kb in the CYP3A4 gene was shown and it is at this site that the transcription factors, LAP and LIP, interact. Variation in the LAP: LIP isoform ratio can largely influence the regulation of CYP3A4 by other well characterized

mechanisms, such as rifampicin induction. Therefore, C/EBPβ isoforms may effectively control CYP3A4 constitutive and inducible expressions and ultimately contribute to the different CYP3A4 phenotypes present in the human population.

C/EBPα is also involved in the constitutive transcription of *CYP3A4* through three proximal elements at -121, -1393 and -1659 bp. Moreover, the C/EBPα-mediated transactivation is synergistically activated in hepatic cells by HNF3γ, which binds at -1718 bp. The HNF3γ site is located 50 nucleotides upstream of the C/EBPα binding site (-1659/-1668), and it is likely that HNF3γ could affect C/EBPα binding through a direct mechanism.

1.5.2 Up-regulation

CYP3A4 is both constitutively expressed and transcriptionally activated by a variety of structurally diverse xeno *CYP3A4* is both constitutively expressed and transcriptionally activated by a variety of structurally diverse xenochemicals. The induction of CYP3A4 is a phenomenon which can determine the toxic vs. therapeutic effects of a drug. CYP3A4 is inducible by a number of clinically important drugs including rifampicin, clotrimazole and dexamethasone, which sometimes cause severe drug-drug interaction responses. The molecular mechanism that underlies this phenomenon is complex, with several nuclear receptors, including PXR, CAR, the glucocorticoid receptor (GR) and the vitamin D receptor (VDR), playing a decisive role.

The human nuclear receptor pregnane X receptor (PXR) is activated by a range of drugs known to induce the *CYP3A4* expression. PXR heterodimerizes with the retinoid X

receptor (RXR) and binds to a response element in the *CYP3A4* promoter (Fig1.5.2). More recent evidence showed the existence of a potent enhancer module, 7.7 kb distal to the transcription start point, which also mediates the transcriptional induction of *CYP3A4* by activators of hPXR. Thus, induction of *CYP3A4* is dependent on the cooperativity between elements within the promoter proximal region of the gene and the distal xenobiotic-responsive enhancer module.

CAR is also capable of trans-activating the expression of the *CYP3A4* gene, both *in vitro* and *in vivo*. CAR regulates the induction of CYP3A4 by the phenobarbital-like class of xenobiotics. In the CYP3A4 5'-upstream region, the induction by both CAR and PXR can occur either by the proximal ER6 motif located at position –160 or by the distal XREM located at –7.7 kb, suggesting that interplay between PXR and CAR is an important determinant of the *CYP3A4* expression. Nevertheless, recent findings have proven that hCAR exhibits a preferential induction of CYP2B6 relating to CYP3A4 owing to its weak binding and the functional activation of the CYP3A4 ER6, which suggest that hCAR is not a major regulator of the *CYP3A4* expression.

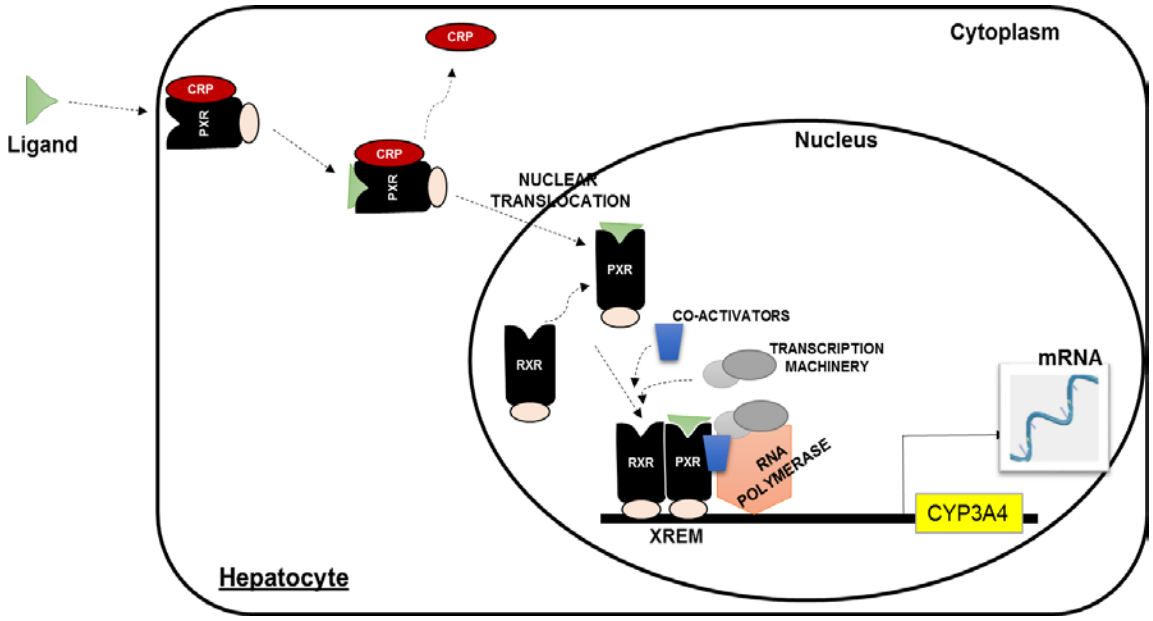

Fig. 1.5.2 Induction of CYP3A4 enzyme via PXR.

1.5.3 Downregulation

Several factors including age, diet, hormone status and disease can also determine the phenotypic variability of CYP3A4. Certain pathological states, in particular those involving a host inflammatory response (i.e. bacterial and viral infection, trauma, burn injury, tissue necrosis, auto-immune disease, etc), are associated with lower drug metabolism in the organism and decreased hepatic CYP content, which ultimately influences the fate and therapeutic efficacy of many drugs. The effects of inflammation on CYP450 levels in liver and cultured primary hepatocytes can be attributed to decreases in the levels of specific CYP450 mRNAs (Morgan, 1997). The decreases in mRNA due to cytokines have been thought to be due to decreased transcription because decrease in the

protein levels is significantly slower. Hence, it is thought that the down-regulation of mRNA is responsible for the reduction in protein levels of DMETs. However, one cannot rule out the possibility of reduced DMET translation and/or mRNA/protein stability.

Many studies have shown the reduction of protein levels of specific forms of DMEs both *in vivo* and *in vitro,* and in most cases, suppression of the mRNAs encoding these enzymes precedes the protein loss. The fact that the magnitudes of the observed decreases in transcription are usually sufficient to account for the decreases in protein and that the mRNA effects can often be shown to precede those on the protein, suggests that the primary mechanism of regulation is transcriptional. However, there are several cases which show that protein turnover and mRNA degradation contribute to this down-regulation.

At the early stages of an inflammatory response, cytokines (mainly IL-1β, TNF-α and IL-6) are produced by monocyte/ macrophages and endothelial cells and are released into the systemic circulation, initiating the so-called *acute phase response*. Evidence from *in vitro* studies using rat and human hepatocytes have revealed that these inflammatory mediators (IL-6, IL-1β, TNFα, oncostatin M, interferon α and γ) are also capable of down-regulating the hepatic P450 function, including CYP3A4 activity. IL-6 causes a moderate induction of the C/EBPβ transcription factor mRNA and a marked increase in the translation of C/EBPβ-LIP, a 20 kDa C/EBPβ isoform lacking a transactivation domain. The adenovirus-mediated expression of C/EBPβ-LIP caused a dose dependent repression of CYP3A4 mRNA, whereas the overexpression C/EBPα and C/EBPβ-LAP (35 kDa) caused a significant induction.

Hepatocyte nuclear factors (HNFs) regulate the basal transcription of many CYP genes. Therefore, a downregulation of the HNF expression or activities could also contribute to the suppression of CYPs. HNF4α, for instance, is required for the basal transcription of rat and human CYP3As. It has been found that the DNA binding activities of HNF1α, HNF3α, and HNF4α were all rapidly reduced in LPS-treated rat liver, with HNF4α displaying the largest decrease at 53%. These findings suggest that the suppression of CYP3As could also be due to the combined effects of LPS on multiple HNFs.

Several other mechanisms for the suppression of the drug inducible CYP3A expression have been described and a role for CAR and PXR in this down-regulation has been proposed. Loss of CYP3A and CYP2B following LPS treatment is associated with a repression of CAR, PXR, and their dimerization partner, RXR. In more recent studies, it has been shown that NFkappaB activation by LPS and TNFα also played a pivotal role in the suppression of the rifampicin-mediated induction of CYP3A4. This occurred through direct interactions of NFkappaB with the PXR: RXR complex, indicating that NF-kappaB activation during inflammatory responses is of particular relevance in mediating the suppression of *CYP3A4* induction by xenobiotics.

1.6 Regulation of PXR activity: Post-translational modifications

PXR is a sensor for endogenous and xenobiotic compounds and a trans-regulator for the expression of many drug metabolism–related genes. The rodent PXR and its human homolog i.e. SXR can be activated by certain xenobiotic and endogenous compounds (Kliewer et al., 1998; Lehmann et al., 1998). The most important drug metabolism gene

regulated by PXR is the Cyp3a subfamily of CYP450s both in mouse and humans. Other genes that are regulated by PXR include multiple drug resistant genes such as Mdr1, Mrp2 & Mrp3 (Synold et al., 2001; Kast et al., 2002), UGT1A1, UGT1A3, UGT1A4, UGT1A6 and UGT1A9 (Xie et al., 2003; Yueh et al., 2003). PXR/RXR heterodimer can also interact with other nuclear receptor pathways (like CAR/RXR) by mutually binding to the regulatory DNA sequences leading to redundancy in regulating the metabolism and clearance of various xenobiotics and endogenous compounds.

PXR gene expression can be regulated by many different stimuli including xenobiotics and metabolites (Aouabdi et al., 2006). PXR gene expression can also activated by farnesoid X receptor (FXR) in response to bile acids. Three alternatively spliced transcripts of PXR that encode different isoforms have been described, one of which encodes two products through the use of alternative translation initiation codons. Additional transcript variants have been shown to exist, although these variants have not been fully described.

While it is well known that the transcriptional activity of PXR is governed by direct binding of ligands, many reports have indicated that cellular signaling pathways modulate the functions of nuclear receptors, including PXR. These aspects shed some light on possible non-liganded mechanisms of receptor activation. Thus far, PXR has been shown to be a subject for phosphorylation, SUMOylation, ubiquitination and acetylation. There is a growing body of evidence that site-specific phosphorylation of PXR provides an important mechanism for PXR-mediated regulation of CYP expression. Series of kinases such as p70 S6K, PKA, PKC, Cdk2 and Cdk5 can phosphorylate and regulate PXR transcriptional

activity. Immunopurified human PXR also has been found to be a target for phosphorylation by such other kinases as glycogen synthase kinase 3 (GSK3), casein kinase II (CK2) and Cdk1. The effects of site-specific phosphorylation of PXR by kinases interfere with a wide variety of its functions involving subcellular localization, dimerization, DNA binding, and coregulatory interaction. While phosphorylation generally may contribute to both activation or termination activity in NRs, direct phosphorylation in the case of human PXR leads mostly to negative response in its transcriptional activity.

1.7 Mitogen activated protein kinases (MAPKs)

Mitogen-activated protein kinases also known as MAP kinases are serine/threonine/tyrosine-specific protein kinases belonging to the CMGC (CDK/MAPK/GSK3/CLK) kinase group. The closest relatives of MAPKs are the cyclin-dependent kinases (CDKs). MAPKs are involved in directing cellular responses to a diverse array of stimuli, such as mitogens, osmotic stress, heat shock and proinflammatory cytokines. They regulate proliferation, gene expression, differentiation, mitosis, cell survival, and apoptosis among many others (Houliston et al., 2001). MAP kinases are found in eukaryotes only, but they are fairly diverse and encountered in all animals, fungi and plants, and even in an array of unicellular eukaryotes. The MAPK signaling pathways generally refers to a family of signaling cascades, which consist of the extracellular signal regulated kinase (ERK 1/2), Jun N-terminal kinase (JNK) and p38 kinase pathways. These cell-signaling components are involved in regulation of DMEs and transporters by modulating the activity of some of nuclear receptors (Ghose et al, 2004, 2008). Based on

in silico analysis of consensus phosphorylation sites for common protein kinases, Lichti-Kaiser *et al*. predicted human PXR to be a target for direct phosphorylation by a MAPK. Recently, JNK was shown to be required for optimal activation of *CYP3A4* gene by NR, VDR (Yasunami et al, 2004). JNK1 and JNK2 are abundantly present in the liver however, JNK1/JNK2 double knockout mice are lethal and there are no well-known *in vivo* inhibitors of JNK and hence, it is difficult to elucidate the role of JNK in signaling *in vivo.*

1.8 Irinotecan

1.8.1 Introduction

Irinotecan (CPT-11, 7-ethyl-10-[4-(1-piperidino)-1-piperidino] carbonyloxy-camptothecin) was approved by FDA in 1996 to be used singly as a second-line agent or as a first-line combination chemotherapy for colorectal cancer. It is a semisynthetic analog of camptothecin, originally isolated from the ornamental tree *Camptothecaacuminata*. It was first discovered and synthesized in Japan in 1983 (Rothenberg 2001). Irinotecan exerts its potent antitumor activity against a wide range of tumors by inhibiting topoisomerase-I (Topo-I), a nuclear enzyme responsible for unwinding DNA required for replication. Irinotecan is a prodrug and is metabolized into an active metabolite, SN-38 (7-Ethyl-10-Hydroxycamptothecin) by carboxylesterases (CES) in the liver. SN-38 is 100-1000 times more potent in destabilizing Topo-I that blocks DNA unwinding and future replication, resulting in interrupted repairs of double strand breaks and S phase arrest followed by cell death (Rudolf et al. 2013; Kawato et al. 1991).

1.8.2 Metabolism/Disposition

Irinotecan undergoes metabolic conversion to SN38 predominantly in the liver by CES mediated cleavage which is far lower in the blood. Oxidation of irinotecan by CYP 3A4/5 enzymes results in two inactive metabolites APC (7-ethyl-10-[4-N-(5-aminopentanoic acid)-1-piperidino] carbonyloxycamptothecin) and NPC (7-ethyl-10-[4-(1-piperidino)-1-amino] carbonyloxycamptothecin). NPC can further be metabolized into SN-38 by CES. SN-38 is then subjected to glucuronidation by several UGT1A (UDP-glucuronosyl transferase) isoformsm and gets converted to SN-38G, which has 1/100 of the antitumor activity. UGT1A1 plays an important role in the biotransformation of SN-38. Irinotecan and its metabolites uptake and transport into the liver are facilitated by *OATP1B1* (SLCO1B1), *ABCB1, MRP1* (ABCC1), *MRP2* (ABCC2), and *MXR/BCRP2* (ABCG2) (Marsh and Hoskins 2010; Han et al. 2009; Kroetz 2006). SN-38 glucuronide (SN-38G) excreted in the intestine are transformed back into SN-38 by bacterial beta-glucoronidases, resulting in accumulation of SN-38 in intestine and reabsorbed into the systemic circulation. These majorly contribute to varied toxicity, specifically dose limiting diarrhea (Brandi et al. 2009; 2006).

Fig. 1.8.2 Metabolites of Irinotecan

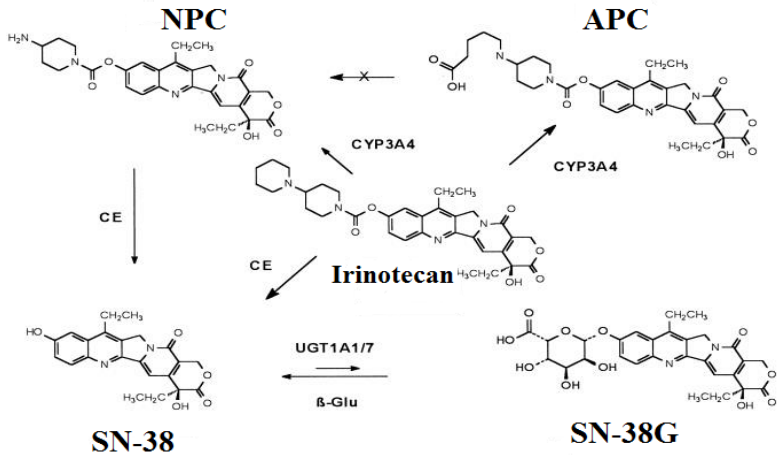

In blood 80% of irinotecan is mainly bound to erythrocytes, whereas SN-38 is bound for at least 99% to albumin and lymphocytes (also to erythrocytes and neutrophils). Both irinotecan and SN-38 are present in two distinguishable forms, an active lactone ring form and an inactive carboxylate form, between which a pH-dependent equilibrium exists. The lactone species is predominantly formed in the acid pH whereas the basic pH favors formation of the carboxylate form. The anti-tumor effect is solely mediated by the lactone form that is essential for interaction with the DNA-enzyme complex. SN-38 lactone form also binds significantly stronger to albumin than the corresponding carboxylate form which explains the better stability of SN-38 *in vivo* compared to irinotecan that does not show any difference in binding to albumin between its two forms (Burke et al. 1995).

1.8.3 Irinotecan treatment in Colorectal Liver Metastasis (CLM)

Colorectal cancer is one of the main causes of cancer-related death, accounting for 677,000 deaths each year worldwide (Rim et al. 2009; Weir et al. 2003). If diagnosed early, colorectal tumors can be cured by a radical resection. Unfortunately, a large number of patients are diagnosed with (distant) metastases either during follow-up or at first presentation. Mostly, metastases spread to liver (Colorectal Liver Metastasis; CLM) and only curative treatment option is hepatic surgical resection of liver metastases (LM), however only 4-15% of the cases are resectable (Adam 2003). Unresectable metastatic liver is majorly because of large size and number (Nordlinger et al. 2007). This has led to evaluate the role of neoadjuvant chemotherapy in the management of these patients (Nordlinger et al. 2008) and were found to render 10% to 30% of initially unresectable patients potentially resectable (Adam 2003).

Until recently, there was no established standard of care in patients with advanced/metastatic colorectal cancer, unresponsive or resistant to 5-fluorouracil (5-FU)-based chemotherapy. However, the introduction of irinotecan has provided a new and effective treatment option in this setting (Vanhoefer et al. 2001; Cunningham et al. 2001). As first-line of therapy, irinotecan in combination of 5FU with oxaliplatin (FOLFIRI or XELIRI) resulted in significantly superior overall response rate (ORR) of between 20-30% to 40-50%. The tumor response rate was almost double in irinotecan treated patients treated to that of 5-FU/LV group (37% vs 21%; $p < 0.05$). The progression-free survival was 6.9 months with 5-FU/LV/irinotecan versus 4.3 months with 5-FU/LV alone ($p < 0.05$) and median overall survival (OS) was 15.9 months versus 13.3 months, respectively ($p < 0.05$)

(Mayer 2000; Saltz et al. 2000). Therefore, addition of irinotecan as combination chemotherapy, provides a statistically significant survival benefit in the first-line treatment of colorectal cancer, thus setting a new standard in the care of colorectal cancer. As second-line of therapy in patients with 5-FU-resistant colorectal cancer, irinotecan monotherapy results in better tumor response rates of 14%-27%, median duration of response was 6.0-9.1 months and median overall survival was 8.3-10.4 months (9.2 months versus 6.5 months, respectively; $p = 0.001$). In addition, progression- free survival was significantly superior with irinotecan (median, 4.2 months versus 2.9 months with 5-FU; $p = 0.03$). These results demonstrated irinotecan monotherapy as the new standard of care in the second-line treatment of 5-FU-pretreated colorectal cancer.

1.8.4 Irinotecan toxicity

1.8.4.1 Causes of toxicity

Dose-limiting toxicities (DLT) of irinotecan hydrochloride are myelosuppression, severe neutropenia and delayed diarrhea. The cytotoxicity of SN-38 is significantly higher than irinotecan itself (Santos et al. 2000). The toxicity profile of irinotecan is dependent on drug dose and schedule, but in all regimens severe diarrhea and neutropenia are the principal dose-limiting toxicities. The incidence of grade 3 or 4 hematological toxicity varies between 5% and 33% depending on irinotecan dosage and regimen (Hoskins et al. 2007). Neutropenia is directly related to the concentration of SN-38 in plasma with higher rates of SN-38 secretion resulting in higher rates of neutropenia.

Irinotecan toxicity is associated with two types of diarrhea; acute and late diarrhea. The acute form is of cholinergic origin and can be prevented in almost all cases by subcutaneous atropine administration. Late diarrhea, occurring more than 24 h after administration of irinotecan (usually at day 5), is prolonged and can be life-threatening, because it may lead to dehydration and electrolyte imbalances especially when it occurs in combination with vomiting. Acute diarrhea is caused by the anti-cholinesterase activity of irinotecan, which destroys the secretory and absorptive functions and properties of the intestinal mucosa. Whereas, severe delayed-onset diarrhea is a result of damaged intestinal mucosa caused by accumulation of SN-38 in intestine due to (i) excessive biliary secretion and (ii) re-activation of SN- 38G in the intestine by bacterial beta-glucoronidases to SN-38 (Saliba et al. 1998). Other suggested mechanisms resulting in severe diarrhea are: (i) reduced rate of SN-38 glucoronidation in the intestines and (ii) increased CES activity. Late diarrhea is treated with intensive courses of oral loperamide that significantly decreases the incidence of grade 3 or 4 late diarrhea during irinotecan treatment ($p= 0.04$) (Benson et al. 2004).

1.8.4.2 Intervention for Irinotecan therapy

Severe intestinal toxicity is still one of the unresolved problems linked to irinotecan administration and constitutes its dose limiting toxicity. Clinical reports have shown that CPT- 11 causes diarrhoea in at least 40% of patients, leading to a premature interruption of chemotherapy (Sargent et al, 2001). Therefore, newer strategies to reduce irinotecan intestinal toxicity have been tested.

One strategy that was using inhibitors of bacterial β-glucuronidases. An oral antibiotic, neomycin, was used to decrease β-glucuronidase activity in the intestinal lumen, and good control of CPT-11-induced diarrhoea in seven colorectal cancer patients was reported. In another clinical trial, simultaneous treatment with oral neomycin and bacitracin was able to prevent the incidence and severity of irinotecan-induced diarrhoea (Kehrer et al, 2001). Apart from using antibiotics, alternative strategies have also been explored to prevent diarrhoea in patients treated with CPT-11. In a hamster model, Ikegami et al showed that by reducing the intestinal SN-38 lactone concentration by increasing the intestinal pH through bicarbonate administration reduced the cellular damage and diarrhoea induced by CPT-11 (Ikegami et al, 2002).

Pregnane X receptor (PXR) is an adopted orphan nuclear receptor that is activated by a wide-range of endobiotics and xenobiotics, including chemotherapy drugs. PXR is expressed in several cancer tissues and the recent evidence strongly points to the differential role of PXR in cancer growth and progression as well as in chemotherapy outcome. Activation of overexpressed PXR in LS174T human colon cancer cells has been found to induce CYP3A4 expression and increased resistance to irinotecan (CPT-11) and SN38 (Raynal et al., 2010), while knockdown of overexpressed PXR reduced CYP3A4 induction and reversed resistance to SN38, suggesting that PXR could alter the outcome of chemotherapy drugs used in the treatment of colorectal cancer. Moreover, LS180 cells overexpressing PXR were found to be less sensitive to irinotecan treatment, suggesting that the PXR pathway is involved in colon cancer irinotecan resistance (Basseville et al., 2011).

This was attributed to the fact that in LS180 cells activation of PXR by SN-38, the active metabolite of irinotecan, resulted in induction of PXR target genes, including CYP3A4, CYP3A5, and MRP2 (Basseville et al., 2011). These studies together suggest that PXR inhibition in colon cancer cells can enhance the efficacy of chemotherapy. It was indeed recently shown in HT-29 colon cancer cells that inhibition of PXR with bitter melon extracts resulted in enhanced doxorubicin effect on the cell proliferation, and sensitized the cells to doxorubicin by reducing the expression of PXR target proteins; MDR1, MRP-2, and BCRP (Kwatra et al., 2013).

1.8.5 Role of "Gut-liver axis"

The interactions between the liver and the gut is through "gut-liver axis" and growing body of evidences suggests malfunction of this axis has a critical role in NAFLD onset and progression. Gut-liver axis is constituted by the intestinal barrier, intestinal microbiota (IM), and liver. Its malfunction may occur through intestinal barrier damage, increased intestinal permeability ("leaky gut"), dysbiosis, and small intestinal bacterial overgrowth (SIBO) (Wigg et al. 2001; Bergheim et al. 2008). Mostly, increased intestinal permeability has been associated clinically with NAFLD and cirrhosis. Leaky gut allows translocations of hepatotoxic bacterial products (PAMPs and DAMPs), endotoxins (Lipopolysaccharide, LPS) and dangerous gut bacteria into liver via mesenteric portal bloodstream, where they activate TLRs present on liver cells (Kupffer cells, stellate cells, and hepatocytes) and induce chronic inflammation (Rivera et al. 2007).

There is accumulating evidence that LPS/TLR4 signaling plays an essential role in the pathogenesis of Colorectal Liver Metastasis. Lipopolysaccharide is a cell wall component of gram-negative bacteria and prototypical ligand for TLR4. LPS-mediated TLR4 activation initiates the pro-inflammatory cascade through activation of MyD88-dependent pathway. TLR activation leads to NF-kB synthesis by stimulating the production of interleukin 1β and activates TNF-α pathway, the pro-inflammatory responses that are ultimately known to contribute towards downregulation of drug metabolizing enzymes and transporters. In both human and animal studies, hepatic steatosis was associated with increased portal LPS levels, through mechanisms involving bacterial overgrowth, and increased intestinal permeability and bacterial translocation (Brun et al. 2007; Cani et al. 2008).

Chapter 2

Hypothesis and Specific Aims

Specific Aims:

Aim 1: We will test the hypothesis that transcriptional regulation of Cyp3a11 enzyme involves an intricate network of transcription factors, epigenetic mechanisms and cell signaling pathways.

Aim 2: We will test the hypothesis that pharmacokinetics of Irinotecan and its metabolites SN38 and SN38G will be altered with changes in drug metabolizing enzyme levels.

Aim 3: We will test the hypothesis that JNK is required for PXR-mediated induction of CYP3A4 *in vitro.*

2.1 Specific Aim 1

Cytochrome P450 (CYP) 3A4 is the most abundant CYP enzyme in the human liver, and it metabolizes ~60% of known drugs. CYP3A4 can be inhibited or induced by drugs, resulting in clinically significant drug-drug interactions that can cause unanticipated adverse reactions or therapeutic failures. This impaired drug metabolism often results in early termination of drug development or withdrawal of drugs from the market. Therefore, the objective of our study was to perform a comprehensive genome-wide mapping and bioinformatics analysis to identify novel mechanisms of CYP3A4 induction and down-regulation *in vivo*. We hypothesize that transcriptional regulation of Cyp3a11 enzyme involves an intricate network of transcription factors, epigenetic mechanisms and cell signaling pathways.

Fig. 2.1: Regulation of Cyp3a11 enzyme by PCN and LPS.

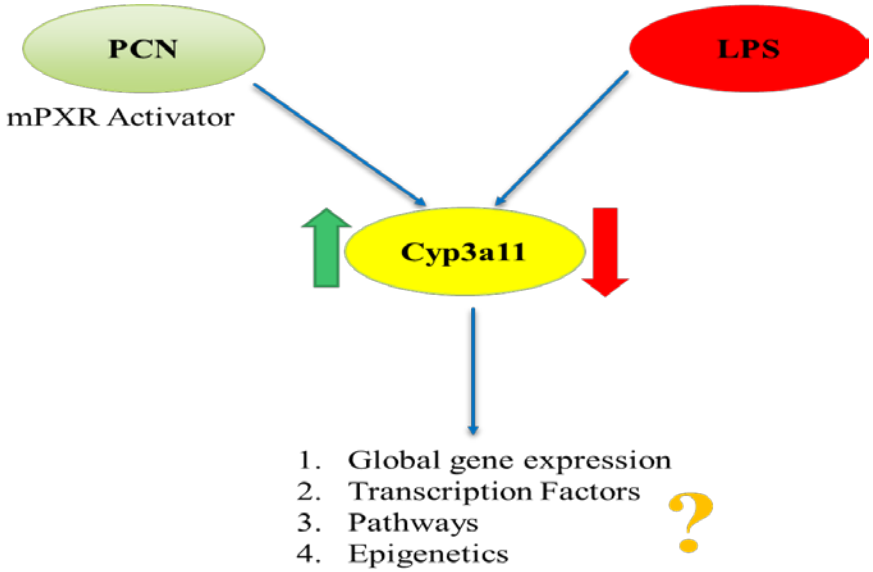

2.2 Specific Aim 2

Irinotecan, a chemotherapeutic agent, is used either singly in the treatment of colorectal cancer or in combination therapy for colorectal liver metastasis (CLM). In CLM patients, disrupted gut barrier has been associated with increased entry of gut-derived bacteria to the liver, which eventually induces hepatic inflammation and leads to alteration of drug metabolizing enzymes (DMEs) such as CYP3A4, UGT1A1 etc. which are responsible for the metabolism of irinotecan to SN38 and SN38 glucuronide. However, if this alteration of DMEs affects the plasma and/or hepatic concentrations of Irinotecan and its metabolites is unknown. Therefore, we hypothesize that downregulation of DMEs during hepatic inflammation alters the pharmacokinetics (PK) of irinotecan and its metabolites *in vivo*. Since the expression/ activity of these DMEs is regulated via nuclear receptors mainly Pregnane X receptor (PXR), we further tested whether activation of PXR would reverse the effect of LPS on PK of irinotecan and its metabolites.

2.3 Specific Aim 3

CYP3A4 is responsible for the metabolism of more than 50% of drugs currently prescribed therapeutically for a wide spectrum of disorders such as cancer, fungal/ bacterial infections, neurological disorders, hepatitis, AIDS etc. Induction of CYP3A4 enzyme expression and activity is known to alter the absorption, disposition, metabolism and/or elimination of co-administered drugs. CYP3A4 gene is both constitutively expressed, as well as transcriptionally induced by structurally diverse xenobiotics and endobiotics. Induction of CYP3A4 usually takes place via activation of nuclear receptors (NRs) especially PXR. Site-specific phosphorylation of PXR has been shown to have a repressive effect on the transcription of its target genes such as CYP3A4. Interestingly, the mitogen activated protein kinase, c-Jun N-terminal kinase (JNK) was shown to be required for optimal activation of CYP3A4 gene by NR, VDR. Therefore, we hypothesize that JNK is required for PXR-mediated induction of *CYP3A4* gene.

Chapter 3

Experimental Methods

3.1 Materials used throughout the dissertation

3.1.1 Compounds

Pregnenolone-16alpha-carbonitrile (#P0543), Hyperforin (dicyclohexylammonium) salt (#H1792), Rifampicin (#R3501) and Curcumin (#C1386) were purchased from Sigma-Aldrich, St. Louis, MO. Lipopolysaccharide (E. coli, Cat # tlrl-pslta), SP600125 (#tlrl-sp60), SB203580 (#tlrl-sb20) and PD098059 (#tlrl-pd98) were purchased from Invivogen, San Diego, CA. Irinotecan hydrochloride injections (NDC # 0703-4434-11) were purchased from Martin Surgical Supplies (Houston, TX, USA). Camptothecin, 7-Ethyl-10-hydroxy-camptothecin (SN-38) and 7-ethyl-10-hydroxycamptothecin glucuronide (SN-38G) were a kind gift from Dr Ming Hu's lab at the University of Houston, TX.

3.1.2 Reagents

Dulbecco's Phosphate-Buffered Saline, 1X without Ca/Mg: 500 ml (21-031-CV, Corning), Dulbecco's Phosphate-Buffered Saline, 1X with calcium and magnesium (21-030-CV, Corning), EGTA (E8145-10G, Sigma), Williams E (12551-032, Invitrogen), Penicillin/streptomycin solution (15140, Invitrogen), Glutamine/Gentamycin (G9654, Sigma), Insulin-transferrin-sodium selenite (I1884, Sigma), Glucagon (G3157, Sigma); Fetal bovine serum (10082-14, Invitrogen), Percoll (P4937, Sigma), Collagenase Type IV (C-5138, Sigma), Trypan blue (T8154-100ML, Sigma), Trizol reagent (T9424, Sigma), Chloroform (C2432, Sigma), Taq man Probes and primers (Sigma), Roche PCR Master Mix (4914058001, Roche Diagnostics), High-Capacity cDNA Reverse Transcription Kit

(4368813, Applied Biosystems), Isopropyl alcohol (JT9037-1, VWR), RNase Inhibitor (N8080119, Applied Biosystems).

3.1.3 Materials

70micron cell strainer (08-771-2, Fisher), 6-well plates BD Primaria culture dish (353846, Corning), Peristaltic pump (VWR International Mini-pump), UV-vis spectrophotometer (Beckman Coulter, DU800), 96-well PCR plate (PCR-96-AB-C, Axygen Scientific), PCR Tubes (20170-012, VWR), Beckman Polytron homogenizer, Cell scrapper (541070, Greiner Bio-One).

3.2 In vivo study requirements

3.2.1 Animals

All animals used in this study followed care of the animals and experimental procedures complied strictly with the Institutional Animal Care and Use Committee guidelines of the University of Houston. Adult, male C57BL/6 mice (Stock #000664), aged 5-6 weeks with approximate weight of 20-22 g were purchased from Jackson Labs (Bar Harbor, Maine, USA). All the animals were maintained in a temperature and humidity controlled environment and 12 h light/dark cycle with free access to water and rodent chow ad libitum.

3.2.2 Treatments

Preparation of Lipopolysaccharide (LPS) solution to be administered intraperitoneally (i.p) at 2 mg/kg dose: 120 μL of the 5 mg/ml stock was freshly reconstituted with 2880 μL saline to prepare 0.2 mg/ml of working solution. 10 μL of working solution was injected for every 1 g of mouse weight.

Preparation of PCN solution to be administered intraperitoneally (i.p) at 50 mg/kg dose: 5 mg/ml PCN stock solution was prepared freshly in corn oil. The solution was sonicated in 37 ^{0}C waterbath for 3 h or until a homogeneous suspension was formed. 10 µL of working solution was injected for every 1 g of mouse weight.

Preparation of irinotecan solution to be administered orally at 10 mg/kg dose: 1 mg/ml irinotecan stock solution was prepared freshly by diluting 5 mg/ml injections in sterile saline. About 200µL of 1 mg/ml irinotecan solution was injected to 20g mouse to achieve 10mg/kg dose.

3.3 RNA isolation and real-time PCR analysis

3.3.1 RNA isolation and quantification

Reagents:

Trizol reagent, Chloroform, Isopropyl alcohol, RNase free water (Life technologies; AM9780) or DEPC water, cell scrapper (541070, Greiner Bio-One), TE buffer (1 ml of 1M Tris-HCl and 0.2 ml EDTA (0.5 M) in 100ml double distilled water, maintained to pH 8.8).

Method:

Total RNA was isolated from mouse liver, primary mouse hepatocytes and HepG2 cells using TRIzol reagent according to the manufacturer's protocol. The initial steps of preparing the suspension from tissue and cells were different but latter steps were all same; (i) Isolation from cell culture plates containing trizol: cells were scrapped with scraper and vigorously pipetted 10-15 times to break the cell wall. Contents of 3 wells with similar treatment were pooled together (~750 µL trizol), (ii) Isolation from mouse liver tissues:

Approximately 0.1 g of liver tissues were collected in 2 ml microcentrifuge tubes containing 0.75 ml TRIzol and homogenized with a hand-held Beckman Polytron homogenizer for ~30 sec at highest speed. After each use, homogenizer was washed in the following sequence- RNA Zap reagent, 70% ethanol, MilliQ water and TRIzol reagent. Throughout the homogenization, the tubes were placed on ice and after completion, samples were incubated at room temperature for 5 min. Then 0.2 ml of chloroform was added. Tube caps were secured and vigorously shaken by hand for 15 seconds and incubated at room temperature for 15 mins. The tubes were then centrifuged at 12,000 rpm for 15 min at 4°C. Centrifugation separated the mixture into a lower red, phenol-chloroform phase, an interphase, and a colorless upper aqueous phase. The aqueous phase was transferred into a clean tube and 0.5 ml of isopropyl alcohol was added, mixed vigorously by shaking, and incubated at room temperature/10 mins. The mixture was centrifuged at 12000 rpm/10 mins/4ºC, which resulted in formation of a whitish gel-like pellet at the bottom of the micro centrifuge tube. The supernatant was removed and 1 ml of 75% ethanol was added to the pellet. The tube was vortexed gently and very briefly (till the pellet was seen floating) and centrifuged again at 7500 rpm/5 mins/4ºC. The ethanol was completely removed (if ethanol still remains, centrifuge once more at 7500 rpm/5 mins/4ºC). The RNA pellet was allowed to dry at RT for 5-8 mins (the pellet should not dry completely as this reduces the solubility). After 8 mins, the pellet was dissolved in 20 µl (if RNA was prepared from HepG2 cells) or 100 µl (if RNA was prepared from liver tissues) of DEPC water. RNA concentration was quantified using UV-vis spectrophotometer at 260 and 280 nm

wavelengths. Total RNA was measured by diluting 1 µL of sample in 500 µL of TE buffer (pH 8.8). The ratio of the readings at 260 nm and 280 nm (A260/A280) provided an estimation of RNA purity with respect to contaminants that absorb in the UV, including protein and phenol. An A260/A280 ratio of >1.8 is indicative of highly purified RNA. Using the following Beer-Lambert law equation: 40 µg/ml x A260 x dilution factor, concentration of RNA (µg/ml) was calculated. An A260 reading of 1.0 is equivalent to ~40 µg/ml single-stranded RNA.

3.3.2 cDNA Synthesis

Reagents:

High Capacity Reverse Transcription Kit (4368813, Applied Biosystems)

Method:

2X Reverse Transcription master mix (per 20 µL reaction) was prepared using the kit components in following volumes (for one sample): 4 µL of 10X RT buffer (1X), 1.6 µL of 25X dNTP mix (100 nm), 4 µL of 10X random primers, 2 µL of multiscribe reverse transcriptase (50 U/µL), 2 µL of RNAase inhibitor (20 U/ µL), 6.4 µL of DEPC water. Volumes of components were adjusted as per required number of reactions. In 0.2 ml thin-coated PCR tubes, 6 µg RNA was prepared in a volume of 20 µl. To this tube, 20 µl of 2X Reverse transcription master mix was added (Total reaction volume was 40 µl). The tubes were gently tapped and placed in the PCR cycler to construct the cDNA. The conditions for PCR were: 25°C for 0-10 min, 37° C for 11-70 min, hold at 37° C for 71-130 min, 85° C for 5 sec, then cooled down to 4° C for 90 min.

3.3.3 RT-PCR

Reagents:

96-well PCR plate, Roche PCR Master Mix (Roche Diagnostics), Taqman primer and probes for Cyp3a11 (FP: GGATGAGATCGATGAGGCTCTG, RP: CAGGTATTCCATCTCCATCACAGT), Cyclophilin (FP: GGCCGATGACGAGCCC, RP: TGTCTTTGGAACTTTGTCTGCA) and GAPDH (FP: CATGGGTGTGAACCATGAGAA, RP: GGTCATGAGTCCTTCCACGAT) were bought from Sigma-Genosys, Houston. Gene expression assays (20X) for CYP3A4 (#Hs00604506_m1), Elk1 (#Mm00468233_g1), Mef2 (#Mm01340842_m1), Nrf2 (#Mm00477784_m1), Pea3 (#Mm00476696_m1), Stat1 (#Mm01257286_m1), Mycmax (#Mm00487804_m1) were purchased from Thermo Fisher Scientific, Waltham, MA. Taqman probes and primers for epigenetic factors- Ezh2, DNMT1, DNMT3a, RunX3 and LSD1 were a kind gift from Dr. Bhagavatula Moorthy, Baylor College of Medicine, Houston, TX.

Method:

RT-PCR was performed in 96-well PCR plate using an ABI PRISM 7300 Sequence System instrument and software (Applied Biosystems, Foster City, CA). Total PCR reaction mixture volume was 25 µl and contained 15 µl of PCR mix reagent and 10 µl of 100 ng of cDNA. The contents of the 15 µl of PCR mix reagent were prepared in following composition: 11.25 µL of Roche PCR Master Mix (1X), 0.075 µL forward primer (100 µM), 0.075 µL reverse primer (100 µM), 0.05 µL TaqMan probe (100 µM) and 3.55 µL of

DEPC water. In the case of 20X master-mix assays bought from Thermo-Fischer, 0.2 µL of the master mix was used as it contained forward primer, reverse primer and probe as a mix. The 96-well plate was tightly sealed with PCR sealing film and tapped to mix the reagents, then centrifuged for 10-15 sec to spin down the reagents. The experiment conditions were 50°C for 2 min (stage 1), denaturing at 95°C for 10 min (stage 2), denaturing at 95°C for 15 sec and annealing at 60°C for 1 min (stage 3, 50 cycles). Cyclophilin was used as house-keeping gene for normalization.

3.4 Immunoblotting for protein analysis

Reagents:

Anti-Lamin A/C (sc-20681) was purchased from Santa Cruz Biotechnology (Santa Cruz, CA). Anti-JNK (#9252) and anti-phospho-JNK (#9251) were purchased from Cell-Signaling (Beverly, MA, USA). Anti-PXR (#PA5-19080) was purchased from Thermo Scientific (Waltham, MA). Homogenization buffer comprising each of 50 mM Tris HCl, 0.5 M NaCl, 2 mM EDTA, 2 mM EGTA, 1% Triton X-100 (X-100; Sigma-Aldrich) and 0.25% deoxycholate, 1 mM sodium fluoride (NaF) (S7920; Sigma-Aldrich), 1 mM sodium vanadate (Na3VO4) (S6508; Sigma-Aldrich), 2 mM of DTT and 100 µL of protease inhibitor cocktail solution per 10 ml of homogenization buffer.

Method:

Preparation of gel: 10% separating gel was first prepared by mixing the following components in a small beaker: 5 ml of 40% acrylamine, 5.2 ml of 1.5 M TB buffer (pH= 8.8), 9.6 ml distilled water, 0.2 ml of 10% SDS, 0.2 ml of 10% APS and 20 µl TEMED. A

10 ml syringe was used to mix all the ingredients together and pour the mix in the gel forming cassette. Using 1 ml pipette, distilled water was added over the mix from one corner in the cassette to prevent the gel from drying. Gel was kept aside to set for ~30 minutes. After 30 mins, water was removed by slightly tilting the cassette and 4% stacking gel was prepared on top by mixing the following components in a beaker and then pouring over the separating gel: 3.8 ml of distilled water, 1.5 ml of 0.5 M TB buffer (pH= 6.8), 0.6 ml of 40% acrylamine, 60 µl of 10% SDS, 30 µl of 10% APS and 6 µl of TEMED.

Immunoblotting analysis was used to determine the protein expression in nuclear extracts or whole cell extracts from HepG2 cells and extracts from mouse livers. Lamin A/C was used as a loading control or as a housekeeping gene for all the nuclear extracts, JNK was used as a control for whole cell extracts and VDAC was used as control for extracts from mouse liver. After determination of protein concentration by BCA assay, the samples were diluted with homogenization buffer. The samples were diluted so as to load at least 10 µg of protein per well in the gel. Then 6X loading dye was added to all the samples in the ratio 4 (sample): 1 (dye). After dilution of the samples with the buffer and dye, the tubes were tightly capped and gently vortexed. The protein samples were then briefly vortexed, spun down and then heated at 90-95°C in a heating block. By this time, the gels, prepared the previous day, were loaded into the chambers to check any leakage of the buffer. After 10 min, the samples were cooled on ice for 10 more min and then spun down for 10 seconds again. The first well of the gel was loaded with 5 µL of protein Fisher-EZ run Pre stained Rec protein ladder (Fisher Scientific, Cat # BP 3603-500) which

consists of a mixture of different proteins with varying molecular weights. Then 10 µL of samples were loaded into the respective wells and the gel was run at 70V electrophoretically on an electrophoresis chamber (Bio-Rad, Hercules, CA, USA) for about 30 minutes followed by running at 150V for 60- 70 minutes. After the run, the gels were transferred onto the nitrocellulose membranes as a sandwich consisting of this sequence: 1 wet sponge, 1 sheet of 3 mm wet paper, 1 pre-wet nitrocellulose membrane, gel, 1 sheet of 3 mm wet paper and then the wet sponge again. Care was taken to avoid any air bubbles in this step. The gel was set up for transfer in the transferring buffer with continuous stirring at 250 mAmp for 90 min at 4°C. After this, the membranes were removed and blocked in a 5% non-fat dry milk (NFDM) solution for 60 minutes on a horizontal shaker to avoid any non-specific binding. Then the membranes were washed 2 times in Tris-buffered saline containing 0.1% Tween-20 (TBST) for 5 min each. The membranes were then incubated overnight at 4°C with the anti-Cyp3a11, anti-VDAC, anti-PXR, anti-Lamin A/C, anti-JNK or anti-P-JNK antibodies in 50 ml conical tubes consisting of 5 ml of 5% bovine serum albumin (BSA, Sigma Aldrich, St. Louis, MO, Cat # A3059) solution prepared in TBST. Following day, the membranes were washed thrice with TBST for 10 minutes each followed by incubation with the goat anti-rabbit IgG-alkaline phosphatase secondary antibody (Santa Cruz Biotechnology Inc., Santa Cruz, CA, Cat # sc-2007) at a dilution of 1:5000 in 5% NFDM for 2 h at room temperature with continuous shaking. Then the membranes were washed for the final 3 times with TBST and incubated with an electro chemiluminescence reagent (~ 1 ml of reagent was added per membrane) for 10 min

covered in dark (I use a box cover and turn off the lights in that lab to protect my membranes from exposure to light). The bands were then analyzed on a FluorChem FC2 Imaging System with chemiluminescence filter initially for 2 min. Depending on the intensity of the bands, exposure time was changed accordingly.

3.5 Cyp3a11 activity assay

Reagents:

Midazolam (MDZ) (Cat # 451028) was purchased from BD Biosciences (San Diego, CA, USA). The Glucose-6-phosphate (Cat # G6378-500UN), MgCl2 (Cat # 208337), glucose-6-phosphate dehydrogenase (Cat # G6378-2KU) and NADP+ (Cat # N0505) were purchased from Sigma-Aldrich, St. Louis, MO. Phenacetin (Cat # 77440) and 1'-hydroxymidazolam (Cat # UC430) were purchased from Sigma Aldrich (St. Louis, MO, USA). Regenerating system solution contained: 3.3 mM of Glucose-6-phosphate, 3.3 mM of MgCl2 and 1.3 mM of NADP+.

Method:

Typical Phase I reactions were carried out in liver microsomes using MDZ as a Cyp3a specific probe substrate. For determining Cyp3a11 activity, 0.05 mg/ml of microsomal protein was incubated with various concentrations of MDZ (0-16 μM). The reaction mixture consisted of 50 mM KPi solution (pH 7.4), 25 μL of regenerating system solution, 10 μL of MDZ stock solutions (25 fold concentrated) and 0.05 mg/ml of final microsomal protein concentration. The reactions were carried out in duplicate and the reaction mixtures were placed in an ice water bath all the time. The reactions were initiated by adding 25 μL

of 100 units/ml of glucose-6-phosphate dehydrogenase solution to get a final concentration of 1 unit/ml in the reaction mixture. The volume of KPi solution was adjusted according to the microsome concentration for which the volume was fixed at 25 μL. The tubes were tightly capped and reversed upside-down to mix the solution properly. The tubes were then incubated for 5 min at 37°C in a shaking water bath (35-40 horizontal oscillations per min). After 5 min, the reactions were stopped by the adding 100 μL of 100% acetonitrile containing phenacetin which was the internal standard (IS, 1 μg/ml).

3.6 Microarray Analysis

Reagents:

Gene Expression MouseWG-6 v2.0 Expression BeadChip Kit (#BD-201-0202) was purchased from Illumina, San Diego, CA.

Methods:

250 ng of total RNA was reverse transcribed, and microarray hybridization performed using the Illumina Gene Expression MouseWG-6 v2.0 Expression BeadChip Kit at the Laboratory for Translational Genomics at Baylor College of Medicine. The transcriptome profile data was quartile-normalized by the Bioconductor lumi package. The Lumi package implemented in the R statistical software, version 2.14.1, was used to perform quality control of the signal intensity data on the transcript probes, background adjustment, variance stabilization transformation, and rank invariant normalization. A detection p value cutoff of 0.01 was required for the normalized intensities to consider a transcript as detected. Differentially Expressed Genes (DEG) were selected following the t-test

comparisons among groups of interest, using the R statistical system. The genes were considered to be differentially expressed for p-value<0.05 and fold change greater than or equal to 1.25x or less than or equal to 0.8x. A graphical representation of the DEGs was generated in the form of heatmaps of mean-centered normalized expression values (z-scores), employing the Euclidean distance metric and the average clustering method, using R statistical software.

3.7 Gene Set Enrichment Analysis

A rank file for each comparison was created based on the log2 fold change of each gene between the respective comparison groups. We next employed the Gene Set Enrichment Analysis (GSEA) methodology and software (Subramanian et al, 2005), against the Molecular Signature database (MSigDB) compendium (Liberzon et al, 2011) of gene sets. Gene Set Enrichment Analysis first finds an aggregate gene set score (termed enrichment score/ES) then runs 1000 permutations to establish a background distribution for ES. The ratio between ES and the average ES is termed Normalized Enrichment Score (NES). GSEA determines whether a key component of a pathway or biological process gene set is significantly and preferentially enriched in up-regulated genes (NES>0, fdr-adjusted Q-value<0.25) or in down-regulated genes (NES <0, fdr-adjusted Q-value <0.25). An established and fertile paradigm for hypothesis generation is that if the NES for a pathway in comparisons stemming from two different treatments are significant but having opposite signs, then the treatments might direct the pathways in opposite directions. The pathway collections KEGG, Reactome, Hallmark, and GOBP (Gene Ontology Biological

Processes) were used to determine enriched pathways. We also used a compendium of putative transcription factors to identify enriched transcription factors targets in the transcriptome footprints analyzed. TransFac Analysis was employed to identify the list of transcription factors which might bind to Cyp3a11 or CYP3A4 promoter regions.

3.8 *In vitro* HepG2 study

3.8.1 HepG2 cell culture

Reagents:

Dulbecco's modified Eagle's medium (Life Technologies, Carlsbad, CA), Fetal bovine serum (Atlanta Biologicals, Flowery Branch, GA), Penicillin-streptomycin (Invitrogen), Trypsin-EDTA (Invitrogen # 25200-056)

Method:

For thawing cells: For seeding cells from a fresh/frozen vial, the vial was thawed in a 37^{o}C water bath and the contents transferred to a 50 ml tube containing 5 ml Dulbecco's modified Eagle's medium (Life Technologies, Carlsbad, CA) supplemented with 10% fetal bovine serum and 1% penicillin-streptomycin. The cells were then centrifuged at 7000 RPM for 5 minutes. The supernatant was carefully aspirated without touching the cell pellet. Cells were suspended in 2 ml fresh medium and homogenously mixed by pipetting gently. Cells were counted using hemocytometer and then diluted according to required concentration. Finally, excess cells were seeded in a 10 cm plate to continue the passage of cells. Plates were incubated at 37^{o}C and 5% CO_2.

For passaging cells: After seeding the cells in a 10 cm plate, media was replaced every 24 hours to maintain proper morphology and provide nourishment to the cells. Upon reaching ~80-90 % confluency, cells were passaged into new plates. For passaging, cells were washed once with 1X PBS and then uplifted by adding 2ml Trypsin-EDTA to the plates. The plates were placed in the incubator for 5 minutes. Finally 3 ml fresh DMEM medium was added to the plate and cells were transferred to a 50 ml tube. The cells were then centrifuged at 7000 RPM for 5 minutes and similar protocol was followed as above to seed the cells.

For freezing cells: Cells were lifted from 10cm plates using Trypsin as mentioned before. The difference is that after centrifugation, cell were re-suspended in DMEM medium containing 20% FBS and 10% DMSO. 1ml freezing medium per cryovial was aliquoted. Immediately frozen cryovial in -80 degrees refrigerator. The vials were transferred to liquid nitrogen cylinder next day. (Try to use cells which have been seeded 24 hours before as the percentage viability is higher upon thawing).

3.9 Plasmid Preparation

3.9.1 Plasmid Description

CYP3A4 Plasmid

p-CYP3A4-pGL3B (-7836/7208ins) luciferase reporter plasmid was obtained as a kind gift from Dr. Rommel G. Tirona, The University of Western Ontario, London, Ontario, Canada. It was prepared as follows (Zhang et al, 2001):

The CYP3A4 proximal promoter region (-1084/+53) was amplified from genomic DNA by long PCR (Expand Long Template PCR System, Roche) using primers described by Goodwin et al. (5'-CATGGATCCTGTTGCTCTTTGCTGGGCTATGTGC-3' and 5'-CATTGCTGGCTGAGGTGGTT-3'). The PCR product was digested with BglII and BamHI and the (-362/+53) fragment was retrieved by gel cleaning (Qiaex II, Qiagen Inc., Valencia, CA, USA) and then cloned into the BglII site in pGL3B (Promega). The CYP3A4 distal xenobiotic response element (PXRE) (-7836/-7208) was amplified from genomic DNA by PCR (AmpliTaq, Roche) using primers 5'-TATTCTAGAGAGATGGTTCAT-3' and 5'-TCTAGATCTCGTCAACAGGTT-3'. The distal PXRE PCR product was initially cloned into pCR2.1-TOPO (Invitrogen, San Diego, CA, USA) and a clone with the insert in the desired orientation was defined by SpeI digest. The distal PXRE insert was then directionally subcloned into the KpnI and XhoI sites in CYP3A4 (-362/+53)/pGL3B vector and the resultant promoter construct [p3A4-362 (-7836/-7208ins)] was sequence verified.

PXR plasmid

h-PXR-pSG5 plasmid was obtained as a kind gift from Dr. Steven Kliewer, UT Southwestern Medical Center, Dallas, Texas, United States. The expression vector pSG5-hPXR was generated by PCR amplification and subcloning of nucleotides 1–1608 of the hPXR clone into the pSG5 expression vector (Stratagene, La Jolla, CA). pSG5-hPXRΔATG was generated by PCR amplification of cDNA encoding amino acids 1–434 of hPXR using oligonucleotides 5'-GGGTGTGGGGAATTCACCACCATGGAGGTGAGACCCAAAGAAAGC-3' (sense)

and 5’-GGGTGTGGGGGATCCTCAGCTACCTGTGATGCCG-3’ (antisense) and insertion into Eco RI/Bam HI– cut pSG5 (Lehmann et al, 1998).

3.9.2 DNA recovery from Whatman paper

Reagents:

10mM Tris buffer (pH= 7.6)

Method:

To recover DNA plasmids from filter paper, a piece of filter paper containing the plasmid was cut and transferred to a microcentrifuge tube. 200 µL Tris buffer was added, briefly vortexed and the set aside to rehydrate for 5 minutes. After 5 minutes, the tube was vortexed for 30 seconds and 5 µL supernatant was used to transform competent bacterial cells.

3.9.3 Bacterial Transformation

Reagents

MAX Efficiency® DH5α Competent Cells, Life Technologies 18258-012, S.O.C. medium (included in the DH5α Kit), Ampicillin powder, 50 ml filter or syringe filter, LB agar, Sterile round-bottom 10-15 ml tube for bacterial culture (or any centrifuge tube), Bunsen burner, 42°C water bath, 37°C baterial culture shaker, 37°C baterial incubator.

Method

100 mg/ml ampicillin was prepared in water and filtered. It was aliquoted and stored -20°C. Lysogeny broth agar mixture was prepared and autoclaved. When the agar cooled down to about 60°C, 100 µg/ml ampicillin was added and agar was poured in 10 cm petri dishes at 25-30 ml/dish (the ampicillin-agar plate can be stored in a bag at 4°C for 1-2 months).

DH5α competent cells were thawed on ice (~3-5 mins.). Now, 5 µL plasmid which was recovered from filter paper was added to 10 µl of DH5α in a sterile round-bottom 10-15 ml tube, and incubated on ice for 30 min. The tube was immersed in 42°C water bath for 45 sec. and incubated on ice for 2 min. 20 vol of SOC medium was then added, and shaken at 200 rpm in the 37°C baterial culture shaker for 1 h. The bacteria were scraped on pre-warmed agar plate, and incubated at 37°C baterial incubator for 16 h or longer. The following day, lots of colonies of bacteria will be seen on the plate.

3.9.4 Midi Prep DNA Preparation

Reagents

QIAGEN Plasmid Midi Kit (cat. nos. 12143), Lysogeny Broth Agar (containing 10g tryptone, 5g yeast extract, 10g NaCl and 15g agar)

Method

One of the bacterial colony after transformation was selected and transferred to a conical flask containing 25 ml Lysogeny agar. The flask was shaken overnight at 37 degrees. Midi prep plasmid preparation was then carried out according to manufacturer's instructions (Qiagen, #12143). The overnight bacterial culture was transferred into two 50 ml tubes and centrifuged at 6000 g for 15 min at 4°C (Make sure both tubes weigh equally). The bacterial pellet was resuspended in 4 ml Buffer P1. 4 ml Buffer P2 was added, mixed thoroughly by vigorously inverting 4–6 times, and incubated at room temperature (15–25°C) for 5 min. (If using LyseBlue reagent, the solution will turn blue). Next, 4 ml prechilled Buffer P3 was added, mixed thoroughly by vigorously inverting 4–6 times. Incubated on ice for 15

min 20 min (If using LyseBlue reagent, mix the solution until it is colorless). Centrifuged at ≥20,000 x g for 30 min at 4°C. In the meantime, a QIAGEN-tip 100 was equilibrated by applying 4 ml Buffer QBT, and column was allowed to empty by gravity flow. The supernatant from previous step was then added to the QIAGEN-tip and it was allowed to enter the resin by gravity flow. The QIAGEN-tip was washed with 10 ml Buffer QC two times. Plasmid DNA was then eluted with 5 ml Buffer QF into a clean 15 ml tube. DNA was precipitated by adding 3.5 ml room-temperature isopropanol to the eluted DNA and mixed. Centrifuged at ≥15,000 x g for 30 min at 4°C. The supernatant was carefully decanted. The DNA pellet was washed with 2 ml room-temperature 70% ethanol and centrifuged at ≥15,000 x g for 10 min. The supernatant was carefully decanted again and pellet was air-dried for 5–10 min and re-dissolved in 1 ml of TE buffer (pH 8.0). The concentration of plasmid was then calculated by measuring absorption at 280 and 260 nm using a Nanodrop Spectrophotometer.

3.10 Transient transfection of HepG2 cells

Reagents

p-CYP3A4-pGL3B luciferase plasmid was obtained as a kind gift from Dr. Rommel G. Tirona, The University of Western Ontario, London, Ontario, Canada. h-PXR-pSG5 plasmid was obtained as a kind gift from Dr. Steven Kliewer, UT Southwestern Medical Center, Dallas, Texas, United States. A custom siRNA sequence (AGAAUGUCCUACCUUCUUUUU) that simultaneously targets JNK1 and JNK2 and a control siRNA targeting luciferase were both synthesized by Dharmacon (Lafayette, CO).

DharmaFECT Duo Transfection reagent was also purchased from Dharmacon. SuperFect Transfection Reagent was purchased from Qiagen (Valencia, CA, #301305).

Method

Following protocol is for transient transfection of HepG2 cells in a 96 well plate. The quantities mentioned below represent the amount needed for 1 well. The day before transfection, 1 * 10^4 cells/well were seeded in 100 µl Growth Medium. Cells were incubated at 37^0C and 5% CO_2 [The optimal confluency at the time of transfection-complex addition is 40-80% (0.5-2.0 * 104 cells/well), although it is preferable to seed less cells (~50% confluency). High cell density leads to insufficient uptake of transfection complexes thereby showing decreased expression of gene of interest. Moreover, overgrown cultures are often more resistant to complete lysis by passive lysis buffer]. After 24 hours i.e. the day of transfection, 2.5 µl of Superfect transfection reagent was diluted in 30µl Serum free medium (14. It is important to use serum free media as FBS and antibiotics present during this step interfere with complex formation and decrease transfection efficiency). All plasmid DNAs (pCYP3A4-pGL3B, hPXR-pSG5 and pRL-TK) were added such that total DNA per well is 0.5 µg (Trans effects- When cells are co-transfected with firefly and Renilla vectors, they can potentially affect each other's reporter gene expression especially if one or both contain very strong promoter elements. Therefore, it is necessary to first optimize both the amount of experimental plasmid (Luciferase plasmid) and the co-reporter plasmid (Renilla plasmid). Ratio of 10:1 or 5:1 for Firefly: Renilla vector is usually feasible). The mix was vortexed for 10 seconds and incubated for

10 minutes at room temperature. During that time, growth medium was gently aspirated from the 96 well plate. After 10 minutes, 150 µl growth medium was added to the cocktail mix. Mixed by inverting the tube three times and immediately transferred to 96 well plate. Cells were incubated with transfection complexes for 5 hours (Incubation with Superfect-DNA complexes for 3-5 hours yields optimal results. Although if excessive cell death is observed, decrease the exposure time). After 5 hours, medium containing the remaining complexes was removed from the cells by gentle aspiration. Cells were washed once with 100 µl PBS and 100 µl fresh cell growth medium/ well was added. Cells were incubated for 24 hours after transfection to obtain maximal levels of gene expression.

For siRNA and plasmid co-transfection, HepG2 cells were transfected with CYP3A4, hPXR, pRL-TK vector and JNK siRNA using DharmaFect Duo reagent. A custom siRNA sequence targeting JNK 1 & JNK2 simultaneously and a control siRNA targeting luciferase were used for these experiments.

3.11 Dual-Glo Luciferase Assays

Reagents

1X Phosphate buffer saline (PBS) without Ca/Mg, 500ml (VWR; 16777-251), Dual Luciferase Reporter Assay System (Promega, E1910), VWR Microplate Shaker, SpectraMax Microplate Reader/ Luminometer

Method

After treatment of HepG2 cells, luciferase assays were carried out. Growth medium containing treatments was gently aspirated from cultured cells. 100 µl PBS was added to

wash the cells once. The plate was briefly swirled to remove detached cells and residual growth medium. PBS was .completely removed from the wells. 20 µl 1X Passive Lysis Buffer was then added and the plate was placed on a shaker/rocker with gentle shaking for 15 minutes at room temperature (Ensure cell monolayer is evenly covered with 1X Passive Lysis Buffer for complete lysis). While the plate was on the shaker, the luminometer was setup to record the luminescence reading. 100 µl Luciferase Assay Reagent II (LAR II) was added directly to wells using Multi channel pipette. The plate was gently tapped to mix the reagent and immediately measured firefly luciferase activity (Never thaw LAR II in water bath as it is heat-labile. Thaw at room temperature and mix before use). 100 µl 1X Stop and Glo Reagent was added next directly to wells using multi-channel pipette. Again, tapped and immediately measured Renilla Luciferase activity (Firefly luciferase and Renilla activity readings should be at least 10 times the baseline reading).

3.12 P450-Glo Assays

Reagents

P450-Glo™ Assay Kit (Promega, # V9002)

Method

HepG2 and HepaRG cells were cultured on white-walled, collagen-coated culture plates. After treatment, cells were lysed and luciferase enzymatic activity was measured using a P450-Glo™ commercial kit as per the manufacturer's protocol (Promega, # V9002). Specific CYP3A4 luminogenic substrate, luciferin-IPA, was added to the wells at a concentration of 3 µM and incubated at 37^{o}C for 60 minutes. Light emission from the

samples was detected by SpectraMax Microplate Reader/ Luminometer and expressed as Relative Light Units.

3.13 Preparation of whole cell extracts

Reagents

All reagents were purchased from Sigma-Aldrich. Sodium fluoride (NaF) (Cat # S7920), Sodium vanadate (Na3VO4) (Cat # S6508), EDTA (Cat # 6381-92-6), EGTA (Cat # E8145), Sodium Deoxycholate (Cat # 302-95-4), Triton X-100 (Cat # 9002-93-1), TRIS (Base) (Cat # 77-86-1), Dithiothreitol (DTT) (Cat # D9779).

Method

The whole cell extracts were prepared from (i) liver tissues by homogenizing ~0.1 g of mouse liver tissue in 1 mL of homogenization buffer or (ii) from hepatocytes by adding 200 μL/well (6-well plate) of buffer, followed by scraping with cell scraper & pipetting ~10 times rigorously. The homogenization buffer consisted of 50 mM Tris HCl (pH 7.5), 0.5M NaCl, 2 mM EDTA, 2 mM EGTA, 1% Triton X-100, and 0.25% deoxycholate. The homogenization buffer was supplemented with 1 mM NaF, 1 mM Na3VO4 and 2 mM DTT just before use. Addition of protease inhibitors like PMSF to homogenization buffer during preparation of cell extracts was avoided as these compounds are mechanism based inhibitors and will inhibit CES enzymes. The liver suspended in buffer was placed in glass homogenizing tubes and minced with few strokes (~20) of dounce A and B. The homogenates were centrifuged at 9,000 rpm/15 min/ 4°C. The supernatants were collected

and stored in aliquots in -80°C. The protein concentrations were determined by bicinchoninic acid (BCA) assay.

3.14 Preparation of nuclear and cytosolic extracts

Reagents

Hypotonic buffer consisted of 10mM HEPES, pH 7.5, 1.5 mM MgCl2, 10 mM KCL, 0.5 mM DTT and 10 μL/mL of protease inhibitor cocktail (P8340; Sigma-Aldrich). Lysis buffer contained 140 mM NaCl, 2 mM EDTA, 1 % NP-40, 50 mM Tris-HCL, pH 7.2 and 10 μL/mL protease inhibitor.

Method

To prepare nuclear and cytosolic extracts from liver cells, a 6-well plate was placed on top of packed ice. The media was quickly aspirated. Then, the plate was washed two times with 1 mL of cold PBS. Ice-cold PBS was added once and swirled gently. PBS was aspirated off and the washing was repeated. 350 μL of hypotonic buffer was added to each well. The cells were then scraped with a cell scraper and transferred to glass homogenizers and then were dounce homogenized (10 strokes of dounce A followed by 10 strokes of dounce B). The solutions were transferred to Eppendorf tubes and spun for 5 minutes at 5000 rpm and 4°C. Pellet was stored and the supernatant was transferred and respun in the same conditions. This time, a smaller pellet will be seen. Collect the supernatant and store in -80°C as cytosolic extracts. 100 μL of lysis buffer was added to the eppendorf tube with the smaller pellet. The contents of that tube were mixed and transferred to the tube containing the bigger pellet. Lysis was done by pipetting up and down ~15 times using P-

1000 pipet. After incubating on ice for 30 min and centrifuging at maximum speed for 5 min the supernatents were collected and stored as nuclear fractions. Protein concentration was determined using the BCA assay.

3.15 BCA Assay for protein quantification

Materials/Reagents

Pierce® BCA protein assay kit (Thermo Scientific, Rockford, IL, Cat # 23225), Albumin (BSA), 96-well flat bottom plate (Corning™ 3585), Biotek plate reader (Biotek, Winooski, VT, USA).

Method

BCA assay was performed in 96-well clear bottom plate using Pierce® BCA protein assay kit. Albumin (BSA) standards were prepared from the stock of 2 mg/ml to get final concentrations of 0.1, 0.2, 0.4, 0.6, and 0.8 mg/ml. Samples were diluted to 10 to 40 times with dd water. The working reagent was prepared by mixing 50 parts of solution A with 1 part of solution B as per the manufacturer's recommendation. In each well, 20 µL of diluted sample or standards were added and reaction was initiated by adding 180 µL of working reagent. The plate was then covered with aluminum foil and incubated for 30 min at 37^{o}C in an incubator. The absorbance was read at 570 nm wavelength on Biotek plate reader. Standard curve was prepared by plotting the average O.D for each BSA standard vs. its concentration in µg/mL and was used to determine the protein concentration of each unknown sample.

3.16 Chromatin Immunoprecipitation Assays

Reagents

Magna ChIP™ HiSens Chromatin Immunoprecipitation Kit (EMD Millipore Inc., #17-10460), PXR antibody was purchased from Santa Cruz (#SC-25381X).

Method

ChIP assays were performed to assess specific binding of PXR complex to the PXR response element on the *CYP3A4* promoter as described in the manufacturer's protocol (EMD Millipore Inc., #17-10460). HepG2 cells were pre-treated with SP (30 μM) or DMSO for 30 minutes, followed by RIF (10 μM) for 24 hours. The cells were then cross-linked with 37% formaldehyde at room temperature for 10 min., washed twice with ice-cold phosphate-buffered saline (PBS) and collected in 1 ml of ice-cold PBS. Cells were pelleted at 800*g* and digested by sonication (15 pulses, 20 sec each, 30 sec. rest in between). The protein-DNA complexes were immunoprecipitated by using ChIP grade anti-PXR antibody. As a negative control, the beads were incubated with lysates without anti-PXR antibody. The chromatin was reverse cross-linked and eluted in 50 μl elution buffer. DNA recovered from this assay was analyzed by end point PCR using primers for PXR binding site in the *CYP3A4* promoter region (forward 5'-AGAACCCAGAACCCTTGGAC-3' and reverse 5'-CTGCCTGCAGTTGGAAGAG-3'). PCR products were analyzed by agarose gel electrophoresis. 10% of the total cell lysate was used as "input". Eluted DNA was further analyzed by real time PCR using same primer mix as mentioned above. ΔΔCt method was used to analyze the difference in fold value in treated vs control groups.

3.17 Pharmacokinetic studies

3.17.1 LC-MS conditions

Materials/Reagents

Irinotecan, camptothecin (CPT), Glacial acetic acid (GAA) and formic acid (FA) were purchased from Sigma–Aldrich (St. Louis, MO, USA). SN-38 and SN-38G were donation from Dr. Ming Hu. Acetonitrile, methanol and water (LC–MS grade) were purchased from EMD (Gibbstown, NJ, USA). Water was deionized by a Milli-Q water purification system of Millipore (Bedford, MA, USA). Acquity UPLC BEH C18 Column (2.1 mm × 50 mm, 300◦A, 1.7 m) from Waters, Milford, MA, USA.

Method

The chromatographic separation was achieved on Acquity UPLC BEH C18 Column. Mobile phase A (0.1% formic acid in water) and phase B (100% acetonitrile) were run as gradient method as follows: 10% B→25% B (0–0.5 min), 25% B→40% B (0.5–1 min), 40% B (1–2.5 min), 40% B→10% B (2.5–4.5 min). The flow-rate was set at 0.4 ml/min, and the column temperature was maintained at 45 °C. Sample injection volume was 10 μL. After chromatographic separation, LC–MS/MS analysis for irinotecan, SN-38, SN-38G and CPT (IS) were performed with API 5500 Qtrap triple quadruple mass spectrometer coupled with a Turbo Ion SprayTM (Applied Biosystem MDS SCIEX, Framingham, MA, USA). The mobile phase was directly introduced into the mass spectrometer via an electrospray ionization (ESI) source operating in the positive mode. Quantification was performed using multiple reaction monitoring (MRM) with following m/z transition transitions: m/z 587.1→124.1 for irinotecan; m/z 393.1→349.1 for SN-38; m/z

569.5→393.1 for SN-38G; m/z 349.0→305.1 for CPT (internal standard, I.S.). The selection of the fragment ions depended on the highest intensity of the fragment. All data were acquired and processed using Analyst®1.5.2 software (AB Sciex, USA).

In order to optimize all the MS parameters, 0.1 μg/ml of the analytes were infused into the mass spectrometer. Some mass spectrometer parameters were identical for all analyte. The curtain gas reached 35 psi. The ionspray voltage was set at 5000 V and the temperature at 550 °C. The nebulizer gas (GS1) and turbo gas (GS2) were 55 and 45 psi. The declustering potential (DP), entrance potential (EP), collision energy (CE) and collision cell exit potential (CXP) were optimized for each analyte (Table.3.8) [The DP were set at 141, 91, 90 and 86 V for irinotecan, SN-38, SN-38G and CPT, respectively. The values of the CE were 57, 38, 40 and 35 V for irinotecan, SN-38, SN-38G and CPT, respectively. The CXP were 8, 8, 7 and 6 V for irinotecan, SN-38, SN-38G and CPT, respectively].

3.17.2 Sample Preparation

Extraction of analytes from whole blood were prepared by precipitation method with 4-10 volumes of organic solvent (50% acetonitrile prepared in water and acidified to 1% by GAA.) For fecal homogenate, 15 volume of acetonitrile was used. Into 1.5 ml centrifuge tube, 25 μL of samples or standard solutions were aliquoted and spiked with 15 μL of IS (0.5 mg/ml of CPT prepared in 94% acetonitrile in methanol and 6% glacial acetic acid) followed by precipitation with 100 to 200 μL of 50% acetonitrile in methanol (1:1). The precipitates were centrifuged at 13000 rpm for 10min. The supernatant was dried under air,

reconstituted with 100 to 250 μL of acidified 50% acetonitrile in water (1:1) and 10 μl of solution was injected into the UPLC–MS /MS system. The prepared samples were kept in an autosampler at 4°C until injection.

3.17.3 Preparation of standard curve

Stock solutions of irinotecan, SN-38 and SN-38G were prepared in DMSO at the concentration of 10 μM. Stock solution of I.S. was prepared in 94% acetonitrile in methanol and 6% glacial acetic acid at 0.5 mg/ml concentration. Calibration curves were prepared by spiking the appropriate standard solution in 25 μL of vehicle treated samples. Effective concentrations of standard samples ranged from 0.006 to 0.2 μM for irinotecan and SN-38G and 0.078 to 5 μM for SN-38. The linearity of each calibration curve was determined by plotting the ratio of the peak areas of analytes to internal standard (CPT). A least-square linear regression method ($1/x^2$ weight) was used to determine the slope, intercept and correlation coefficient of linear regression method. The lower limit of quantification (LLOQ) was determined based on the signal-to-noise ratio of at least 10:1.

3.17.4 Pharmacokinetic Analysis

For quantification of analytes in plasma, LC-MS/MS method was utilized. In order to quantitate CPT-11, SN-38, SN-38G and CPT in plasma an API 5500 Qtrap triple quadrapole mass spectrophotometer (Applied Biosystems/MDS SCIEX, Foster City, CA, USA) equipped with a Turbospray TM source was used by multiple reaction monitoring (MRM) method operated in a positive ion mode. The optimization of the LC-MS/MS conditions for analysis of irinotecan and its metabolites was performed as follows. The m/z

transition for irinotecan was 587.1/124.1, m/z transition for SN-38 was 393.1/349.1, m/z transition for SN-38G was 569.5/393.1, m/z for CPT was 349.0/305.1 in positive ion mode. The instrument dependent and compound dependent parameters for all the compounds were optimized as described. The following compound dependent parameters were optimized: declustering potential (DP), entrance potential (EP), cell exit potential (CXP) and the collision energy (CE). The following instrument dependent parameters were optimized for the compounds: ion spray voltage, ion source temperature, nebulizer gas (gas 1), turbo gas (gas 2) and the curtain gas. The flow rate of the sample during Mass method optimization was set between 7 - 20 μL/min. The UPLC conditions for the compounds were: system, Waters Acquity™ (Milford, MA, USA) with DAD detector; column, Acquity UPLC BEH C18 column (50×2.1mm I.D., 1.7μm, Waters); mobile phase A, 0.1% formic acid; mobile phase B, 100%, acetonitrile; gradient, 0-0.5 min, 10% B, 0.5-1 min, 25% B, 1-2 min, 40% B, 2-2.5 min, held constant at 40% B, 2.5-3 min, 10% B, respectively. Flow rate was 0.4 ml/min, column temperature, 45 degree; injection volume, 10 μL.

The PK data was analyzed using the WinNonlin 3.3 PK modeling software from Pharsight Corporation (Mountain View, California). The data was fitted to a non-compartmental model for pharmacokinetic analysis of CPT-11 and its metabolites. Pharmacokinetic parameters, including maximum plasma concentration (Cmax), time to reach Cmax (Tmax), elimination rate constant (ke), half-life (t1/2), rate at which drug is cleared from the body (CL), volume of distribution (Vd) and plasma exposure or area under the curve (AUC) were directly derived from WinNonlin.

Chapter 4

Genomic profiling to identify novel mechanisms of transcriptional regulation of Cytochrome P450 3a enzyme

4.1 Abstract

Cytochrome P450 (CYP) 3A4 is the most abundant enzyme in the human liver; metabolizing ~60% of known drugs. Impairment in CYP3A4 metabolism leads to unanticipated adverse reactions or therapeutic failures; culminating in early termination of drug development or withdrawal of drugs from the market. The role of key regulators (i.e. transcription factors (TFs), epigenetic modulators, cell signaling pathways etc.) in transcriptional up or down-regulation of *CYP3A4* is not fully understood and needs further investigation. We performed a comprehensive genome-wide mapping and bioinformatics analysis using DNA microarray in a mouse model of CYP3A induction (using potent PXR activator pregnenolone-16alpha-carbonitrile [PCN]) followed by down-regulation using lipopolysaccharide (LPS) (bacterial endotoxin which induces cytokines that suppresses *CYP3A* levels). The objective of our study was to identify novel changes in opposite directions in TFs, epigenetic modulators, pathways etc. by PCN and LPS in mouse liver. We found that 114 genes were significantly upregulated (UR) (~5 folds) with PCN and 834 genes were significantly downregulated (DR) (~5 folds) with LPS as compared to control. With combined LPS and PCN treatment, 1896 genes were differentially expressed (UR: 1075, DR: 821) as compared to control. We identified 514 TFs, altered by PCN and LPS in opposite directions, and among these, 285 were found to have binding sites on Cyp3a11 (mouse homolog of CYP3A4). In silico analysis revealed that repressed targets of epigenetic markers such as HDAC1, HDAC3 and EZH2 were further suppressed by LPS and induced by PCN in our study. Therefore, novel regulators that are potentially involved

in both up-regulation & down-regulation of CYP3A4 were identified. Ultimately, characterization of these regulators will lead to the development of targeted strategies to treat disorders due to impaired drug metabolism.

4.2 Introduction

Cytochrome P450 3A (CYP3A) is the most abundant family of drug metabolizing enzymes (DMEs), responsible for the disposition of more than 50% of currently prescribed drugs (Guengerich, 1999; Veith et al, 2009; Wilkinson et al, 2005, Zanger et al, 2013). A review of 121 new molecular entities (NMEs), approved by FDA during 2003 and 2008, indicated that CYP3A was the main CYP enzyme involved in the disposition of these NMEs (Zhang et al, 2009). Clinical importance of CYP3A can be assessed from numerous reports which show that down-regulation of *CYP3A* expression/activity in diseases leads to failure of therapy and/or potentially harmful adverse drug reactions (Lynch et al, 2007; Palleria et al, 2013). For example, ketoconazole (a strong CYP3A inhibitor) treatment increased the AUC and Cmax of romidepsin by ~25% and 10% respectively in patients with advanced cancer (Laille et al, 2015). Romidepsin, a CYP3A substrate, is indicated for the treatment of cutaneous T-cell lymphoma and its increased plasma concentrations lead to thrombocytopenia. Similarly, treatment with an anti-fungal agent and a CYP3A4 inhibitor drug voriconazole enhanced the AUC for oxycodone, an opioid receptor agonist, resulting in increased toxicity of oxycodone in cancer patients (Watanabe et al, 2011). On the other hand, a clinically relevant decrease was observed in faldaprevir (hepatitis C virus protease inhibitor) exposure when co-administered with an antiretroviral efavirenz (CYP3A inducer). Faldaprevir doses were thus doubled in order to manage the disease (Sabo et al, 2014). A variability in plasma drug concentrations of this magnitude presents a major therapeutic problem in dosage optimization. Therefore, in order to reduce/ prevent these

drug-drug interactions and/or adverse drug reactions, it is crucial to gain an understanding of the complete molecular mechanism behind regulation of CYP3A enzyme.

CYP3A is both constitutively expressed as well as transcriptionally induced/ inhibited by a variety of structurally diverse xenobiotics. Multiple signaling pathways contribute to the complex regulation of the *CYP3A* genes. Constitutive expression of CYP3A is regulated via basal transcription factors such as HNF4, HNF1, AP1, C/EBPα, C/EBPβ, HNF3γ, USF1 etc. by binding to the constitutive liver enhancer module (CLEM4) and distal enhancer module (XREM) of *CYP3A4* promoter (Jover et al., 2002; Matsumura et al, 2004; Rodriguez-Antona et al, 2003; Martinez-Jimenez et al, 2005; Tirona et al, 2003; Biggs et al., 2007). Xenobiotic-mediated induction of *CYP3A* is indirect and involves activation of nuclear receptors such as pregnane X receptor (PXR), constitutive androstane receptor (CAR), glucocorticoid receptor (GR) and vitamin D receptor (VDR) (Luo et al, 2004; Pascussi et al, 2003). However, among them, PXR is considered to be the most important and critical determinant of hepatic CYP3A enzyme activity and expression (Kojima et al, 2007; Liu et al, 2008). PXR is expressed in the cytosol and is activated upon binding with structurally diverse drug ligands, including barbiturates, rifampicin, statins, pregnenolone 16α-carbonitrile (PCN) and many others. Upon activation, PXR is translocated in the nucleus, where it hetrodimerizes with retinoid X receptor (RXR), and enhances *CYP3A* transcription by binding to AGGTCA-like direct repeat (DR-3) and everted repeat regions (ER-6) on *CYP3A* gene (Goodwin et al, 1999; Timsit & Negishi, 2007; Liu et al., 2008; Pascussi et al., 2008). Expression of PXR itself, however, can be modulated by a number

of cell signaling components activated in pathophysiological conditions and this can impact the expression and activity of Cyp3a enzyme. Cell-signaling kinases such as protein kinase A (Ding et al, 2005a; Litchi-Kaiser et al, 2009), protein kinase C (Ding et al, 2005b) etc. phosphorylate PXR, and this impacts its downstream transcriptional ability to induce *CYP3A.* Epigenetic changes such as DNA methylation, histone protein modification and microRNAs (miRNAs) have also been implicated in regulation of CYP3A enzyme. Impact of miRNAs on CYP3A gene expression can be direct or indirect. miR-27b directly regulated CYP3A4 gene expression (Pan et al., 2009), while miR-148a targets nuclear receptors such as PXR (NR1I2), thereby influencing CYP3A4 expression levels and the metabolism of its xenobiotic drug substrates (Takagi et al., 2008).

In contrast to induction of *CYP3A* being xenobiotic-mediated, downregulation of hepatic *CYP3A* has mainly been reported in various pathophysiological conditions especially infections and inflammation. Studies have shown that the gram-negative bacterial endotoxin, lipopolysaccharide (LPS) induces acute phase response (Crawford et al, 1998) in animals which can lead to decreased expression and activity of *Cyp3a11* (Morgan, 1989; Renton and Nicholson, 2000), ultimately leading to decreased hepatic drug metabolism (Monshouwer et al., 1996a). Multiple mechanisms have been proposed to explain the effect of LPS to downregulate *CYP3A*. LPS treatment of mice suppresses *PXR* mRNA levels and causes modification in nuclear export of the RXRα (Ghose et al., 2004). Binding of the PXR/RXRα to conserved sequences of *Cyp3a11* was also reduced by LPS, thereby suppressing *Cyp3a11* mRNA (Ghose et al., 2004). LPS has also been shown to activate

toll-like receptors (TLRs) on the hepatocytes and Kupffer cells, which leads to the induction of pro-inflammatory cytokines, IL-1β, IL-6 and TNF-α in the immune cells (Renton, 2004; Aitken et al., 2006). These increased levels of cytokines in turn downregulate *Cyp3a* gene expression by activating downstream mediators such as JNK or NF-κB (Yu et al., 1999; Tan et al., 2004 Ghose et al, 2008). Translocation of NF-κB was shown to increase binding between NF-κB and RXRα, which interfered with the formation of PXR-RXRα and thereby suppressed *CYP3A4* expression (Gu et al, 2006).

Although numerous mechanisms, both *in vitro* and *in vivo*, have been proposed to explain altered *CYP3A* expression levels; global changes at the whole genome level have not yet been investigated. Therefore, the objective of our study was to perform a comprehensive genome-wide mapping and bioinformatics analysis to identify novel mechanisms of *Cyp3a11* (mouse homolog of CYP3A4) down-regulation *in vivo*. For this purpose, we utilized the model of CYP3A up-regulation by PCN (mouse specific PXR activator) followed by CYP3A downregulation by LPS. The rationale of using this model was to identify genes, gene pathways, transcription factors and epigenetic modulators which are being altered (induced or downregulated) by PCN and LPS in opposite directions. By finding such subsets of factors which are either induced by PCN and downregulated by LPS or induced by LPS and downregulated by PCN, we hoped to identify potential regulators involved in Cyp3a transcription which can be targeted for further investigation. In addition, we compared and contrasted the effect of combined treatment of PCN and LPS to their individual transcriptome changes.

4.3 Materials and methods

4.3.1 Materials

5-Pregnen-3β-ol-20-one-16α-carbonitrile (#P0543) was purchased from Sigma-Aldrich (St. Louis, MO). Lipopolysaccharide (E. coli, #tlrl-pslta) was purchased from InvivoGen (San Diego, CA). RNeasy Mini Kit (#74104) was obtained from Qiagen (Valencia, CA). Mouse WG-6 v2.0 expression BeadChip Kit was obtained from Illumina (San Diego, CA). 96-well PCR plate, Roche PCR Master Mix (Roche Diagnostics), Taqman primer and probes for Cyp3a11 (FP: GGATGAGATCGATGAGGCTCTG, RP: CAGGTATTCCATCTCCATCACAGT) and Cyclophilin were bought from Sigma-Genosys, Houston. Gene expression assays (20X) for CYP3A4 (#Hs00604506_m1), Elk1 (#Mm00468233_g1), Mef2 (#Mm01340842_m1), Nrf2 (#Mm00477784_m1), Pea3 (#Mm00476696_m1), Stat1 (#Mm01257286_m1), Mycmax (#Mm00487804_m1) were purchased from Thermo Fisher Scientific, Waltham, MA. Taqman probes and primers for epigenetic factors- Ezh2, DNMT1, DNMT3a, RunX3 and LSD1 were a kind gift from Dr. Bhagavatula Moorthy, Baylor College of Medicine, Houston, TX.

4.3.2 Animals and Treatments

Adult C57Bl/6 mice (~6 weeks, male, Jackson Labs, Stock no. 000664) were allowed to acclimate to the animal care facility for 7 days. The mice were maintained in a temperature and humidity controlled environment, and all animal protocols were approved by the Institutional Animal Care and Use Committee. They were fed standard mice food and water *ad libitum* and maintained in a 12 h day/night cycle. Mice were treated with PCN (50

mg/kg/day) or corn oil I.P. for 3 days followed by LPS (2 mg/kg/day) or saline I.P. for 16 hours. After treatment, animals were anesthetized with isoflurane and euthanized by survical dislocation while under deep anesthesia. The liver tissues were harvested for further analysis.

4.3.3 Real-time PCR

We used a total of 4 animals per treatment group. Total RNA from liver samples in mice treated with PCN/LPS was isolated using the RNeasy kit as per the manufacturer's standard protocols (Qiagen, Valencia, CA). Following total RNA isolation, sample concentration was assayed using a Nanodrop-8000 (Thermo Scientific, Wilmington, DE, USA) and quality checks were done using the NanoDrop spectrophotometer and the Agilent Bioanalyzer. RNA quality parameters were as follows: the 260/280 and 260/230 ratios needed to be greater than 1.8. Further the RNA Integrity Number (RIN) was analyzed using the Agilent Bioanalyzer. The samples needed to have RIN values of 7–10 and with a range of 1–1.5. cDNA was synthesized from the isolated total mRNA using the High Capacity Reverse Transcription Kit from Applied Biosystems. Real-time PCR was performed using an ABI PRISM 7300 Sequence Detection System instrument and software (Applied Biosystems; Foster City, CA) as described previously (Shah et al., 2014; Ghose et al. 2004, 2009). In short, each reaction mixture (total of 25 ml) contained 50–100 ng cDNA, 300 nM forward primer, 300 nM reverse primer, 200 nM fluorogenic probe, and 15 ml TaqMan Universal PCR Master Mix. We extrapolated the quantitative expression values from standard curves and these values were normalized to cyclophillin.

4.3.4 Immunoblotting

Whole liver extracts were prepared as described previously (Ghose et al., 2011) and the protein concentration was determined using the bicinchoninic acid assay acc ording to the manufacturer's protocol (Pierce, Rockford, IL). Equal amounts of protein (10 mg) were analyzed by SDS-polyacrylamide gel electrophoresis and transferred onto a nitrocellulose membrane. The membranes were then probed with rabbit anti-Cyp3a11 antibody, followed by probing with a goat anti-rabbit IgG-alkaline phosphatase secondary antibody. The membranes were then washed and incubated with Tropix CDP star nitroblock II ECL reagent as per the manufacturers' instructions (Applied Biosystems). The membranes were analyzed using FlourChem FC imaging system (Alpha Innotech). The images were quantified by densitometer using AlphaEase software.

4.3.5 Cyp3a11 Activity Assay

Mouse liver microsomes were prepared as described previously (Ghose et al., 2011) and protein concentration of the microsomal fractions was determined using a BCA protein assay kit (Pierce, Rockford, IL, USA) using bovine serum albumin (BSA) as the standard. Cyp3a11 enzyme activity was determined using mouse liver microsomes using the Cyp3a substrate, midazolam (MDZ) as described previously, with minor modifications (He et al., 2006). The formation of 1′-OHMDZ from MDZ was used as a specific indicator for mouse Cyp3a11 activity. In brief, 0.1 mg of total microsomal protein was incubated with MDZ (0-16 μM), 1.3 mM NADPH and reaction cofactors in 50 mM potassium phosphate buffer (pH 7.4). The reaction was initiated by addition of glucose-6-phosphate dehydrogenase (1

unit mL-1). After 5 min, the reactions were stopped by the addition of equal volume of acetonitrile containing phenacetin as the internal standard (IS). The incubation mixture was centrifuged at 13,000 rpm at 4°C for 10 min and the supernatant was transferred to a 96-well auto-sampling plate for LC-MS/MS analysis. The identity of 1′OHMDZ and IS was verified by comparing with authenticated standards. The data were fit to standard Michaelis Menten rate equation.

4.3.6 Microarray Analysis

250 ng of total RNA was reverse transcribed, and microarray hybridization performed using the Illumina Gene Expression MouseWG-6 v2.0 Expression BeadChip Kit at the Laboratory for Translational Genomics at Baylor College of Medicine. The transcriptome profile data was quartile-normalized by the Bioconductor lumi package. The Lumi package implemented in the R statistical software, version 2.14.1, was used to perform quality control of the signal intensity data on the transcript probes, background adjustment, variance stabilization transformation, and rank invariant normalization. A detection p value cutoff of 0.01 was required for the normalized intensities to consider a transcript as detected. Differentially Expressed Genes (DEG) were selected following the t-test comparisons among groups of interest, using the R statistical system. The genes were considered to be differentially expressed for p-value<0.05 and fold change greater than or equal to 1.25x or less than or equal to 0.8x. A graphical representation of the DEGs was generated in the form of heatmaps of mean-centered normalized expression values (z-

scores), employing the Euclidean distance metric and the average clustering method, using R statistical software.

4.3.7 Pathway enrichment and transcription factor analysis

A rank file for each comparison was created based on the log2 fold change of each gene between the respective comparison groups. We next employed the Gene Set Enrichment Analysis (GSEA) methodology and software (Subramanian et al, 2005), against the Molecular Signature database (MSigDB) compendium (Liberzon et al, 2011) of gene sets. Gene Set Enrichment Analysis first finds an aggregate gene set score (termed enrichment score/ES) then runs 1000 permutations to establish a background distribution for ES. The ratio between ES and the average ES is termed Normalized Enrichment Score (NES). GSEA determines whether a key component of a pathway or biological process gene set is significantly and preferentially enriched in up-regulated genes (NES>0, fdr-adjusted Q-value<0.25) or in down-regulated genes (NES <0, fdr-adjusted Q-value <0.25). An established and fertile paradigm for hypothesis generation is that if the NES for a pathway in comparisons stemming from two different treatments are significant but having opposite signs, then the treatments might direct the pathways in opposite directions. The pathway collections KEGG, Reactome, Hallmark, and GOBP (Gene Ontology Biological Processes) were used to determine enriched pathways. We also used a compendium of putative transcription factors to identify enriched transcription factors targets in the transcriptome footprints analyzed. TransFac Analysis was employed to identify the list of transcription factors which might bind to Cyp3a11 or CYP3A4 promoter regions.

4.3.8 Statistical Analysis

Real-time PCR data were shown as the mean and analyzed with Student's t test or one-way analysis of variance for all groups, followed by pairwise comparisons. Significant values are represented as $P < 0.05$.

4.4 Results

4.4.1 Cyp3a11 gene expression, protein expression and activity

We analyzed gene expression of Cyp3a11 after treatment with PCN and LPS using qPCR to validate our model. We observed that treatment with PCN upregulated Cyp3a11 gene expression by 16-folds and LPS downregulated Cyp3a11 gene expression significantly by almost 90% as compared to control. Combined treatment of PCN and LPS showed significantly higher Cyp3a11 gene expression as compared to control; however its expression reduced by almost 50% with combined treatment as compared to PCN treatment alone. Although values for fold change varied, microarray data also showed that PCN upregulated (~2.41-folds) and LPS significantly downregulated (~2.6-folds) *Cyp3a11* gene expression (Table 4.4.2A, B, C); in concordance with qPCR data. The Cyp3a11 protein levels were also considerably up-regulated by PCN treatment and downregulated ~50% by LPS as compared to control treatment. To determine whether the transcriptional changes in *Cyp3a11* resulted in altered Cyp3a mediated drug metabolism, PCN and/or LPS treated mice were injected with sleep-inducing drug Midazolam (MDZ), which is predominantly metabolized by Cyp3a. Significantly higher MDZ was metabolized in PCN treated mice as observed with higher formation rate of 1'-OHMDZ; primary metabolite of MDZ. LPS treatment alone, on the other hand, decreased formation rate of 1'-OHMDZ significantly as compared to control. Combined treatment of LPS with PCN significantly induced and at the same time attenuated Cyp3a11 activity as compared to control and individual PCN treatment respectively.

A

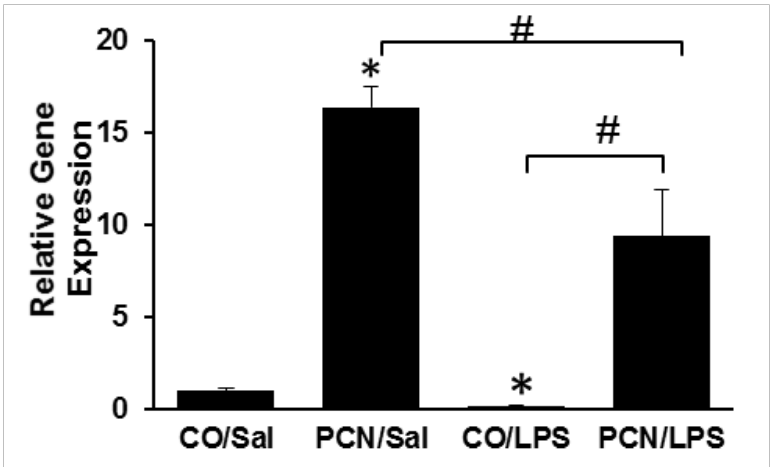

Actual fold change normalized to Cyclophilin

S.No	CO/Sal	PCN/Sal	CO/LPS	PCN/LPS
1	0.881	5.703	0.163	10.515
2	1.185	15.732	0.164	8.962
3	1.120	17.403	0.119	7.650
4	0.855	16.712	0.155	7.350
Average	1.010	16.388	0.150	8.619
SD	0.167	0.824	0.021	1.445

B

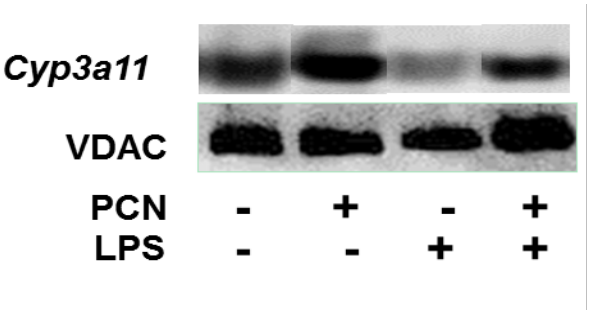

C

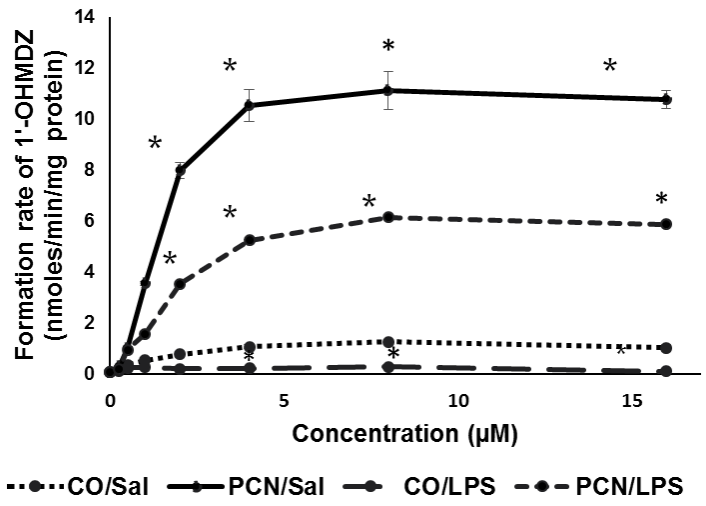

	Rate Avg				SD			
uM	**CO/Sal**	**PCN/Sal**	**CO/LPS**	**PCN/LPS**	**CO/Sal**	**CO/LPS**	**PCN/Sal**	**PCN/LPS**
0	0.07	0.06	0.06	0.07	0	0	0	0.010
0.25	0.2	0.28	0.11	0.2	0.01	0	0.01	0.020
0.5	0.36	1.01	0.25	0.94	0.02	0.02	0.01	0.020
1	0.54	3.54	0.26	1.57	0.08	0.04	0.08	0.040
2	0.77	7.98	0.21	3.53	0.11	0.08	0.3	0.020
4	1.07	10.53	0.23	5.25	0.07	0.06	0.64	0.040
8	1.26	11.12	0.28	6.15	0.01	0.03	0.74	0.050
16	1.02	10.76	0.11	5.87	0.14	0.04	0.36	0.030

Fig. 4.4.1 Validation of alteration of Cyp3a11 levels by PCN and LPS.

(**A**) Real-time RT-PCR analysis of Cyp3a11 gene expression (**B**) protein expression of Cyp3a11 (**C**) Cyp3a11 enzyme activity from the livers of mice treated with corn oil or PCN (50mg/kg/day) for 3 days followed by saline or LPS (2mg/kg/day) for 16 h. *$p<0.05$ as compared to control treatment. #$p<0.05$ as compared to PCN or LPS treatment alone.

4.4.2 Differentially expressed genes upon PCN and/or LPS treatment

Gene expression analysis using DNA microarray was carried out to identify common genes which are upregulated by PCN and downregulated by LPS or downregulated by PCN and upregulated by LPS. As reflected in the heatmaps and venn diagrams, after three days PCN treatment, a total of 79 genes were down-regulated (DR: 79) and 114 genes were up-regulated (UR: 114) (Fig. 4.4.2 A -E). With 16 hours LPS treatment however, 834 genes were downregulated and 864 genes were found to be significantly upregulated. With combined PCN and LPS treatment, a total of 821 genes showed significant downregulation and 1075 genes were up-regulated at the whole mouse liver genome level. Table 4.4.2A represents the top 15 genes based on fold change, which were differentially expressed among all the global changes upon PCN and/or LPS treatment as compared to control. PCN treatment led to significant alterations in gene expression of numerous drug metabolizing enzymes such as glutathione S transferases, Cyp3a11, Cyp2b10, carboxylesterases etc. On the other hand, LPS upregulated many inflammatory mediators such as chemokines, CD14 etc. Interestingly, with combined treatment of PCN and LPS, we saw a very similar trend in genetic changes as observed with LPS treatment alone.

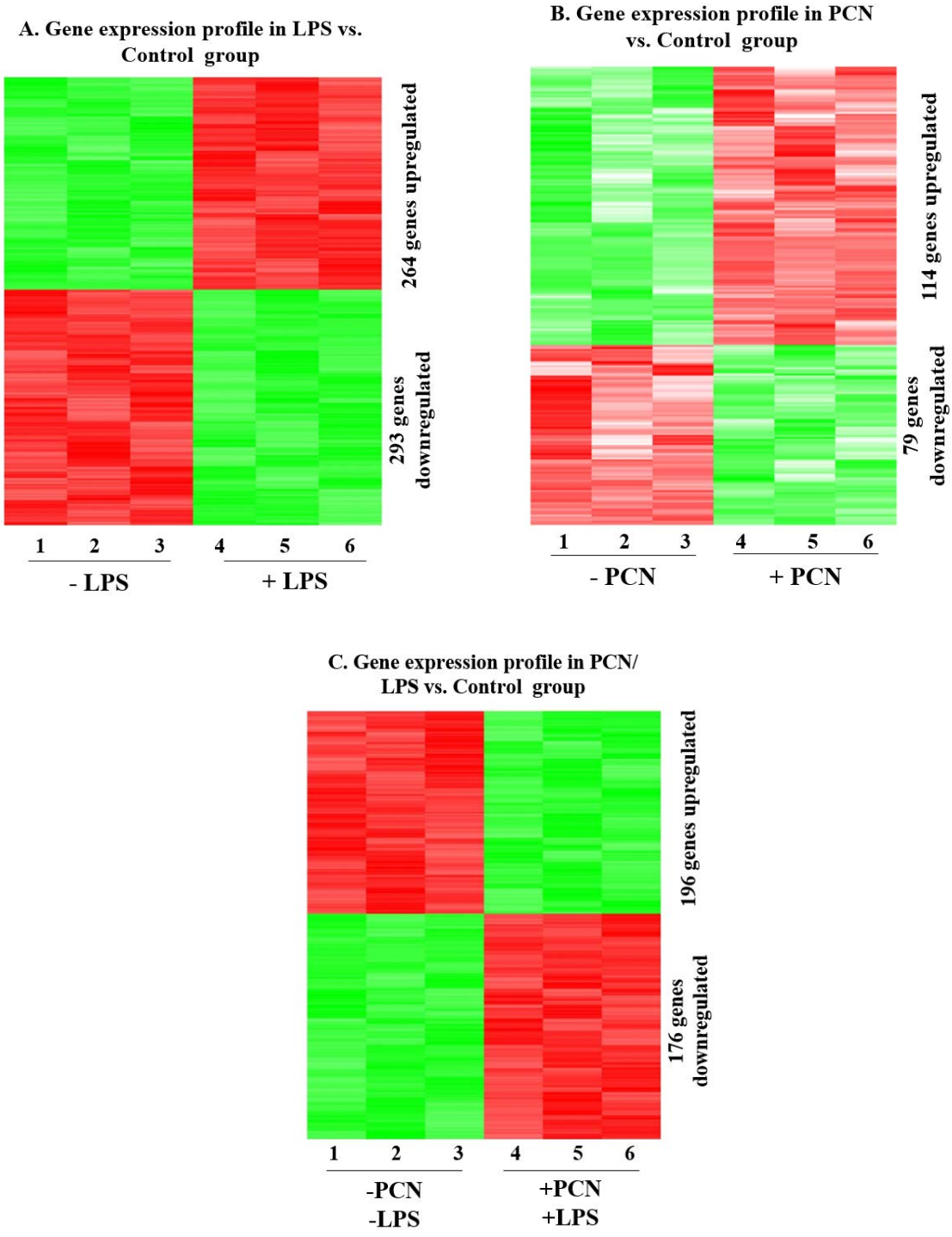
A. Gene expression profile in LPS vs. Control group
264 genes upregulated
293 genes downregulated
1 2 3 4 5 6
- LPS
+ LPS
B. Gene expression profile in PCN vs. Control group
114 genes upregulated
79 genes downregulated
1 2 3 4 5 6
- PCN
+ PCN
C. Gene expression profile in PCN/ LPS vs. Control group
196 genes upregulated
176 genes downregulated
1 2 3 4 5 6
-PCN
-LPS
+PCN
+LPS

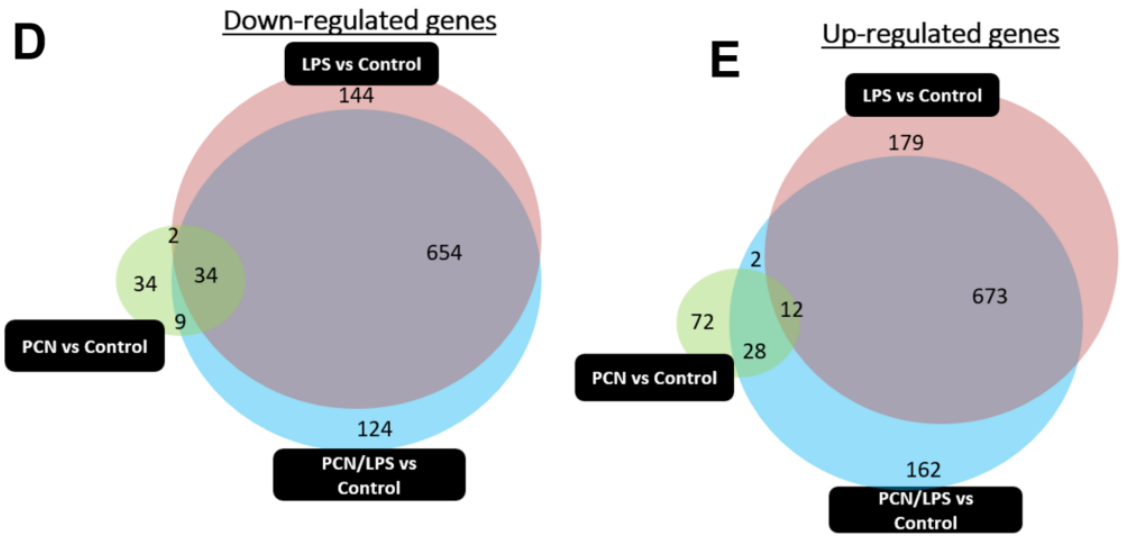

Fig. 4.4.2 PCN and LPS treatment leads to robust yet distinct transcriptomic changes.

(**A-C**) Heatmaps of the differentially expressed genes (DEGs); Red: upregulated DEGs as compared to control; Green: downregulated DEGs as compared to control. (**D-E**) Venn diagrams showing number of upregulated and downregulated DEGs by PCN treatment, LPS treatment and combined PCN/LPS treatment as compared to control.

PCN vs Control		LPS vs Control		PCN/LPS vs Control		PCN/LPS vs PCN/Sal		PCN/LPS vs CO/LPS	
Up	Down	Up	Down	Up	Down	Up	Down	Up	Down
GSTA1	CYP4A14	REG3B	CAR3	S100A8	HSD3B5	CXCL9	THRSP	CYP3A11	CYP4A14
GSTM3	CML2	S100A8	HSD3B5	S100A9	HAMP2	SAA3	CAR3	CES6	FDPS
CYP2C55	EGFR	S100A9	CPS1	SAA3	CAR3	S100A9	AQP8	GSTA1	IDI1
CES6	EGR1	SAA3	THRSP	REG3B	AQP8	S100A8	HAMP2	CYP3A25	REG3A
GSTA2	ARRDC3	CXCL9	HAMP2	CRYBB3	THRSP	REG3B	HSD3B5	GSTM3	SC4MOL
CYP2B10	IDB2	CRYBB3	ELOVL3	CXCL9	VSIG4	CRYBB3	ELOVL6	GSTA2	SLC25A25
AKR1B7	CYP2C67	CXCL1	VSIG4	CXCL1	ELOVL3	CD14	GSTA1	POR	CYP51
CYP3A11	GNAT1	CD14	INMT	CD14	CPS1	CXCL1	CYP2C55	HSD17B6	PPP1R3C
GSTM6	G0S2	LCN2	ACSS2	LCN2	ACSS2	CCL5	G6PC	CYP2C55	LSS
GSTM2	RNASE4	ADH7	AQP8	MT2	G6PC	LCN2	ACSS2	AKR1B7	CRELD2
HSD17B6	ACOT1	MT2	CLEC4G	SAA2	CLEC4G	SAA2	GSTM3	CYP2B10	
CYP2B23	AOX3	CPNE8	CYP2A5	CHI3L3	SLC2A2	MT2	SLC2A2	GSTM2	
DDIT4	CYP2C70	MT1	UPP2	CES6	ACAA1B	CYP17A1	CHRNA4	SLCO1A4	
CYP3A25	RNASE4	SAA2	G6PC	ADH7	NUDT7	GBP2	CPS1	GSTM6	
CSAD	HSD3B5	STEAP4	GSTM6	MT1	AOX3	CHI3L3	GSTM6	CES3	

Table 4.4.2A Top 15 differentially regulated genes by PCN, LPS and combined PCN/LPS treatment as compared to control, PCN alone or LPS alone.

B

	Fold Change		
Gene Symbol	PCN vs control	LPS vs control	PCN/LPS vs control
GSTM3	5.16	-1.59	1.54
CYP2C55	4.92	-1.14	1.24
CES6	3.88	-0.64	3.53
GSTA1	3.83	-2.24	
GSTA2	3.48	-2.48	
CYP3A11	2.41	-2.64	2.15
GSTM6	2.11	-2.89	-1.34
GSTM2	1.95	-1.87	
HSD17B6	1.72	-1.50	0.88
GSTM2	1.68	-1.22	0.66
CYP3A25	1.36	-2.40	0.94
GSTT3	1.13	-1.28	-0.90
EPHX1	1.12	-0.60	
GSTA4	1.20	-1.46	-0.78
INMT	1.05	-3.47	-2.24

C

	Fold Change		
Gene Symbol	PCN vs control	LPS vs control	PCN/LPS vs control
SAA4	-0.92	2.68	2.26
2200001I15RIK	-0.85	1.05	0.89
LRG1	-0.74	1.45	1.50
LCAT	-0.67	0.83	0.86
LDHA	-0.64	1.15	1.12
IIGP2	-0.62	0.94	1.00
ACTB	-0.61	0.61	
IGTP	-0.59	1.05	0.98

Table 4.4.2B Top genes differentially regulated in opposite directions B) Induced by PCN and down-regulated by LPS C) Down-regulated by PCN and induced by LPS as compared to control.

4.4.3 Pathway analysis of differentially expressed genes (DEGs)

Biological processes that were enriched and differentially modulated in the transcriptome footprint of the treated mice were identified using gene set enrichment analysis (GSEA). We focused on pathways that were regulated in opposite directions between PCN and LPS treatments. In addition we studied the effect of co-treatment of PCN and LPS on these differentially regulated pathways. Fig. 4.4.3 shows the major biological processes for the group of genes that were differentially regulated ($Q<0.25$; Normalized Enrichment Score/NES has opposite signs between PCN and LPS treatment). Broadly, all the major biological pathways were classified into 3 main types: a) Drug metabolism pathways; representing subgroups such as CYP450 metabolism or glucuronidation (Fig. 3A) b) Inflammatory pathways; representing subgroups such as Interferon-γ, interferon-α, TNFα signaling etc. Signal Transduction pathways; representing subgroups such as protein kinase cascade, mitogen activated protein kinase signaling etc. All the drug metabolism pathways were found to be positively enriched by PCN and negatively enriched by LPS. LPS attenuated PCN-mediated positive enrichment of all pathways. On the other hand, both the inflammatory pathways and the signal transduction pathways were mainly negatively enriched by PCN and positively enriched by LPS. Similar to the pattern observed in DEGs

with combined PCN and LPS treatment, most of the pathways were enriched in the same direction as LPS treatment.

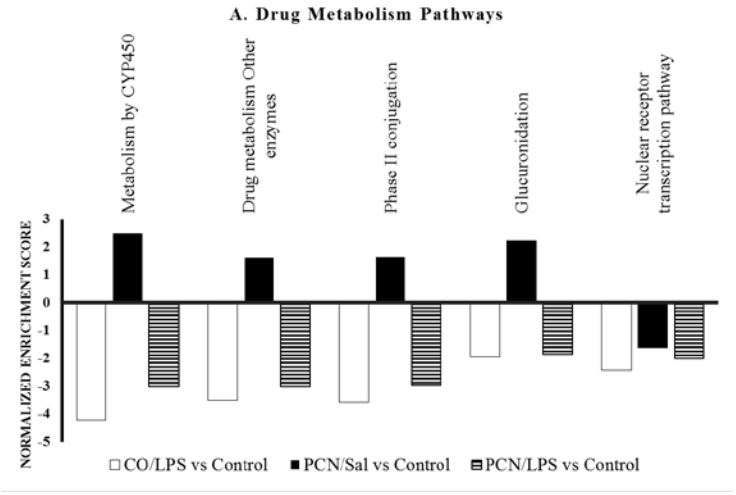

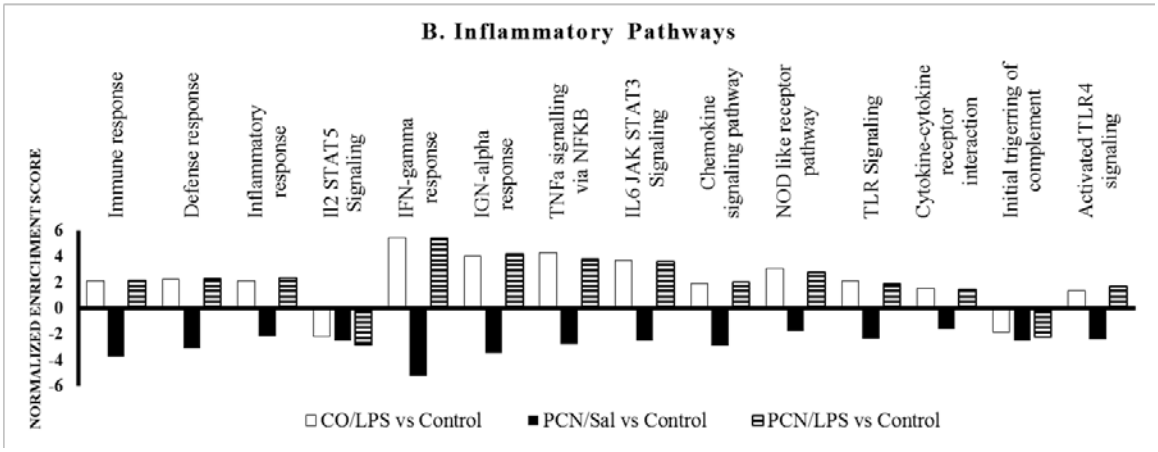

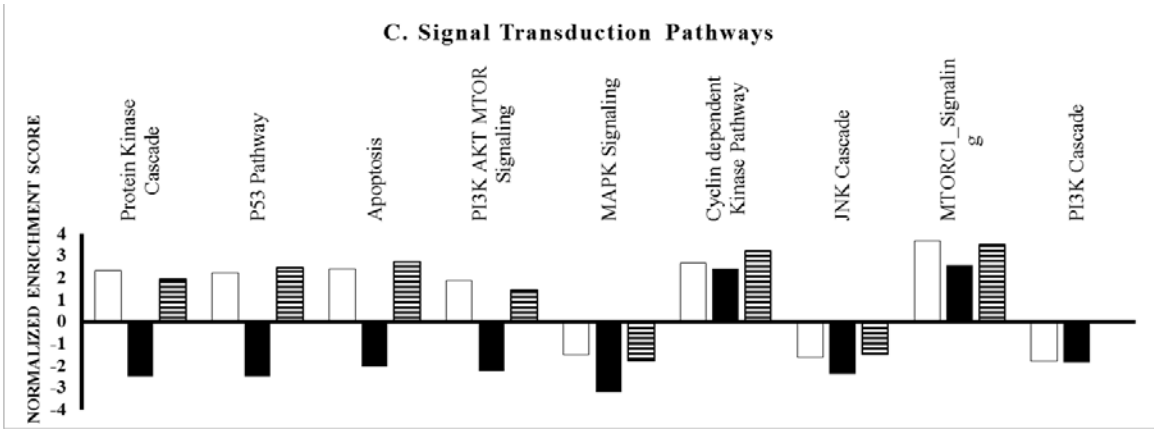

Fig. 4.4.3 Gene Set Enrichment Analysis (GSEA) reveals distinct modulation of pathways between PCN and LPS treatment.

Mice were treated with corn oil or PCN (50mg/kg/day) for 3 days followed by saline or LPS (2mg/kg/day) for 16 h. Biological processes enriched in the transcriptome footprint of liver mRNA from treated mice were identified using Gene Set Enrichment Analysis (GSEA). The Normalized Enrichment Score (NES) is reported for select enriched pathways (fdr-adjusted Q-value < 0.25). Key differences were observed in (A) Drug metabolism pathways (B) Inflammatory Pathways and (C) Signal Transduction pathways.

4.4.4 Differentially expressed transcription factors upon PCN and/or LPS treatment

Next, we sought to analyze the transcription factors (TF) that were responsible for modulating the gene expression changes under PCN and/or LPS treatment in the mouse liver. Transcription factors which were preferentially induced or suppressed by PCN and/or LPS treatment and were differentially modulated were determined via GSEA and shown in Fig. 4. The top transcription factors driving the expression of upregulated and downregulated genes are shown in Table 2. After three days PCN treatment alone, a total of 562 transcription factors were negatively enriched and only 3 transcription factors were positively enriched i.e. MEF2, NFE2 and PPARγ. Among these three, MEF2 was the only transcription factor that was also negatively enriched with LPS. With 16 hours LPS treatment however, 472 transcription factors were negatively enriched and 65 transcription factors were found to be significantly positively enriched. In PCN/LPS group, 536 TFs were differentially expressed (Upregulated: 35, Downregulated: 501) as compared to CO/Sal. Using TRANSFAC based motif-analysis, we identified TFs which are altered by PCN or LPS (in same or opposite direction) and might bind to *Cyp3a11* promoter sequence (Table 3) and *CYP3A4* promoter sequence (Table S1). Till now, transcription factors- HNF4α, CREB, HNF1, PXR, CAR, RXRα, AP1, C/EBPβ, HNF3γ, USF1, COUP, C/EBPα are known to bind to Cyp3a gene and regulate its constitutive expression. Through TransFac analysis, we found novel transcription factors which could also be involved in this pathway such as- Stat1, Stat5b, Pax4, Mycmax, Pea3 etc. Although these transcription factors are not known to regulate drug metabolizing enzymes till date, they have been

involved in repressing other genes and maintaining the cellular functions. We carried out confirmatory studies to validate the microarray changes of these transcription factors, however, ChIP assay studies need to be performed to confirm whether they are actually binding to the Cyp3a11 gene.

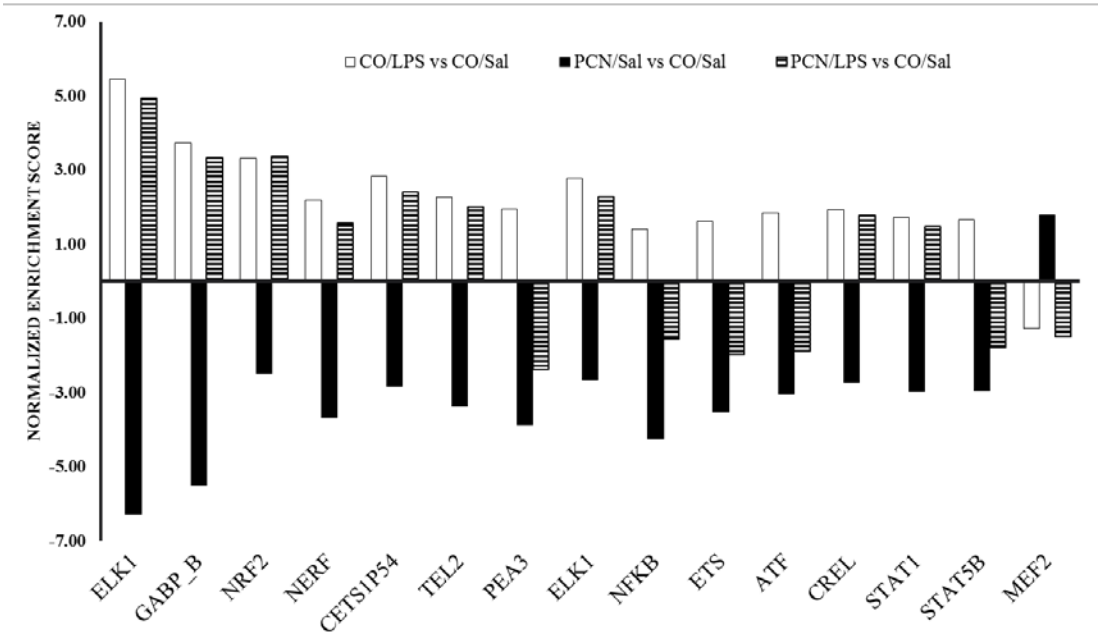

Fig. 4.4.4A Gene Set Enrichment Analysis (GSEA) reveals distinct modulation of transcriptional regulators.

Enrichment of transcriptional regulators in the transcriptomic response of mouse livers exposed to corn oil or PCN (50mg/kg/day) for 3 days followed by saline or LPS (2mg/kg/day) for 16 h was assessed using GSEA. An extensive search was carried out for

transcriptional regulators that were enriched (Q < 0.025) but with targets changed in opposite direction with PCN and LPS as compared to control. We report transcriptional regulators with a positive NES (acting primarily as transcriptional activators for Cyp3a11) and those with a negative NES (acting primarily as transcriptional repressors for cyp3a11).

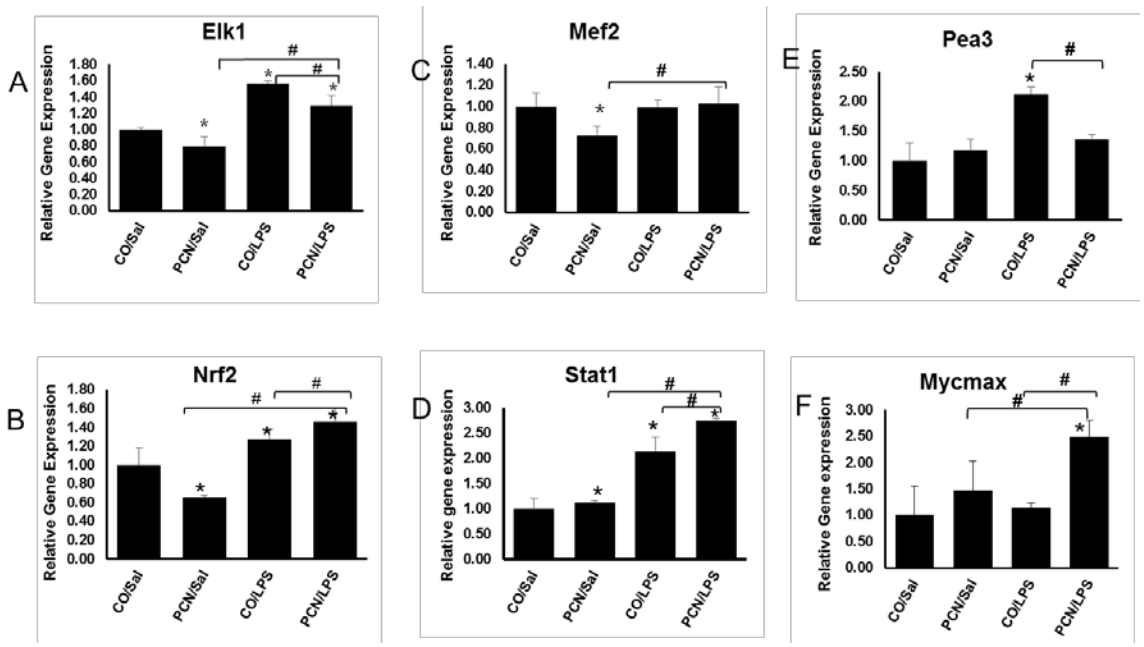

Fig. 4.4.4B Real-time qPCR analysis for validation of gene expression of transcription factors.

Mice were treated with corn oil or PCN (50mg/kg/day) for 3 days followed by saline or LPS (2mg/kg/day) for 16 h. A few selected candidate genes from the list of transcription factors that were differentially regulated between PCN and LPS treatment were chosen for validation of gene expression. *p<0.05 as compared to control treatment. #p<0.05 as compared to PCN or LPS treatment alone.

PCN vs Control		LPS vs Control		PCN/LPS vs Control		PCN/LPS vs PCN/Sal		PCN/LPS vs CO/LPS	
Up	Down	Up	Down	Up	Down	Up	Down	Up	Down
MEF2	SP1	ELK1	FOXO4	ELK1	FOXO4	ELK1	FOXO4		SP1
PPARG	ELK1	GABP_B	SP1	NRF2	FREAC2	GABP_B	SP1		MAZ
NFE2	FOXO4	NRF2	FREAC2	GABP_B	SP1	NRF2	FREAC2		E12
	MAZ	CETS1P54	E12	CETS1P54	NFAT	ETS2_B	MAZ		LEF1
	ETS2_B	TEL2	NFAT	TEL2	MAZ	STAT5B	LEF1		NFY
	LEF1	NFKB	MYC	NFKAPPAB65	LEF1	HNF4	AP4		FOXO4
	E12	COUP	MAZ	NFE2	E12	CETS1P54	NFAT		NFAT
	GABP_B	AP1	AP4	CREL	AP4	NERF	MEF2		ELK1
	NFAT	PEA3	LEF1	IRF	MYOD	TEL2	E12		MYOD
	FREAC2	CREL	HNF3	MAX	ERR1	IRF	MYOD		LEF1
	AP4	ATF	ERR1	BACH1	LEF1	STAT5A	MYC		MEIS1
	HNF3	CREB	HNF1	USF	MYC	NFKB	ERR1		AP4
	PU1	BACH1	CHX10	ICSBP	CHX10	PU1	CHX10		FREAC2
	PAX4	MYCMAX	MYOD	AP1	HNF3	ICSBP	NFY		PU1
	MYC	ATF6	NKX25	NERF	MEF2	SP1	MEIS1		E4F1

Table 4.4.4A Top 15 differentially enriched transcription factors by PCN, LPS and combined PCN/LPS treatment as compared to control, PCN alone or LPS alone.

PCN↓ LPS↓	PCN↓ LPS↑
FREAC2	NFKB
NFAT	PEA3
LEF1	STAT1
HNF1	STAT5B
CHX10	AP2
ERR1	CETS1P54
HNF3	CREB
MYOD	PAX4
GATA1	COUP
FOXO4	HSF
USF2	MYCMAX
PAX4	PTF1BETA
NFY	
NF1	
SREBP1	

Green: Known activators

Table 4.4.4B Altered transcription factors predicted to have putative binding sites on Cyp3a11 promoter using TRANSFAC analysis.

4.4.5 Epigenetic Regulation

To understand the role of epigenetic modulators in regulating Cyp3a11 at the transcriptional level, GSEA analysis was carried out against the molecular signature database compendium of annotated gene sets. Fig. 6 shows targets of epigenetic modulators which are differentially enriched by PCN and LPS in opposite directions. Targets of methylation by modulators such as HDAC1, HDAC3, EZH2 etc. are suppressed in these collection of data sets and our data shows that these targets might be further suppressed by PCN and relieved by LPS. Changes by these epigenetic modulators have been reported in numerous in vitro and in vivo models and we believe that the same epigenetic modulators could also be involved in regulation of Cyp3a11 expression and activity via PCN and LPS. We also carried out RT-qPCR analysis in our treated liver tissues to investigate whether the actual gene expression of epigenetic markers is altered by PCN and/or LPS. We found that both EZH2 and DNMT3a were significantly down-regulated with PCN treatment as compared to control, in accordance with our GSEA data (Fig. 7A and 7B). Gene expression of DNMT1, however, was significantly induced by PCN (Fig. 7B). With LPS treatment alone, gene expression of two epigenetic markers was induced significantly- Ezh2 and DNMT1, as compared to control. Combined treatment of PCN and LPS significantly reduced the gene expression of EZH2; thereby showing that PCN can attenuate effect of LPS in regulating targets of EZH2. Confirmatory studies showing that Cyp3a11 is indeed a target of methylation by these epigenetic markers need to be carried out for further validation.

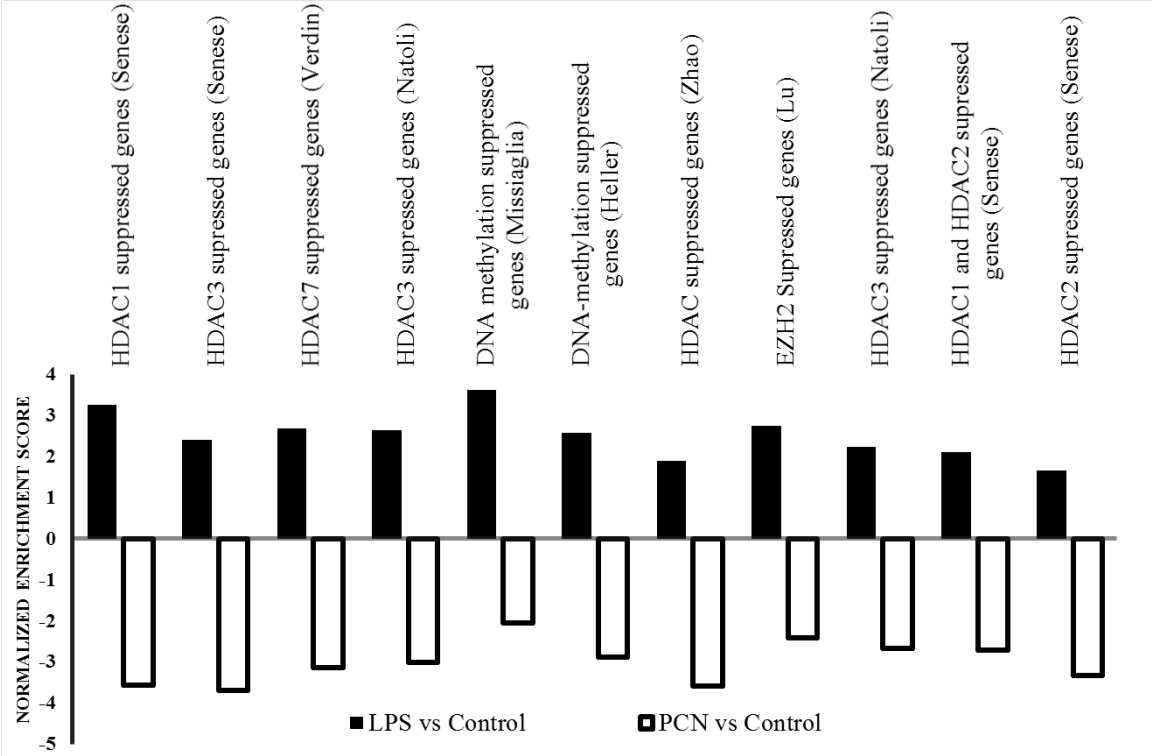

Fig 4.4.5A Gene Set Enrichment Analysis (GSEA) reveals distinct modulation of epigenetic modulators.

Enrichment of epigenetic mechanisms in the mouse livers exposed to corn oil or PCN (50mg/kg/day) for 3 days followed by saline or LPS (2mg/kg/day) for 16 h was assessed using GSEA. An extensive search was carried out for epigenetic regulators that were enriched ($Q < 0.025$) but with targets changed in opposite direction with PCN and LPS as compared to control.

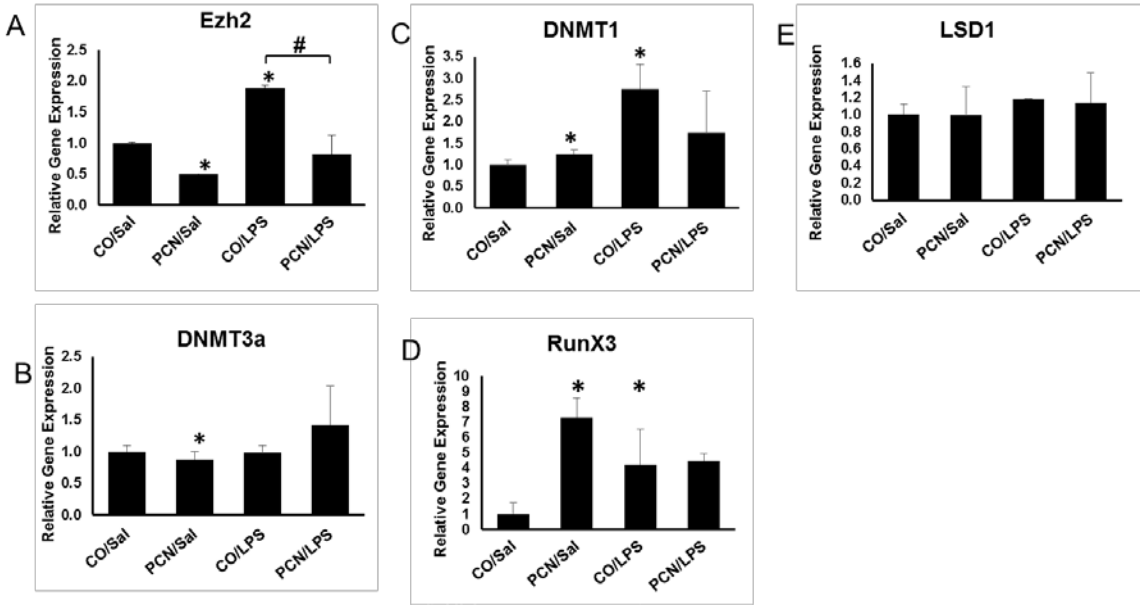

Fig 4.4.5B Real-time qPCR analysis for validation of gene expression of epigenetic modulators- Ezh2, DNMT1, DNMT3a, RunX3 and LSD1.

Mice were treated with corn oil or PCN (50mg/kg/day) for 3 days followed by saline or LPS (2mg/kg/day) for 16 h. A few selected candidate genes from the list of epigenetic factors that were differentially regulated between PCN and LPS treatment were chosen for validation of gene expression. *$p<0.05$ as compared to control treatment. #$p<0.05$ as compared to PCN or LPS treatment alone.

4.5 Discussion

The key findings of this study were the identification of novel differentially regulated genes, molecular pathways, transcription factors and epigenetic mechanisms potentially involved in the regulation of Cyp3a11 (mouse homolog of CYP3A4) enzyme. Numerous mechanisms of alteration of drug metabolizing enzymes especially *Cyp3a* have been reported but a comprehensive study of all the genomic changes that are associated with up-regulation and down-regulation of Cyp3a has not been reported till yet. We found robust changes in mouse genomic profile upon treatment with PCN, *Cyp3a* inducer, as well as LPS, endotoxin responsible for downregulation of *Cyp3a*.

Genes that were maximally upregulated by PCN mainly included DMEs such as CYP2C55, carboxylesterases, CYP2B10, glutathione S-transferases, aldo-keto reductases and so on. These results were fairly expected as next generation sequencing has previously been shown to have PXR-binding sites on glutathione S-transferases (Cui et al., 2010), carboxylesterases and most of the other drug metabolizing enzymes. Most studies of the effects of PCN on the liver have traditionally focused on the function and inducibility of enzymes involved in drug metabolism. Our results showed that, this steroid, acting specifically through PXR, simultaneously induced or repressed hundreds of genes apart from DMEs, including epidermal growth factor receptor (EGFR), early growth response protein 1 (EGR1), arrestin domain containing protein 3 (ARRDC3), cysteine sulfinic acid decarboxylase (CSAD) and so on. Since multiple EGR1 binding sites have previously been identified within the 5′-regulatory promoter region of the *CYP2B6* gene (Inoue and

Negishi, 2008, 2009), its altered gene expression may imply potential involvement in the regulation of *Cyp3a11* also. With LPS treatment alone, gene expression pattern of most of the inflammatory mediators was found to be differentially regulated such as Serum amyloid A3 (SAA3), chemokine ligand 9 (CXCL9), cluster of differentiation 14 (CD14), metallothionein 2 (MT2) etc. Combined treatment of PCN and LPS showed interesting results. Although different genes were maximally altered in both directions by LPS alone and PCN/LPS co-treatment, most of the changes with co-treatment followed the trend of LPS treatment alone.

Although, genome wide expression analysis with DNA microarray has become a mainstay of genomics research (Schena et al, 1995; Lockhart et al, 1996); the challenge no longer lies in obtaining differential gene expression patterns, but rather in interpreting the results to gain insights into biological mechanisms. One way to do that is to use an analytical tool-gene set enrichment analysis (GSEA), in which all DEGs are ranked according to their differential expression and then assigned different gene sets based on known biological similarities. GSEA analysis then determines the degree of representation of the members of a particular gene set towards the top (positive enrichment) or bottom (negative enrichment) of the entire ranked list (Subramanian et al, 2005). Since, genomic profiling after PCN and LPS treatment identified genes whose functions are related to drug metabolism, or are involved in cell cycle kinetics and mediating inflammation, we broadly selected pathways belonging to three major groups- drug metabolism (DM), inflammatory regulation (IR) or signal transduction (ST) mechanisms for enrichment analysis. We

observed that most of the drug metabolism pathways were positively enriched by PCN and negatively enriched by LPS, consistent with changes in *Cyp3a11* gene expression. With combined treatment however, negative enrichment was observed for DM pathways. Taking a closer look into the subsets of genes belonging to these pathways, we found that although *Cyp3a11* is positively enriched, multiple drug metabolizing enzymes such as glutathione S transferase A3, aldo-keto reductase 1C6 or alcohol dehydrogenase 1 are negatively enriched, which shifts the total enrichment score of the pathway in the negative direction by both PCN and LPS treatment. In contrast to DM pathways, most of the IR and ST pathways were found to be negatively enriched by PXR activation and positively enriched by LPS as well as combined treatment. Understanding which pathways are enriched by PCN and LPS is crucial as these upstream changes ultimately trigger downstream components which might be involved in transcriptional regulation of *Cyp3a11*.

Gene transcription of *Cyp3a11* is regulated, in large part, by transcription factor (TF) proteins that bind to genomic cis-regulatory elements in a sequence-specific fashion. TF genes are usually not significantly up- or downregulated in microarray experiments. Their activity is mainly regulated at the level of ligand binding or at the posttranscriptional level (Everett et al, 2010). Therefore we carried out GSEA analysis to find the top transcription factors whose targets were maximally enriched by PCN and LPS in opposite directions. One such transcription factor which was altered maximally was Elk1; an ETS family transcription factor responsible for target gene transcription upon mitogen activated protein kinase-signaling pathway stimulation (Besnard et al, 2011). Elk1 negatively enriched by

PCN and positively enriched by LPS; combined treatment following the LPS trend. In fact, most of the transcription factors such as Tel2, Pea3, Stat1, Stat5b etc. which are changed in opposite directions were negatively enriched by PCN and positively enriched by LPS treatment, suggesting that these transcription factors might be negatively regulating basal *Cyp3a11* expression. This fact was strengthened by previous reports showing that loss of Stat5b increased gene expression of *Cyp3a* in mice (Park et al, 1999). LPS-mediated activation of NF-κB has also been shown to play a significant role in downregulation of Cyp3a enzyme (Gu et al, 2006; Abdulla et al, 2005). On the other hand, myocyte enhancer factor 2 (Mef2) was the only transcription factor which was positively enriched by PCN and negatively enriched by LPS in our data. Mef2 regulates cell differentiation, proliferation, morphogenesis, survival and apoptosis of a wide range of cell types (Potthoff et al, 2007) and previous microarray analysis has revealed that a number of drug metabolizing enzymes such as Cyp1b1 and nuclear receptors such as Ahr are downregulated in the absence of Mef2 (Luoffo et al, 2015). Although the actual gene expression of *Mef2* was not induced by PCN in our data, it might still be involved in altering the expression of its downstream genes. Further studies to understand the role of Mef2 in regulation of *Cyp3a* enzyme need to be carried out.

Furthermore, TRANSFAC analysis was carried out to investigate whether these enriched transcription factors have any binding sites on Cyp3a promoter/ enhancer regions. TRANSFAC (TRANScription FACtor database) is a manually curated database of eukaryotic transcription factors, their genomic binding sites and DNA binding profiles.

The contents of the database can be used to predict potential transcription factor binding sites. Some transcription factors which are already known to bind to *Cyp3a* eg. HNF1, HNF3, CREB and COUP were also picked up by TRANSFAC, validating our analysis. Other transcription factors which may have potential binding sites on Cyp3a are listed in Table 3 and real-time qPCR was performed to investigate whether PCN and LPS alter the gene expression of these transcription factors. These findings would provide novel insights into the mechanisms involved in regulation of human *CYP3A4* and suggest new therapeutic targets to treat disorders due to altered drug metabolism.

Lastly, recent studies have demonstrated that many other factors such as epigenetics (Ingelman-Sundberg et al, 2013) and micro RNAs (miRNAs) (Yu et al, 2016) may modulate DME gene expression and cause variations in drug metabolism and toxicity. The effect of epigenetic processes on pharmacologically relevant genes and ultimately drug response is a rather new area of research (Ingelman-Sundberg & Gomez, 2010). Among all the epigenetic changes, changes in DNA methylation profiles determine whether there is a permissive chromatin state for the transcription machinery to access gene promoter regions and initiate transcription (Bird, 2002; Reik, 2007). DNA methylation is a key epigenetic mechanism and a covalent modification, resulting in stable gene silencing (Suzuki et al, 2008). In our data, we found that genes which are suppressed by DNA methylation by modulators such as enhancer of zeste homolog 2 (Ezh2) in previous studies (Lu et al, 2010) were further suppressed by PCN and this effect was relieved by LPS. We further carried out RT-PCR analysis to measure the gene expression of methylation

modulator Ezh2 in our model. We found that Ezh2 gene expression was suppressed by PCN and induced by LPS, implicating that Ezh2 could also have a significant role in regulation of Cyp3a enzyme. Future studies to study whether Ezh2 actually methylates Cyp3a11 need to be carried out. Enrichment of histone-3-lysine-27 trimethylation (H3K27me3) in promoters and gene-bodies has also been associated with inactivation of gene transcription (Lan et al., 2007; Swigut and Wysocka, 2007). Li *et al* found that increased H3K27me3 within the margins of the *Cyp3a16* gene may be responsible for switching off its gene expression in livers of adult mice (Li et al, 2009). In addition to being homologous in DNA and protein sequences to the human CYP3A isoforms, mouse *Cyp3a11* and *Cyp3a16* also mimic a developmental switch as human *CYP3A4* and *CYP3A7* (Hart et al., 2009). In our GSEA analysis, we found that genes downregulated in liver tumors by H3K27me3 (Acevedo et al, 2008) were further suppressed by PCN and relieved by LPS. This could imply that although H3K27me3 might be responsible for the switch of *Cyp3a16* to *Cyp3a11*; high levels of H3K27me3 could be responsible for decreased expression of *Cyp3a11* in adult liver. However, further methylation specific studies need to be carried out to confirm the involvement of H3K27me3 in regulation of *Cyp3a11* in adult mice. Apart from epigenetic modulation, microRNA-27b (miR-27b) or mouse microRNA-298 (mmu-miR-298) has previously been shown to downregulate *CYP3A4* expression (Pan et al, 2009). Hence, GSEA analysis to understand the involvement of miRNAs in regulation of *Cyp3a11* was carried out, however PCN and LPS

did not significantly enrich any miRNAs in opposite directions in our model (data not shown).

In conclusion, we carried out whole transcriptome analysis to understand novel molecular mechanisms associated with downregulation of *Cyp3a11* enzyme. Using high-throughput microarray technology, we screened large numbers of genes to detect changes stimulated by PCN, LPS as well as their combined treatment. Potential transcription factors which are altered by PCN and LPS in opposite directions and might be involved in regulation of Cyp3a gene were identified such as Pea3 and Stat1. Their differential gene expression was validated and future studies entail chromatin immunoprecipitation assays to investigate their binding on Cyp3a promoter. Results from this study will further enhance our understanding of the intricate network of different cell signaling pathways and epigenetic mechanisms with nuclear receptors such as PXR. In addition, Cyp3a might be a potential target of DNA methylation by epigenetic modulators such as Ezh2 and hence its exact role needs to be further investigated. Since PXR is involved with regulation of a number of DMEs other than Cyp3a, these pathways, transcription factors and epigenetic modulators could be involved in regulation of numerous other genes controlled by PXR.

Chapter 5

Role of alteration of Cyp3a on pharmacokinetics of its substrate- Irinotecan, a chemotherapeutic agent

5.1 Abstract

Irinotecan, a chemotherapeutic agent, is used either singly in the treatment of colorectal cancer or in combination therapy for colorectal liver metastasis (CLM) and is currently undergoing clinical trials for various other metastatic cancers. Colorectal cancer is the third most common cause of cancer related deaths in the United States, usually associated with CLM. In CLM patients, disrupted gut barrier has been associated with increased entry of gut-derived bacteria to the liver, which eventually induces hepatic inflammation through Toll-like receptor (TLRs) signaling pathway. Activation of TLR4 by Lipopolysaccharide (LPS) has been found to downregulate drug metabolizing enzymes (DMEs) such as CYP3A4, UGT1A1 etc. which are responsible for the metabolism of irinotecan to SN38 and SN38 glucuronide. Alteration of DMEs could potentially influence the plasma and/or hepatic concentrations of Irinotecan and its metabolites, leading to enhanced toxicity or failure of therapy. Therefore, the first purpose of our study was to establish whether LPS, by downregulating DMEs, alters the pharmacokinetics (PK) of irinotecan and its metabolites *in vivo*. Expression/ activity of these DMEs is regulated via nuclear receptors mainly Pregnane X receptor. Hence, we wanted to find out whether induction of DMEs, via activation of PXR, would be able to reverse the effect of LPS on PK of irinotecan and its metabolites. PXR is expressed in human colon cancer cells and accumulating evidence strongly points to its differential role in cancer progression and thereby chemotherapy outcome. Therefore, through our LPS and PCN model, we would be able to enhance our understanding on effect of alteration of DMEs on PK and differential organ distribution of

irinotecan and its metabolites *in vivo*. Ultimately, by activating PXR, our purpose is to find interventions for effective irinotecan chemotherapy, with minimum side effects.

5.2 Introduction

Irinotecan, a topoisomerase 1 inhibitor, was first approved by FDA in 1996 in combination therapy and then in 2000 as a first-line agent for treatment of colorectal cancer. Colorectal cancer is one of the main causes of cancer-related deaths, accounting for 677,000 deaths each year worldwide (Rim et al. 2009; Weir et al. 2003). If diagnosed early, colorectal tumors can be cured by a radical resection. Unfortunately, a large number of patients are diagnosed with hepatic metastasis from colorectal cancer at the time of primary cancer diagnosis or during follow-up after resection and only curative option is surgically removing the metastatic liver (Niederhuber et al, 1993). However, most of the cases are unresectable because of tumor's large size and number (Nordlinger et al. 2007). Preoperative chemotherapy with irinotecan provides an effective treatment option in patients with metastatic colorectal cancer as it significantly improves overall response rate (ORR) by 40-50% and facilitates hepatic resection in previously unresectable metastatic liver (Vanhoefer et al. 2001; Cunningham et al. 2001).

Antitumor activity of irinotecan is mediated via inhibition of topoisomerase-I (Topo-I), a nuclear enzyme responsible for unwinding DNA required for replication. Once irinotecan reaches the systemic circulation, it is metabolized into an active metabolite, SN-38 (7-Ethyl-10-Hydroxycamptothecin) by carboxylesterases (CES) in the liver. SN-38 is 100-1000 times more potent in destabilizing Topo-I that blocks DNA unwinding and future replication, resulting in interrupted repairs of double strand breaks and S phase arrest followed by cell death (Rudolf et al. 2013; Yashiro et al. 2011; Kawato et al. 1991). As

shown in Fig. 1, irinotecan is first bioactivated by carboxylesterases (CES) to form the toxic metabolite, 7-ethyl-10-hydroxycamptothecin (SN-38) (Weekes et al. 2009) which is detoxified to inactive SN-38 glucuronide (SN-38G) predominantly by uridine diphosphate glucuronosyltransferases (UGT) 1A1 enzyme. Apart from CES, oxidation of irinotecan by cytochrome P450 (CYP) 3A enzymes forms two inactive metabolites: APC [7-ethyl-10[4-N-(5-aminopentanoicacid)-1-piperidino] carbonyloxycamptothecin] and NPC [7-ethyl-10[4-amino- 1 piperidino] carbonyloxycamptothecin]. NPC is further converted to SN-38 by the CES. Irinotecan and its metabolites are subjected to extracellular efflux by P-glycoprotein (MDR1), multidrug resistance-related protein-2 (MRP2) and breast cancer resistance protein *(BCRP2* (ABCG2)) (Marsh and Hoskins 2010; Han et al. 2009; Kroetz 2006) and are subsequently eliminated in bile or urine. SN-38G is deconjugated to SN-38 by intestinal bacterial β-glucuronidase (Saliba et al. 1998; Sparreboom et al. 1998; Takasuna et al. 2006).

Although increased response rates with irinotecan chemotherapy have been observed, its widespread use is limited due to severe toxicities. Accumulation of SN-38 in intestine severely damages intestinal mucosa that results in delayed-onset life threatening diarrhea (Hecht, 1998). Moreover, damaged intestinal mucosa increases intestinal permeability ("leaky gut"), which ultimately leads to increased dysbiosis and small intestinal bacterial overgrowth (SIBO) (Wigg et al. 2001). Hepatotoxic bacterial products such as PAMPs, DAMPs, endotoxins (Lipopolysaccharide, LPS) and dangerous gut bacteria thus translocate into liver via mesenteric portal bloodstream, where they activate TLRs present

on liver cells (Kupffer cells, stellate cells, and hepatocytes) and induce chronic inflammation (Rivera et al. 2007). We and others have shown that activation of hepatic TLR4 by LPS suppresses expression of drug metabolizing enzymes (DMEs) and transporters (Ghose et al. 2009). However, whether this alteration of DMEs such as Cyp3a etc. leads to alteration of pharmacokinetics of Irinotecan and its metabolites is not known yet. Therefore, our first objective was to determine the effect of administration of LPS on PK of irinotecan and its metabolites SN38 and SN38G *in vivo*.

Drug-metabolizing enzymes play a vital role in the elimination of irinotecan and thus slightest alteration in expression/activity of DMEs that metabolize irinotecan, will have a significant impact on its pharmacokinetic properties. Indeed, clinically irinotecan pharmacokinetics and disposition was affected by various compounds now identified as ligands of the xenosensor PXR (Pregnane X Receptor, NR1I2) such as rifampicin (Yonemori et al, 2004) or St. John's wort (Mannel et al, 2004). PXR is also the main nuclear receptor responsible for induction of DMEs such as CYP3A and UGT1A1, which are involved in disposition of irinotecan. Therefore, considering the metabolic profile of irinotecan, our second objective was to assess whether PCN (mouse PXR activator) administration could revert the effect of LPS on altered PK of irinotecan as well as its metabolites.

5.3 Materials and methods

5.3.1 Materials

Pregnenolone-16alpha-carbonitrile (#P0543) was purchased from Sigma-Aldrich, St. Louis, MO. Lipopolysaccharide (E. coli, Cat # tlrl-pslta) was purchased from Invivogen, San Diego, CA. Camptothecin (CPT; internal standard (I.S)) was purchased from Sigma-Aldrich, St. Louis, MO. Irinotecan hydrochloride (NDC-0703-4437-11) for injections was procured from Martin Surgicals, Houston, TX. SN-38 and SN-38G were a kind gift from Dr. Ming Hu's lab at the University of Houston, TX. LC-MS grade solvents were purchased for chromatography from VWR international, LLC (Suwanee, GA, USA). Unless specified, all other materials were purchased from Sigma-Aldrich (St Louis, MO, USA).

5.3.2 Animals and treatments

Adult, male C57BL/6 mice (Stock #000664), aged 5-6 weeks with approximate weight of 20-22 g were purchased from Jackson Labs (Bar Harbor, Maine, USA). All the animals were maintained in a temperature and humidity controlled environment and 12 h light/dark cycle with free access to water and rodent chow ad libitum. All animals used in this study followed care of the animals and experimental procedures complied strictly with the Institutional Animal Care and Use Committee guidelines of the University of Houston.

C57Bl/6 mice (n=4/ group) were administered PCN (50 mg/kg/day) I.P. or corn oil for three days. On day four, mice were co-administered LPS (2 mg/kg) or saline I.P. and irinotecan hydrochloride solution (10 mg/kg) by oral gavage.

5.3.3 Collection of whole blood and tissues

After irinotecan administration, approximately 10-15 μL of whole blood samples were collected at predetermined time points (0, 15, 30, 60, 120, 240, 360, 480, 600 and 1440 mins) from the tail vein in heparinized Eppendorf tubes. The heparinized tubes were prepared on the day before the experiment by coating the tubes with Qtips immersed in a solution of 1000 units heparin prepared in deionized water.

After collecting blood from tail vein at last time point, following euthanasia, whole blood, liver, intestine and kidneys were collected. Blood was taken by inferior venacava (IVC) puncture, centrifuged at 13000 rpm for 10 min at 4°C to obtain serum and stored at –80°C. Livers, intestine and kidney samples for each mouse were snap frozen in liquid nitrogen and stored at -80°C until further analysis.

5.3.4 RNA preparation and qRT-PCR

Total RNA was isolated from mouse liver using TRIzol reagent (Sigma-Aldrich, St Louis, MO, U.S.A) according to the manufacturer's protocol. cDNA was synthesized using the High Capacity Reverse Transcription Kit from Applied Biosystems. Real-time PCR was performed using an ABI PRISM 7300 Sequence Detection System instrument and software (Applied Biosystems) as described previously (Ghose et al. 2004). Briefly, each reaction mixture (total of 25μl) contained 50-100 ng of cDNA, 300 nM forward primer, 300 nM reverse primer, 200 nM fluorogenic probe, and 15 μl of TaqMan Universal PCR Master Mix. Quantitative expression values were normalized to cyclophilin.

5.3.5 LC-MS/MS sample preparation

CPT-11, SN-38, SN-38G and CPT stock solutions (1mM) were prepared in 50% methanol solution, aliquoted and stored in -80°C. ~10 µl of whole blood sample from the mouse was diluted in 40 µl blank plasma and 5 µl of IS (CPT, 1 µg/ml) and vortexed briefly. Standard samples were prepared by serial dilutions of 45 µl of the highest standard (1000 ng/ml of CPT-11, SN-38 and SN-38G) with 45 µl blank plasma. Then 5 µl of 1 µg/ml of IS was added and the tubes were briefly vortexed. A mixture of 450 µl acetonitrile (ACN) and 450 µl methanol was added to the samples and standards and the tubes were vortexed for 30 sec and centrifuged at 13,200 rpm for 15 min. The supernatant organic solvent (~825 µl) was transferred to clean eppendorf tubes and evaporated in a gentle stream of air at room temperature. The dried extracts were reconstituted in a solution of 50%ACN/50% methanol/1% glacial acetic acid.

5.3.6 Pharmacokinetic studies and analysis

For quantification of analytes in plasma, LC-MS/MS method was utilized. In order to quantitate CPT-11, SN-38, SN-38G and CPT in plasma an API 5500 Qtrap triple quadrupole mass spectrophotometer (Applied Biosystems/MDS SCIEX, Foster City, CA, USA) equipped with a Turbospray TM source was used by multiple reaction monitoring (MRM) method operated in a positive ion mode. The optimization of the LC-MS/MS conditions for analysis of irinotecan and its metabolites was performed as follows. The m/z transition for irinotecan was 587.1/124.1, m/z transition for SN-38 was 393.1/349.1, m/z transition for SN-38G was 569.5/393.1, m/z for CPT was 349.0/305.1 in positive ion mode. The instrument dependent and compound dependent parameters for all the compounds

were optimized as described. The following compound dependent parameters were optimized: declustering potential (DP), entrance potential (EP), cell exit potential (CXP) and the collision energy (CE). The following instrument dependent parameters were optimized for the compounds: ion spray voltage, ion source temperature, nebulizer gas (gas 1), turbo gas (gas 2) and the curtain gas. The flow rate of the sample during Mass method optimization was set between 7 - 20 μL/min. The UPLC conditions for the compounds were: system, Waters Acquity™ (Milford, MA, USA) with DAD detector; column, Acquity UPLC BEH C18 column (50×2.1mm I.D., 1.7μm, Waters); mobile phase A, 0.1% formic acid; mobile phase B, 100%, acetonitrile; gradient, 0-0.5 min, 10% B, 0.5-1 min, 25% B, 1-2 min, 40% B, 2-2.5 min, held constant at 40% B, 2.5-3 min, 10% B, respectively. Flow rate was 0.4 ml/min, column temperature, 45 degree; injection volume, 10 μL.

The PK data was analyzed using the WinNonlin 3.3 PK modeling software from Pharsight Corporation (Mountain View, California). The data was fitted to a non-compartmental model for pharmacokinetic analysis of CPT-11 and its metabolites. Pharmacokinetic parameters, including maximum plasma concentration (Cmax), time to reach Cmax (Tmax), elimination rate constant (ke), half-life (t1/2), rate at which drug is cleared from the body (CL), volume of distribution (Vd) and plasma exposure or area under the curve (AUC) were directly derived from WinNonlin.

5.3.7 Statistical Analysis

All data presented as mean ± S.D from 4-5 mice per group. The data were analyzed by un-paired student's t-test using GraphPad Prism 5.2 software (GraphPad Inc., La Jolla, CA) and *$p < 0.05$ was considered to be statistically significant.

5.4 Results

5.4.1 PCN and LPS alter the gene expression of Cyp3a11 and Ugt1a1 in opposite directions

Firstly, we measured Cyp3a11 and Ugt1a1 expression because these are the main DMEs involved in metabolism of Irinotecan. We observed that treatment with LPS downregulated Cyp3a11 gene expression significantly by almost 90% and similarly PCN upregulated Cyp3a11 gene expression by 16 folds as compared to control (Fig. 5.4.1A). Combined treatment of PCN and LPS showed significantly higher gene expression as compared to control and Cyp3a11 expression reduced by almost 50% with combined treatment as compared to PCN treatment. Alteration of *Ugt1a1* expression with LPS and PCN was significant but not as robust as *Cyp3a11* expression. Treatment with LPS alone reduced the mRNA expression of Ugt1a1 by ~50% as compared to control. With PCN on the other hand, significant up-regulation of Ugt1a1 was observed.

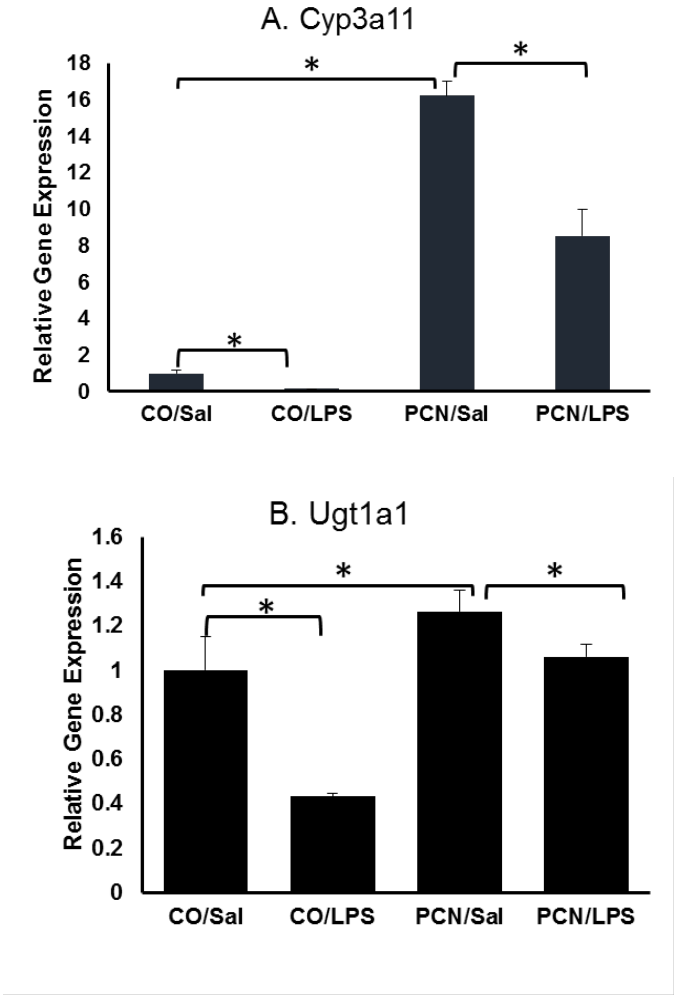

S.No	CO/ Sal	CO/LPS	PCN/Sal	PCN/LPS
1	0.957	0.454	1.328	1.131
2	1.233	0.434	1.296	0.977
3	1.004	0.453	1.128	1.083
4	0.845	0.407	1.356	1.089
Average of Ugt1a1 fold change	1.009	0.437	1.277	1.070
SD	0.163	0.022	0.102	0.065

Fig. 5.4.1 Regulation of DME genes by PCN and LPS.

C57Bl/6 mice (n=4/ group) were administered PCN (50 mg/kg/day) I.P. or corn oil for three days followed by treatment with LPS (2 mg/kg) or saline I.P. for 16 hours. Livers were harvested and gene expression of (**A**) Cyp3a11 and (**B**) Ugt1a1 in mouse liver (n=4) is represented as ± S.D. and standardized for cyclophilin mRNA levels. * $p<0.05$

5.4.2 Pharmacokinetic analysis of irinotecan and its metabolites with LPS treatment

In order to measure alteration in PK of irinotecan and its metabolites, we performed pharmacokinetic (PK) studies after treatment of LPS in C57Bl/6 mice. The data was analyzed by non-compartmental analysis using WinNonLin software 3.3 (Pharsight Corporation Mountain View, California). The plasma PK data revealed significantly higher plasma AUC and Cmax of irinotecan after LPS treatment as compared to control, as expected. However, plasma AUC and Cmax of metabolites of irinotecan i.e. SN38 and SN38-G did not change significantly as compared to control.

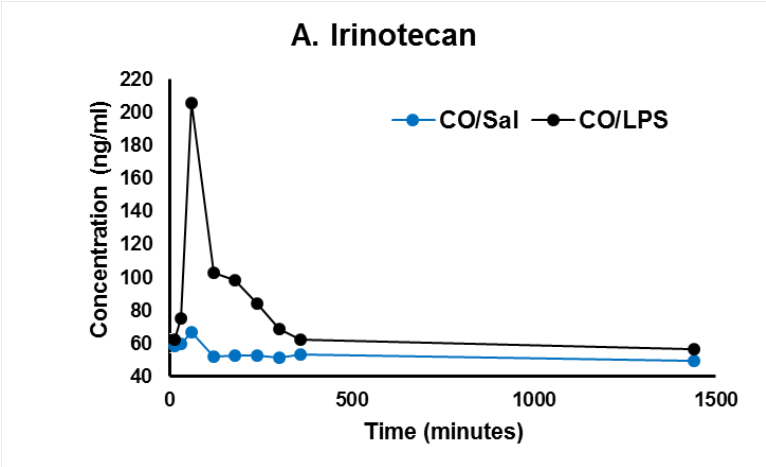
A. Irinotecan
CO/Sal
CO/LPS
Concentration (ng/ml)
220
200
180
160
140
120
100
80
60
40
0
500
1000
1500
Time (minutes)

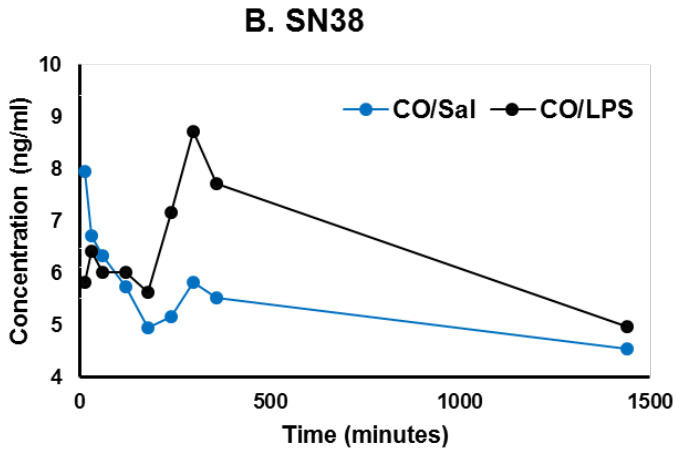
B. SN38
CO/Sal
CO/LPS
Concentration (ng/ml)
10
9
8
7
6
5
4
0
500
1000
1500
Time (minutes)

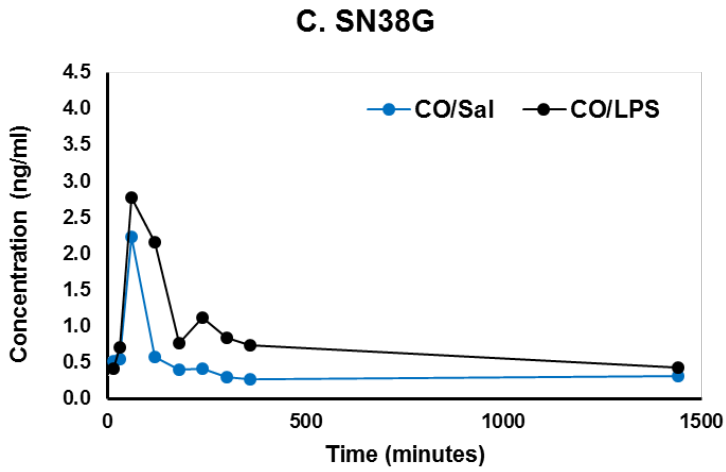
C. SN38G
CO/Sal
CO/LPS
Concentration (ng/ml)
4.5
4.0
3.5
3.0
2.5
2.0
1.5
1.0
0.5
0.0
0
500
1000
1500
Time (minutes)

Fig. 5.4.2 PK profile of irinotecan, SN38 and SN38-G after treatment with LPS

C57Bl/6 mice (n=4/ group) were administered LPS (2 mg/kg) or saline I.P. and irinotecan hydrochloride solution (10 mg/kg) by oral gavage and whole blood samples were collected at predetermined time points (0, 15, 30, 60, 120, 240, 360, 480, 600 and 1440 mins) from the tail vein in heparinized Eppendorf tubes. Plasma concentrations versus time profiles from 0 to 24 h for irinotecan (**A**), SN-38 (**B**) and SN-38G (**C**) are shown. Plasma samples were processed as described earlier. n = 4. Data are shown as mean ± S.D.

5.4.3 Pharmacokinetic analysis of irinotecan and its metabolites with PCN and LPS treatment

Lastly, in order to measure whether treatment with PXR activator would reverse the effect of alteration in PK of irinotecan and its metabolites by LPS, we performed pharmacokinetic (PK) studies after treatment of PCN and LPS in C57Bl/6 mice. The data was analyzed by non-compartmental analysis using WinNonLin software 3.3 (Pharsight Corporation Mountain View, California). For the parent compound i.e. irinotecan, significantly higher plasma AUC and Cmax as compared to control was observed as before (Table 5.4.3). Interestingly, PCN treatment also increased plasma concentration of irinotecan and SN38 as compared to control, although it was not significant. Combined PCN and LPS treatment showed higher plasma concentrations for both parent and metabolites as compared to control.

Parameter	Saline	LPS	PCN	LPS + PCN
A. Irinotecan				
AUC (min*ng/ml)	75199.5 ± 1803.2	**106617.8 ± 3725.03**	77352.19 ± 3345.42	111603.2 ± 30938.8
Cmax (ng/ml)	68.60 ± 9.65	**205.50 ± 2.12**	76.33 ± 7.92	117.80 ± 40.23
Tmax (min)	160 ± 17.21	60	37.5 ± 25.98	97.5 ± 66.5
B. SN38				
AUC (min*ng/ml)	7574.15 ± 163.14	8759.82 ± 1684.28	9135.13 ± 2340.2	13473.36 ± 6311.85
Cmax (ng/ml)	7.95 ± 1.47	7.21 ± 1.67	16.99 ± 11.33	23.57 ± 2.26
Tmax (min)	30 ± 25.98	150 ± 137.48	26.25 ± 22	142.5 ± 113.25
C. SN38-G				
AUC (min*ng/ml)	519.97 ± 80.14	1045.24 ± 412.95	491.85 ± 71.92	914.37 ± 423
Cmax (ng/ml)	1.66 ± 0.96	2.80 ± 1.41	0.89 ± 0.27	2.60 ± 1.2
Tmax (min)	45 ± 25.9	120 ± 34.6	86.25 ± 22.5	150 ± 103.92

Table 5.4.3 Pharmacokinetic parameters of irinotecan and its metabolites

Pharmacokinetics parameters of irinotecan, SN-38 and SN-38G were calculated using WinNonlin 5.2 software. Data are shown as mean ± S.D. * indicates statistical significance at $p<0.05$ when compared to the lean group.

A. Irinotecan

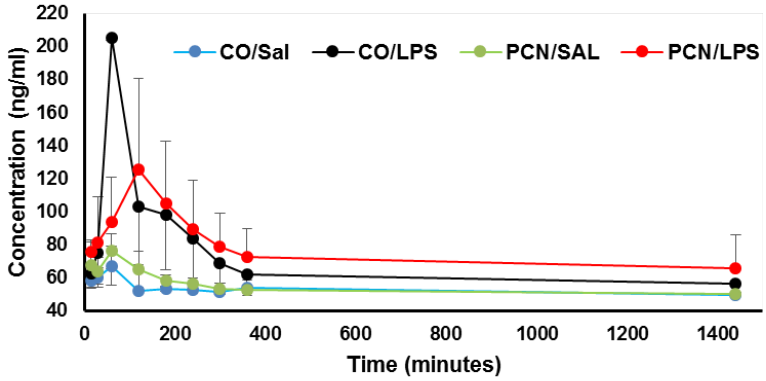

B. SN38

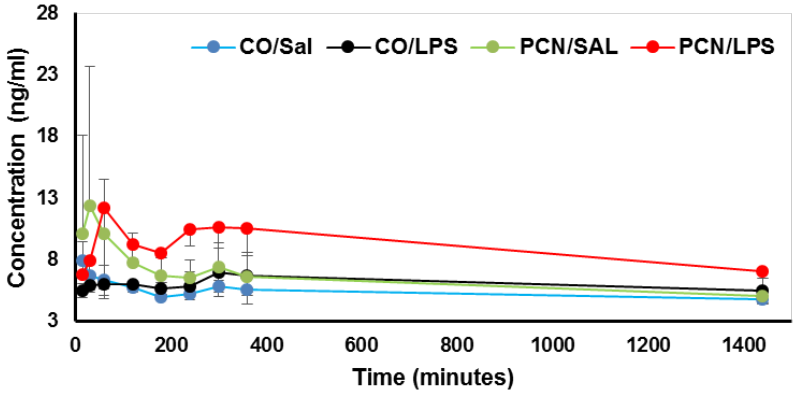

SN38G

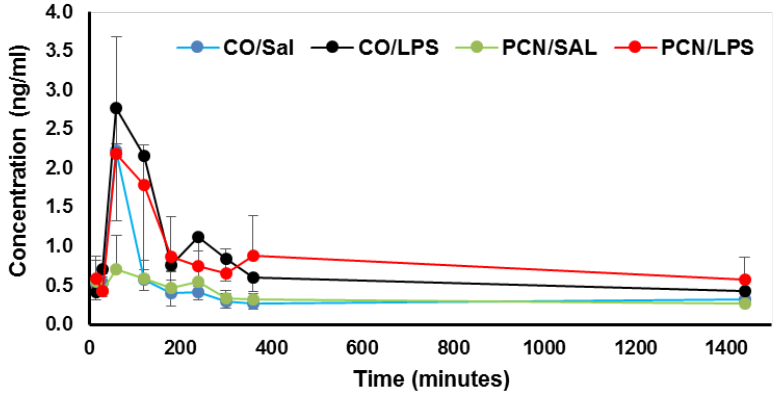

CPT11

	CO/Sal					CO/LPS					PCN/SAL						PCN/LPS					
Time	Mouse 1	Mouse 2	Mouse 3	Average	SD	Mouse 1	Mouse 2	Mouse 3	Average	SD	Mouse 1	Mouse 2	Mouse 3	Mouse 4	Average	SD	Mouse 1	Mouse 2	Mouse 3	Mouse 4	Average	SD
15	62.8	55	57.1	58.30	4.04	59.4	66.3	61.3	62.33	3.56	68.7	81.3	52.8		67.60	14.28	83.7	73.7	70.5		75.97	6.89
30	64.3	55.9		60.10	5.94	67.7	65.7	92.5	75.30	14.93	71.7	61.4	53.9	69.5	64.13	8.13	112	59.3	72.6		81.30	27.41
60	68.3	54.9	78.4	67.20	11.79		207	204	205.50	2.12	80.5	68	67.2	89.2	76.23	10.58	108	62.5	111		93.83	27.18
120	52.7	51.3	53	52.33	0.91	67.4	104	138	103.13	35.31	79.4	55.2	58.9	67.3	65.20	10.74	161	68.1	90.2	183	125.58	55.10
180	52.6	51.7	54.7	53.00	1.54	61	125	109	98.33	33.31	58.5	53.4	57.5	62.8	58.05	3.86	130	81.4	65.3	143	104.93	37.43
240	51.9	51.3	55.1	52.77	2.04	56.7	92.5	103	84.07	24.27	59.4	56.4	52.7		56.17	3.36	125	70.9	60.7	102	89.65	29.39
300	51.9	50.8	51.1	51.27	0.57	54.9	76.3	75.2	68.80	12.05	58.3	50.8	51.2	53.4	53.43	3.45	97.4	68.3	55.3	93.3	78.58	20.15
360	51.2	59.1	50.7	53.67	4.71	54.6	63.6	68.7	62.30	7.14	53.4	52.4	50.1	53.5	52.35	1.58	94.1	66.2	53	77	72.58	17.39
1440	49.7	49.5	49.5	49.57	0.12	50.1	59.4	60	56.50	5.55	51.6	49.5	50	50.2	50.33	0.90	95.6	53.2	51	62.8	65.65	20.61

SN38

	CO/Sal					CO/LPS					PCN/SAL						PCN/LPS					
Time	Mouse 1	Mouse 2	Mouse 3	Average	SD	Mouse 1	Mouse 2	Mouse 3	Average	SD	Mouse 1	Mouse 2	Mouse 3	Mouse 4	Average	SD	Mouse 1	Mouse 2	Mouse 3	Mouse 4	Average	SD
15	9.57	6.69	7.58	7.95	1.47	5.47	6	4.93	5.47	0.54	5.19	19.3	5.7		10.06	8.00	6.4	7.01	7.06		6.82	0.37
30	7.05	5.65	7.44	6.71	0.94	6.35	6.09	5.23	5.89	0.59	5.13	8.55	6.85	29.1	12.41	11.22	6	7.12	10.6		7.91	2.40
60	6.21	5.19	7.6	6.33	1.21	6.3		5.74	6.02	0.40	4.97	9.19	10.5	15.7	10.09	4.42	6.19	6.88	13.6	22.1	12.19	7.40
120	5.68	5.39	6.14	5.74	0.38	5.9		6.15	6.03	0.18	5	7.81	7.16	10.9	7.72	2.44	8.98	8.37	8.67	10.9	9.23	1.14
180	5.04	4.89	4.96	4.96	0.08	6.01		5.24	5.63	0.54	4.68	7.25	6.94	7.97	6.71	1.42	6.05	7.79	6.89	13.5	8.56	3.37
240	5.19	5.16	5.18	5.18	0.02	5.35	7.12	5.04	5.84	1.12	5.14	6.97	5.52	8.35	6.50	1.47	9.11	11.9	9.46	11.2	10.42	1.35
300	5.76	5.39	6.32	5.82	0.47	6.27	9.15	5.37	6.93	1.97	5.03	8	6.9	9.69	7.41	1.96	7.53	10.6	6.98	17.4	10.63	4.79
360	5.49	5.72	5.36	5.52	0.18	5.81	8.55	5.66	6.67	1.63	4.58	6.74	5.74	9.24	6.58	1.98	6.75	8.45	7.2	19.8	10.55	6.21
1440	4.68	5.15	4.44	4.76	0.36	4.55	6.56	5.38	5.50	1.01	4.6	4.84	5.22	5.47	5.03	0.39	8.07	5.14	5.34	9.72	7.07	2.22

SN38G

	CO/Sal					CO/LPS					PCN/SAL						PCN/LPS					
Time	Mouse 1	Mouse 2	Mouse 3	Average	SD	Mouse 1	Mouse 2	Mouse 3	Average	SD	Mouse 1	Mouse 2	Mouse 3	Mouse 4	Average	SD	Mouse 1	Mouse 2	Mouse 3	Mouse 4	Average	SD
15		0.557	0.487	0.52	0.05	0.452	0.49	0.301	0.41	0.10	0.465	0.907	0.262		0.54	0.33	0.851	0.483	0.43		0.59	0.23
30	0.716	0.553	0.355	0.54	0.18	0.583	0.612	0.933	0.71	0.19	0.513	0.304	0.272	0.633	0.43	0.17	0.681	0.287	0.307		0.43	0.22
60	2.29		2.16	2.23	0.09	1.94	4.44	1.94	2.77	1.44	0.376	0.287	1.05	1.12	0.71	0.44	1.17		1.46	3.91	2.18	1.51
120	0.686	0.429	0.602	0.57	0.13	0.709	3.75	2.03	2.16	1.52	0.28	0.689	0.525	0.84	0.58	0.24	2.38		1.53	1.46	1.79	0.51
180	0.335	0.282	0.586	0.40	0.16	0.709		0.808	0.76	0.07	0.291	0.436	0.399	0.766	0.47	0.20		0.597	0.565	1.46	0.87	0.51
240	0.49	0.299	0.456	0.42	0.10	0.673	1.57		1.12	0.63	0.505	0.752	0.37		0.54	0.19		0.709	0.964	0.59	0.75	0.19
300	0.258	0.408	0.232	0.30	0.10	0.612	1.16	0.741	0.84	0.29	0.305	0.293	0.242	0.484	0.33	0.11		0.797	0.305	0.874	0.66	0.31
360	0.245	0.213	0.354	0.27	0.07	0.387	0.716	0.711	0.60	0.19	0.309	0.325	0.229	0.406	0.32	0.07	1.52	0.683	0.329	1.01	0.89	0.51
1440	0.329	0.332	0.288	0.32	0.02	0.273	0.529	0.474	0.43	0.13	0.249	0.203	0.382	0.241	0.27	0.08		0.29	0.55	0.868	0.57	0.29

Raw Data

Fig. 5.4.3 PK profile of irinotecan, SN38 and SN38-G after treatment with PCN and LPS

C57Bl/6 mice (n=4/ group) were administered PCN (50 mg/kg/day) I.P. or corn oil for three days. On day four, mice were co-administered LPS (2 mg/kg) or saline I.P. and irinotecan hydrochloride solution (10 mg/kg) by oral gavage. Whole blood samples were collected at predetermined time points (0, 15, 30, 60, 120, 240, 360, 480, 600 and 1440 mins) from the tail vein in heparinized Eppendorf tubes. Plasma concentrations versus time profiles from 0 to 24 h for irinotecan (**A**), SN-38 (**B**) and SN-38G (**C**) are shown. Plasma samples were processed as described earlier. n = 4. Data are shown as mean ± S.D.

5.5 Discussion

In this work, we address whether PXR-mediated alteration of CYP3A expression could interfere with the metabolism of irinotecan used in treatment of colorectal liver metastasis and thereby, could potentially be used to reduce its toxicity. First we showed that Lipopolysaccharide (LPS) administration increased the plasma concentration of Irinotecan and its metabolites *in vivo*. This was fairly expected as we and others have shown that activation of hepatic TLR4 by LPS suppresses expression of drug metabolizing enzymes (DMEs) and transporters (Ghose et al. 2009). Unexpectedly, activation of PXR by PCN further increased the plasma concentrations of the metabolites of irinotecan i.e. SN38 and SN38-G with combined PCN and LPS treatment.

Although highly efficacious, SN-38 (primary metabolite of Irinotecan) is highly toxic and the intestinal epithelial cells undergo considerable stress due to its accumulation in the gut. Lipopolysaccharide (LPS) is a bacterial endotoxin, and its production is increased during intestinal damage. Although it is well known that LPS downregulates drug metabolizing enzymes i.e. Cyp3a11, Ugt1a1 and carboxylesterases (Mao et al, 2011) expression, the impact of this alteration on PK of irinotecan and its metabolites is unknown. We found that plasma concentrations of the parent were increased significantly upon LPS administration as compared to control. Although we observed increased plasma concentrations of SN38 and SN38-G with LPS, this effect was not significant. This could possibly due to the fact that LPS does not downregulate the expression of phase 2 enzyme- *Ugt1a1* as robustly as *Cyp3a11*.

Gastrointestinal toxicity was substantially reduced when antibiotics or inhibitors of bacterial glucuronidase were used in combination with irinotecan. However, the use of broad spectrum of antibiotics often leads to severe disruption of the microbial homeostasis in the intestine and can result in other negative consequences. A promising alternative would be to use an agent which would reverse the expression of DMEs and thus might prevent accumulation of SN38 in the body by increasing the clearance of irinotecan. Therefore, we used PCN, a specific mouse PXR activator, to induce DMEs after LPS administration and studied the PK of irinotecan. PXR plays a major role in the metabolism of xenobiotics in liver and intestine via induction of drug-metabolizing enzymes and accumulating evidence strongly points to the differential role of PXR in cancer growth and progression as well as in chemotherapy outcome. Upon PCN administration, we did not see significant alteration in the parent concentration, however, PCN potentiated the effect of LPS on the PK of its metabolites SN38 and SN38G. Higher plasma concentrations of SN38 could probably be due to increased expression of PXR target genes, MDR1, MRP-2 and BCRP, upon PCN administration, which are also involved with effluxing SN38 from the hepatocytes into the bile and ultimately systemic circulation via the gut. Apart from that, since we only measured plasma concentration, it would be interesting to note whether the actual hepatic and intestinal concentration of irinotecan and its metabolites is altered by PXR activation.

Chapter 6

Role of via c-Jun-N-terminal kinase in pregnane X receptor mediated induction of cytochrome P450 3A4

6.1 Abstract

Cytochrome P450 (CYP) 3A4 is the most abundant drug metabolizing enzyme, and is responsible for the metabolism of ~50% of clinically available drugs. Induction of CYP3A4 impacts the disposition of its substrates and leads to harmful clinical consequences such as failure of therapy. In order to prevent such undesirable consequences, molecular mechanisms of regulation of CYP3A4 need to be fully understood. *CYP3A4* induction is primarily regulated by the xenobiotic nuclear receptor, pregnane-X-receptor (PXR). After ligand binding, PXR is transported to the nucleus, where it binds to the *CYP3A4* promoter and induces its gene expression. It is known that PXR function is modulated by phosphorylation(s) by multiple kinases. In this study, we determined the role of the c-Jun-N-terminal kinase (JNK) in PXR-mediated induction of CYP3A4 enzyme *in vitro*. HepG2 cells were transfected with CYP3A4 luciferase and PXR plasmid followed by sequential treatment with JNK inhibitor and rifampicin (RIF, specific PXR activator). Treatment with JNK inhibitor (SP600125; SP) significantly attenuated RIF-mediated *CYP3A4* reporter activity as well as gene expression and enzyme activity. JNK knockdown by siRNA (targeting both JNK 1 and 2) also attenuated CYP3A4 induction by RIF. Interestingly, SP treatment attenuated JNK activation by RIF. Furthermore, treatment with RIF increased PXR nuclear levels and binding to the *CYP3A4* promoter; SP attenuated these effects. This study shows that JNK is a novel mechanistic regulator of CYP3A4 induction by PXR.

6.2 Introduction

The cytochrome P450 (CYP450) 3A4 enzyme is the most important contributor of hepatic and intestinal metabolism in adults (Guengerich, 1995; Leeder & Okey, 1996; Krishna & Klotz, 1994; Wilkinson, 2005). CYP3A4 is responsible for the metabolism of more than 50% of drugs currently used therapeutically for a wide spectrum of disorders such as cancer, fungal/ bacterial infections, neurological disorders, hepatitis, AIDS etc (Guengerich, 1999; Veith et al, 2009; Zanger et al, 2013). Moreover, CYP3A4 enzyme plays a crucial endogenous role in bile acid detoxification and metabolism of steroid hormones (Waxman et al, 1991; Araya et al, 1999).

Induction of CYP3A4 enzyme expression and activity is known to alter the absorption, disposition, metabolism and/or elimination of co-administered drugs (Thummel & Wilkinson, 1998). A recent study showed that St. John wort's supplementation significantly increased the clearance and decreased the mean area under the curve (AUC) of the chemotherapeutic drug docetaxel (Goey et al, 2014). Similarly, a phase 1 trial showed that concomitant administration of the chemotherapeutic agent, bexarotene induced CYP3A4, leading to 50% reduction of AUC of the CYP3A4 substrate, atorvastatin, a lipid-lowering agent (Wakelee et al, 2012). Therefore, induction of CYP3A4 enzyme could result in drug-drug interactions (DDIs), failure of therapy or drug toxicities in patients.

CYP3A4 gene is both constitutively expressed, as well as transcriptionally induced by structurally diverse xenobiotics and endobiotics. Induction of CYP3A4 usually takes

place via activation of nuclear receptors (NRs). A number of clinically important drugs bind to and activate NRs such as pregnane-X-receptor (PXR), constitutive androstane receptor (CAR), glucocorticoid receptor (GR) and vitamin D-receptor (VDR) to induce CYP3A4 (Pascussi et al, 2003; Luo et al, 2004). Among these NRs, PXR is primarily responsible for regulating the induction of CYP3A4 (Goodwin et al, 2002, Xie et al, 2004). PXR has a large ligand-binding domain and can be activated by structurally diverse hydrophobic moieties such as rifampicin, ritonavir, clotrimazole etc (Harmsen et al, 2007; Lehmann et al, 1998). PXR is localized in the cytosol and upon binding with a ligand, it is activated and translocated into the nucleus where it hetrodimerizes with retinoid-X–receptor (RXR). This heterodimer binds to the proximal PXR response element (PXRE) and distal xenobiotic responsive enhancer module (XREM) on *CYP3A4* promoter and lead to its induction (Kliewer et al, 1998). Hence, PXR-mediated *CYP3A4* gene activation is a critical determinant of metabolism, transport and elimination of potentially toxic chemicals, including steroids, xenobiotics & other toxins from the body. Therefore, the mechanism of *CYP3A4* regulation by PXR needs to be fully elucidated.

There is a growing body of evidence that site-specific phosphorylation of PXR provides an important mechanism for PXR-mediated regulation of CYP3A4 (Staudinger et al, 2011). So far, phosphorylation of PXR has been shown to have a repressive effect on the transcription of its target genes. PXR has been shown to be a substrate for cyclic AMP-dependent protein kinase A (PKA), although specific phosphorylation sites are unknown. It was reported that PKA interaction with PXR represses *CYP3A4* gene transcription in a

species specific manner (Ding et al, 2005a; Litchi-Kaiser et al, 2009). Similarly, other kinases such as cyclin-dependent kinase (Cdk2 & 5) directly phosphorylate PXR, and this led to inhibition of *CYP3A4* expression. Cdk2 phosphorylated PXR at Ser350 position which led to repression of *CYP3A4* gene expression in HepG2 cells (Lin et al, 2008). Activation of protein kinase C (PKC) signaling by pro-inflammatory cytokines led to inhibition of PXR transcriptional activity in hepatocytes (Ding et al, 2005b). Furthermore, p70 S6K, a ribosomal protein, was shown to directly phosphorylate PXR *in vitro* at site Thr57, repressing PXR activity (Pondugula et al, 2009). Although direct phosphorylation of PXR is not involved, recent studies have shown that casein kinase 2 (CK2)-mediated phosphorylation of heat shock protein 90 (HSP90) stabilizes PXR and induces its downstream genes (Kim et al, 2015). HSP90 is a 90-kDa molecular chaperone and cytoplasmic retention protein which binds to and sequesters PXR in the cytosol (Squires et al, 2004). Interestingly, the mitogen activated protein kinase (MAPK), c-Jun N-terminal kinase (JNK) was shown to be required for optimal activation of *CYP3A4* gene by NR, VDR (Yasunami et al, 2004). MAPKs consist of two additional members, extracellular signal-regulated kinase (ERK 1/2) and p38 kinase (Zhou et al., 2009). These are serine/threonine kinases which transduce extracellular signals from activated receptors on cell surface to different cellular responses by phosphorylating transcriptional factors or downstream kinases (Houliston et al., 2001).

The goal of this investigation was to determine the role of JNK in PXR-mediated induction of *CYP3A4* gene. We observed that inhibition of JNK significantly attenuated

the induction of CYP3A4 reporter activity, gene expression as well as enzyme activity by PXR ligands (rifampicin or hyperforin) in human hepatic cell lines. Further, activation of JNK was observed upon treatment of HepG2 cells with rifampicin. Lastly, JNK inhibitors attenuated ligand-induced PXR nuclear import and binding to the *CYP3A4* promoter.

To our knowledge, this is the first study showing that JNK is required for PXR-mediated induction of CYP3A4. To date, PXR phosphorylations have been associated with attenuation of CYP3A4 induction by PXR. Therefore, JNK may play a novel role in promoting CYP3A4 induction by PXR. These findings may provide insight into understanding functional interactions between cell signaling pathways and drug metabolism and their consequences in drug efficacy and/or toxicity.

6.3 Materials and methods

6.3.1 Materials

HepG2 cells were purchased from ATCC (Manassas, VA). HepaRG cells were purchased from Thermo Fisher Scientific (Waltham, MA, # HPRGC10). Rifampicin (#R3501), Hyperforin (dicyclohexylammonium) salt (#H1792), Curcumin (#C1386) and Dimethyl sulfoxide (DMSO) were purchased from Sigma-Aldrich (St. Louis, MO). SP600125 (#tlrl-sp60), SB203580 (#tlrl-sb20) and PD098059 (#tlrl-pd98) were purchased from InvivoGen (San Diego, CA). A custom siRNA sequence (AGAAUGUCCUACCUUCUUUUU) that simultaneously targets JNK1 and JNK2 and a control siRNA targeting luciferase were both synthesized by Dharmacon (Lafayette, CO). DharmaFECT Duo Transfection reagent was also purchased from Dharmacon. SuperFect Transfection Reagent was purchased from Qiagen (Valencia, CA, #301305). p-CYP3A4-pGL3B luciferase plasmid was obtained as a kind gift from Dr. Rommel G. Tirona, The University of Western Ontario, London, Ontario, Canada. h-PXR-pSG5 plasmid was obtained as a kind gift from Dr. Steven Kliewer, UT Southwestern Medical Center, Dallas, Texas, United States. pRL-TK vector (#E2241), Dual-Glo® luciferase reporter assay kit (#E1910) and P450-Glo™ CYP3A4 Assay (Luciferin-IPA) (#V9002) was purchased from Promega (Madison, WI). Antibodies against phospho-JNK (#9251), JNK (#9252) were purchased from Cell Signaling (Beverly, MA), PXR (#PA5-19080) was purchased from Thermo Scientific (Waltham, MA) and Lamin A/C (#sc-20681) was purchased from Santa Cruz Biotechnology (Dallas, TX). Goat Anti-Rabbit IgG HRP Conjugate antibody (#1706515) was purchased from Bio-Rad

(Hercules, CA). Donkey Anti-goat IgG-HRP (#sc-2020) was purchased from Santa Cruz Biotechnology (Dallas, TX). ChIP grade PXR antibody was purchased from Santa Cruz (#SC-25381X). Chromatin Immunoprecipitation assay was performed using the Magna ChIP™ HiSens Chromatin Immunoprecipitation Kit (#17-10460) purchased from EMD-Millipore (Billerica, MA).

6.3.2 Cell culture and Transfection

HepG2 cells were maintained in Dulbecco's modified Eagle's medium (Life Technologies, Carlsbad, CA) supplemented with 10% fetal bovine serum (Atlanta Biologicals, Flowery Branch, GA). In brief, cells were seeded in 96 well/ 24 well or 6 well format depending on the type of assay at 60-80% confluency. After 24 hours, cells were transfected with CYP3A4, hPXR and pRL-TK vector using SuperFect transfection reagent. For siRNA experiments, co-transfection of plasmids and siRNA was carried out with DharmaFect Duo reagent. A custom siRNA sequence targeting JNK 1 & JNK2 simultaneously and a control siRNA targeting luciferase were used for these experiments. HepG2 cells were transfected with JNK1/2 siRNA along with CYP3A4 luciferase and PXR plasmid using DharmaFect Duo reagent for 24 hours before treatment. HepaRG^{TM} cells were cultured according to the manufacturer's protocol. Cryopreserved cells were thawed with Williams E Medium containing HepaRG^{TM} Thawing/ Plating medium supplement. Cells were seeded in 96 well plates at a density of 0.1 million cells/ml. The cells were allowed to recover at 37°C with a 5% CO_2.

6.3.3 Dual-Glo Luciferase Assay

After 24 hours transfection, cells were pretreated with 30 μM SP600125 (SP; specific JNK 1/2/3 inhibitor) or 25 μM Curcumin (JNK Pathway inhibitor) or 10 μM SB203580 (p-38 inhibitor) or 25 μM PD098059 (ERK inhibitor) for 30 minutes followed by treatment with 1 μM Hyperforin or 10 μM Rifampicin (RIF) or DMSO as control for 24 hours. Following treatment, cells were lysed and Dual-Glo® luciferase assay was carried out, according to manufacturer's instructions (Promega, #E1910). Briefly, cells were lysed using passive lysis buffer. Dual-Glo® Luciferase buffer containing Dual-Glo® Luciferase substrate was added to the lysed cells and firefly luciferase activity was recorded. Stop and Glo® reagent was added next to the same wells to measure Renilla luciferase activity as internal control.

6.3.4 Real time-PCR

Total RNA was isolated from HepG2 cells using TRIzol reagent according to the manufacturer's protocol (Sigma Aldrich; St Louis, MO). cDNA was synthesized using the High Capacity Reverse Transcription Kit from Applied Biosystems. Real-time PCR was performed using an ABI PRISM 7300 Sequence Detection System instrument and software (Applied Biosystems; Foster City, CA) as described previously (Shah et al., 2014; Ghose et al, 2004, 2007). In short, each 25 μl reaction mixture contained 50-100 ng of cDNA, 300 nM forward primer, 300 nM reverse primer, 200 nM fluorogenic probe, and 15 μl of TaqMan Universal PCR Master Mix. We extrapolated the quantitative expression values from standard curves and these values were normalized to GAPDH.

6.3.5 P450-Glo Activity Assay

HepG2 and HepaRG cells were cultured on white-walled, collagen-coated culture plates. After treatment, cells were lysed and luciferase enzymatic activity was measured using a P450-Glo™ commercial kit as per the manufacturer's protocol (Promega, # V9002). Specific CYP3A4 luminogenic substrate, luciferin-IPA, was added to the wells at a concentration of 3 μM and incubated at 37^{o}C for 60 minutes. Light emission from the samples was detected by SpectraMax Microplate Reader/ Luminometer and expressed as Relative Light Units.

6.3.6 Immunoblotting

Whole cell extracts and nuclear and cytosolic extracts were prepared as described previously (Ghose et al., 2007, 2011) and the protein concentration was determined using the bicinchoninic acid (BCA) assay according to the manufacturer's protocol (Pierce, Rockford, IL, U.S.A). Equal amounts of protein (30 μg) were analyzed by SDS-polyacrylamide gel electrophoresis and transferred onto a nitrocellulose membrane. The membranes were probed with specific antibodies, followed by incubation with goat anti-rabbit IgG-HRP secondary antibody or donkey anti-goat IgG secondary antibody. The membranes were then washed and incubated with HyGlo HRP Antibody detection reagent (Denville Scientific, #E2500) as per the manufacturers' instructions. The immunoreactive bands were detected by chemiluminescence method and the band density was analyzed by Image J software (National Institutes of Health, Bethesda, Maryland).

6.3.7 Chromatin Immunoprecipitation (ChIP) Assay

ChIP assays were performed to assess specific binding of PXR complex to the PXR response element on the *CYP3A4* promoter as described in the manufacturer's protocol (EMD Millipore Inc., #17-10460). HepG2 cells were pre-treated with SP (30 μM) or DMSO for 30 minutes, followed by RIF (10 μM) for 24 hours. The cells were then cross-linked with 37% formaldehyde at room temperature for 10 min., washed twice with ice-cold phosphate-buffered saline (PBS) and collected in 1 ml of ice-cold PBS. Cells were pelleted at 800*g* and digested by sonication (15 pulses, 20 sec each, 30 sec. rest in between). The protein-DNA complexes were immunoprecipitated by using ChIP grade anti-PXR antibody. As a negative control, the beads were incubated with lysates without anti-PXR antibody. The chromatin was reverse cross-linked and eluted in 50 μl elution buffer. DNA recovered from this assay was analyzed by end point PCR using primers for PXR binding site in the *CYP3A4* promoter region (forward 5'-AGAACCCAGAACCCTTGGAC-3' and reverse 5'-CTGCCTGCAGTTGGAAGAG-3'). PCR products were analyzed by agarose gel electrophoresis. 10% of the total cell lysate was used as "input". Eluted DNA was further analyzed by real time PCR using same primer mix as mentioned above. ΔΔCt method was used to analyze the difference in fold value in treated vs control groups.

6.3.8 Statistical Analysis

Data are shown as the mean and analyzed with Student's t test or one-way analysis of variance for all groups, followed by pairwise comparisons. Significant values are represented as $P < 0.05$.

6.4 Results

6.4.1 Induction of *CYP3A4* luciferase activity by PXR was mediated by JNK

To determine the role of JNK in induction of *CYP3A4* reporter gene expression, we co-transfected HepG2 cells with plasmids expressing *CYP3A4* reporter gene and PXR, followed by treatment with the PXR ligand, RIF in the presence of JNK inhibitors. *CYP3A4* reporter activity increased ~8 folds in the presence of 10 μM RIF as compared to control (Fig. 6.4.1A). This *CYP3A4* reporter induction by RIF was significantly attenuated by treatment with SP (Fig 6.4.1A), indicating that JNK may be involved in regulating CYP3A4 induction by PXR. We observed that PD098059 (ERK inhibitor) co-treatment also inhibited *CYP3A4* luciferase activity but not SB203580 (p38 inhibitor) (Fig. 6.4.1C). In addition, we also studied the effect of curcumin, a JNK pathway inhibitor on *CYP3A4* reporter expression. As shown in Fig. 1A, 15 μM curcumin significantly attenuated RIF-mediated *CYP3A4* induction by almost 50%. We further confirmed these findings by treating HepG2 cells with another PXR ligand, hyperforin in the presence of the SP (Fig. 6.4.1B). *CYP3A4* luciferase activity was induced ~4 folds by 2 μM hyperforin at 24 hours, and this induction was significantly attenuated by SP. SP had no effect on *CYP3A4* luciferase activity in the absence of RIF or hyperforin, indicating that JNK likely does not affect the basal expression of *CYP3A4* gene.

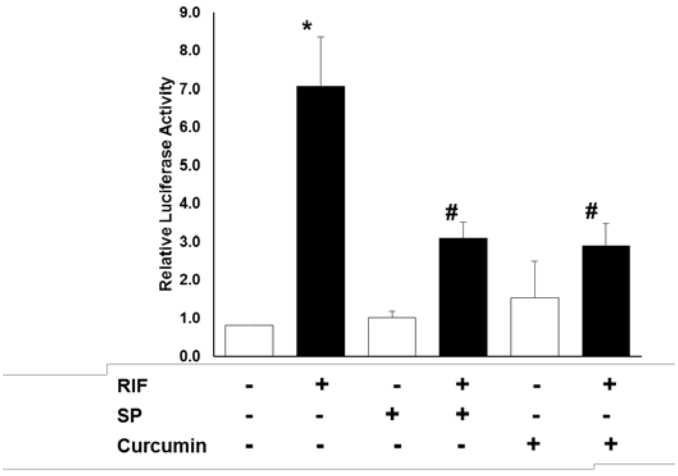

Raw Values

S.No	DMSO/ DMSO	DMSO/ RIF	SP/ DMSO	SP/ RIF	Curcumin/ DMSO	Curcumin/ RIF
1	0.851	7.989	0.942	3.416	2.137	2.603
2	0.810	6.145	1.091	2.769	0.940	3.163
Average	0.830	7.067	1.017	3.092	1.539	2.883
SD	0.029	1.304	0.105	0.458	0.847	0.396

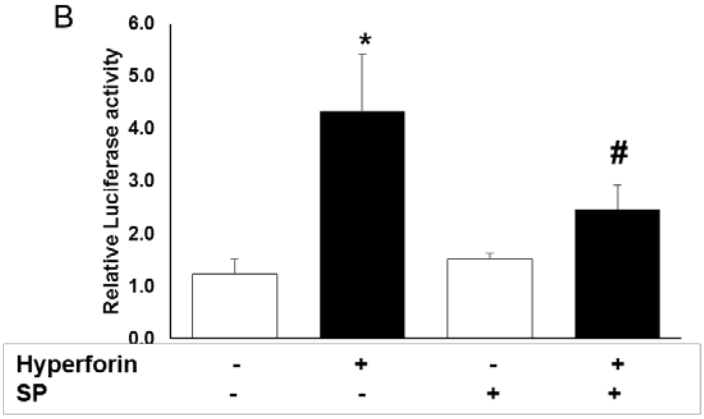

Raw Values

S.No	DMSO/DMSO	DMSO/HYP	SP/DMSO	SP/HYP
1	0.967	3.305	1.534	1.941
2	0.983	3.919	1.361	2.549
3	1.495	5.849	1.645	-
4	1.473	4.250	1.515	2.877
Average	1.229	4.331	1.514	2.455
SD	0.294	1.085	0.117	0.475

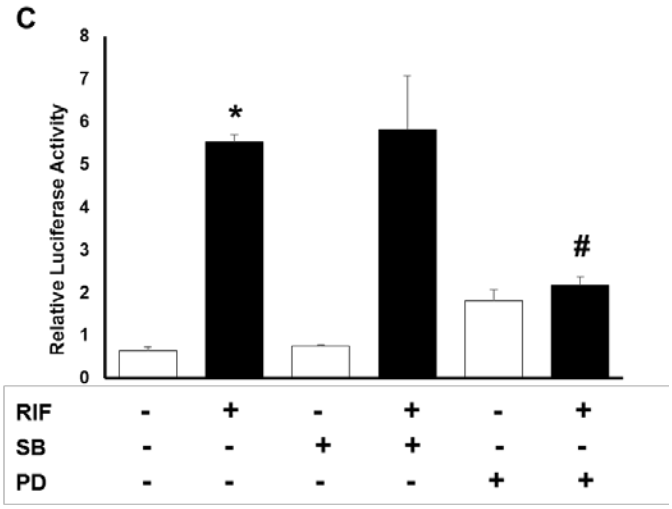

	DMSO/ DMSO	DMSO/ RIF	SB/ DMSO	SB/RIF	PD/ DMSO	PD/RIF
1	0.710	6.071	0.766	3.910	1.985	0.834
2	0.575	5.844	0.746	5.678	1.627	1.113
3	-	4.426	-	7.537	-	4.812
4	-	5.742	-	6.161	-	1.952
Average	0.643	5.521	0.756	5.821	1.806	2.178
SD	0.096	0.161	0.015	1.250	0.253	0.198

Fig. 6.4.1 Induction of *CYP3A4*–luciferase activity by RIF was attenuated by JNK inhibitors.

CYP3A4 luciferase reporter was co-transfected with PXR plasmid into HepG2 cells. Cells were pre-treated with vehicle (DMSO) or 30 μM SP/ 25 μM Curcumin for 30 mins. followed by **A)** 10 μM RIF for 24 h or **B)** 2 μM hyperforin for 48 h or **C)** cells were pre-treated with vehicle (DMSO) or 10 μM SB203580 (p-38 inhibitor) or 25 μM PD098059 (ERK inhibitor) for 30 mins. followed by 10 μM RIF for 24 h and harvested for luciferase activity assays as described under Materials and Methods. The error bars represent the standard deviation from the mean of triplicate assays of an individual experiment. * $p<0.05$ as compared to control treatment. # $p<0.05$ as compared to SP or Curcumin treatment alone.

6.4.2 Knockdown of JNK decreases CYP3A4 luciferase gene expression

To further confirm our results, we investigated the effect of simultaneous knockdown of JNK1 and JNK2 (using a siRNA that targets a homologous region present in both kinases) on CYP3A4 reporter gene induction (Fig 6.4.2). Knockdown of JNK1/2 expression dramatically reduced the ability of RIF to induce *CYP3A4* luciferase activity in HepG2 cells, validating our previous data with pharmacological inhibitors.

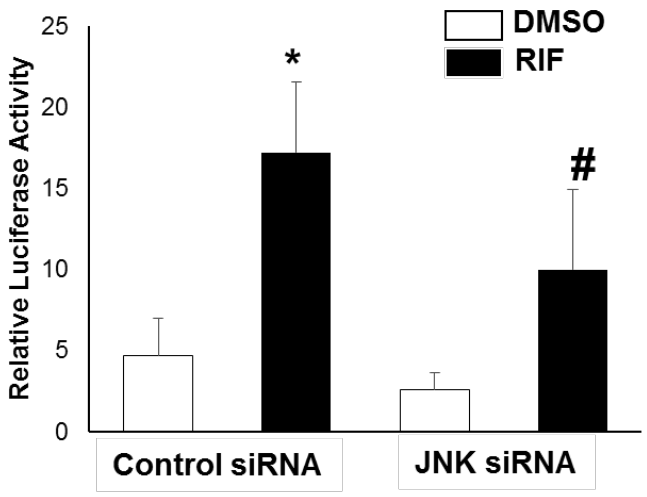

	Cont. siRNA		JNK siRNA	
S.No	DMSO	RIF	DMSO	RIF
1	3.229	15.698	1.403	3.831
2	5.010	14.729	3.722	14.153
3	1.884	17.562	1.837	10.020
4	8.745	24.511	2.204	6.467
5	4.342	13.566	4.008	-
6	4.809	-	2.505	15.431
AVERAGE	4.670	17.213	2.613	9.980
SD	2.310	4.334	1.041	4.931

Fig. 6.4.2 Induction of *CYP3A4* luciferase activity by RIF was attenuated by JNK siRNA.

Custom-made JNK1/2 siRNA was co-transfected with *CYP3A4* luciferase plasmid and PXR plasmid in HepG2 cells. Following transfection, cells were pre-treated with the vehicle (DMSO) or 30 μM SP for 30 mins. followed by 10 μM RIF for 24 h. Cells were lysed, and relative *CYP3A4* luciferase activity was determined. * $p<0.05$ as compared to vehicle control. # $p<0.05$ as compared to non-targeting control siRNA transfected cells.

6.4.3 Induction of CYP3A4 gene expression by PXR was mediated by JNK

To determine the role of JNK in regulating endogenous *CYP3A4* gene expression, HepG2 cells co-treated with SP and RIF were lysed to prepare mRNA and *CYP3A4* gene expression was analyzed. RIF treatment significantly induced *CYP3A4* gene expression from 2 to 12 hours; SP treatment significantly attenuated this induction (Fig. 6.4.3A). These results are in agreement with our CYP3A4 luciferase activity data in transfected HepG2 cells. Since significant attenuation of CYP3A4 reporter gene activity was observed with ERK inhibitor, we also carried out gene expression studies using the ERK inhibitor, PD098059; we found that PD098059 had no effect on RIF-induced *CYP3A4* mRNA levels (Fig. 6.4.3B).

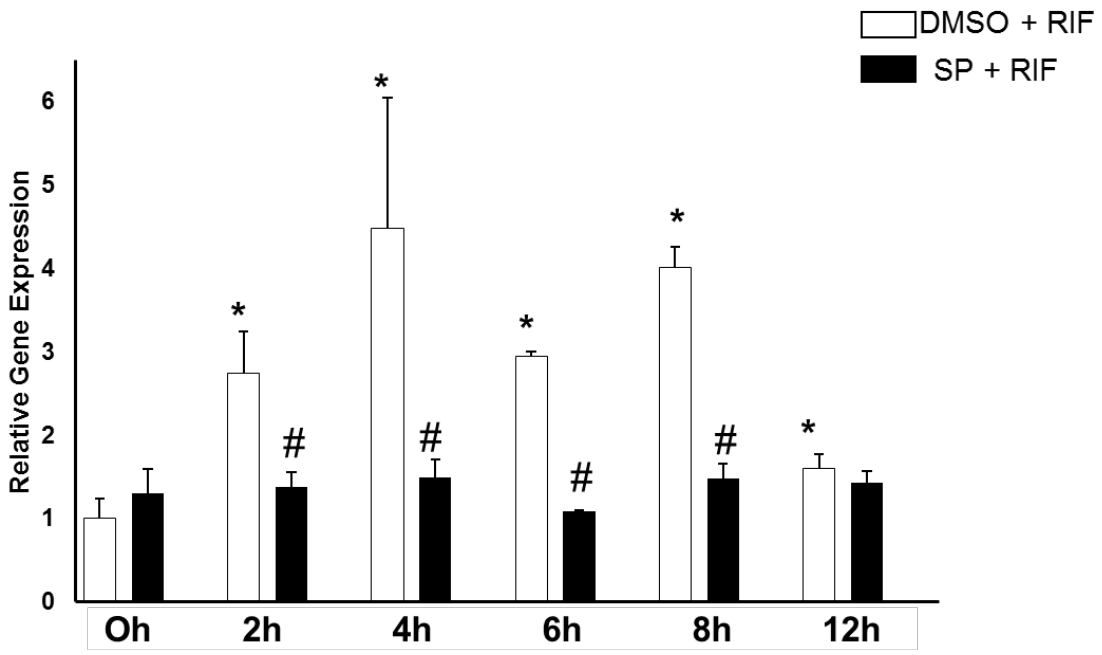

S.No	DMSO/ RIF 0H	SP/ RIF 0H	DMSO/ RIF 2H	SP/ RIF 2H	DMSO/ RIF4H	SP/ RIF 4H	DMSO/ RIF 6H	SP/ RIF6H	DMSO/ RIF 8H	SP/ RIF 8H	DMSO/ RIF12H	SP/ RIF12H
1	1.025	1.648	2.886	1.212	6.281	1.681	3.018	1.131	4.263	1.376	1.863	1.650
2	0.760	1.333	2.257	1.390	4.335	1.641	3.099	1.074	4.266	1.654	1.545	1.346
3	1.284	1.019	3.282	1.613	3.141	1.240	2.939	1.129	3.800	-	1.508	1.384
Avg.	1.023	1.334	2.808	1.405	4.585	1.521	3.019	1.111	4.109	1.515	1.639	1.460
SD	0.26	0.31	0.52	0.20	1.59	0.24	0.08	0.03	0.27	0.20	0.19	0.17

Fig. 6.4.3A Induction of *CYP3A4* gene expression by RIF was attenuated by SP. HepG2 cells were pre-treated with vehicle (DMSO) or 30 μM SP for 30 mins. followed by 10 μM RIF for 0, 2, 4, 6, 8 & 12 h. Relative CYP3A4 mRNA expression (0h samples are set as 1) levels are plotted at different times. * $p<0.05$ as compared to DMSO + RIF 0 h group for each time point. # $p<0.05$ as compared to DMSO + RIF for each time point.

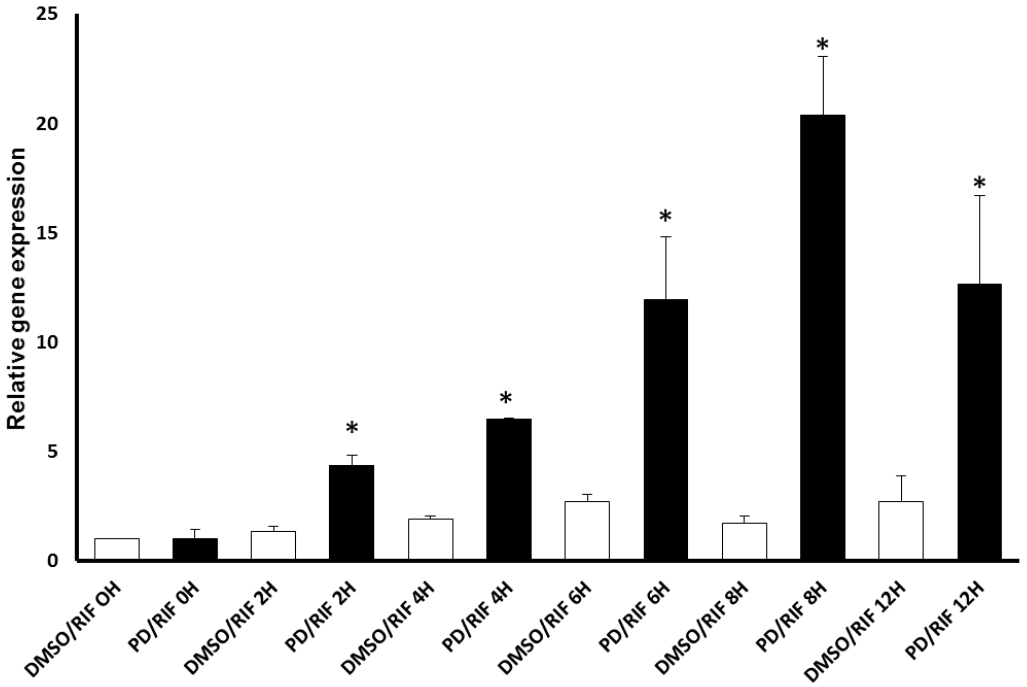
Relative gene expression
25
20
15
10
5
0
*
*
*
*
DMSO/RIF OH
PD/RIF 0H
DMSO/RIF 2H
PD/RIF 2H
DMSO/RIF 4H
PD/RIF 4H
DMSO/RIF 6H
PD/RIF 6H
DMSO/RIF 8H
PD/RIF 8H
DMSO/RIF 12H
PD/RIF 12H

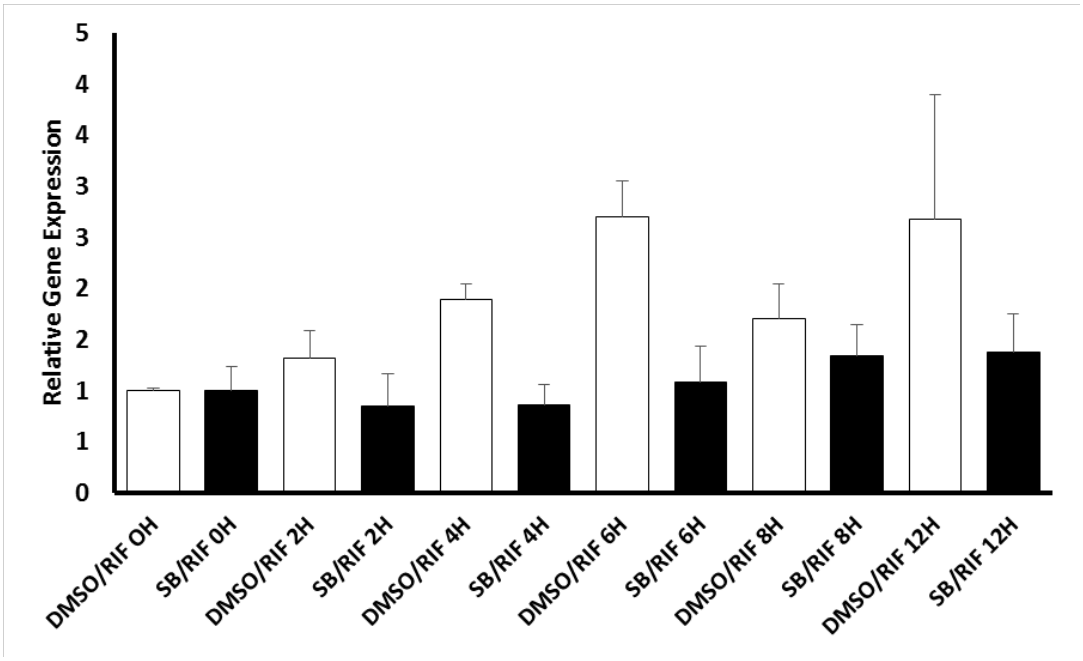
Relative Gene Expression
5
4
4
3
3
2
2
1
1
0
DMSO/RIF OH
SB/RIF 0H
DMSO/RIF 2H
SB/RIF 2H
DMSO/RIF 4H
SB/RIF 4H
DMSO/RIF 6H
SB/RIF 6H
DMSO/RIF 8H
SB/RIF 8H
DMSO/RIF 12H
SB/RIF 12H

Fig. 6.4.3B Induction of *CYP3A4* gene expression by RIF in presence or absence of SB and PD. HepG2 cells were pre-treated with vehicle (DMSO) or 25 μM PD or 10 μM SB for 30 mins. followed by 10 μM RIF for 0, 2, 4, 6, 8 & 12 h. Relative CYP3A4 mRNA expression (0h samples are set as 1) levels are plotted at different times. * $p<0.05$ as compared to DMSO + RIF 0 h group for each time point. # $p<0.05$ as compared to DMSO + RIF for each time point.

6.4.4 Induction of CYP3A4 enzyme activity by PXR was mediated by JNK

We performed P450-Glo™ assay to determine the role of JNK in PXR-mediated induction of CYP3A4 enzyme activity. As shown in Fig.6.4.4A, treatment of HepG2 cells with RIF significantly induced CYP3A4 enzyme activity (~2 times) as compared to control, and SP attenuated this induction of CYP3A4 enzyme activity as measured by the metabolism of the CYP3A4-specific substrate, luciferin IPA. In order to confirm our findings, we also conducted CYP3A4 activity assays in HepaRG™ cells, which are terminally differentiated hepatic cells derived from a human hepatic progenitor cell line that retains many characteristics of primary human hepatocytes (Parent et al, 2004). We observed a similar trend in HepaRG™ cells; RIF treatment significantly induced CYP3A4 enzyme activity from 4-12 h; while no such induction was observed in the presence of JNK inhibitor, SP (Fig.6.4.4B). Consistent with our gene expression results, SP does not affect CYP3A4 enzyme activity in the absence of RIF, indicating that JNK is likely not involved in regulating basal CYP3A4 activity.

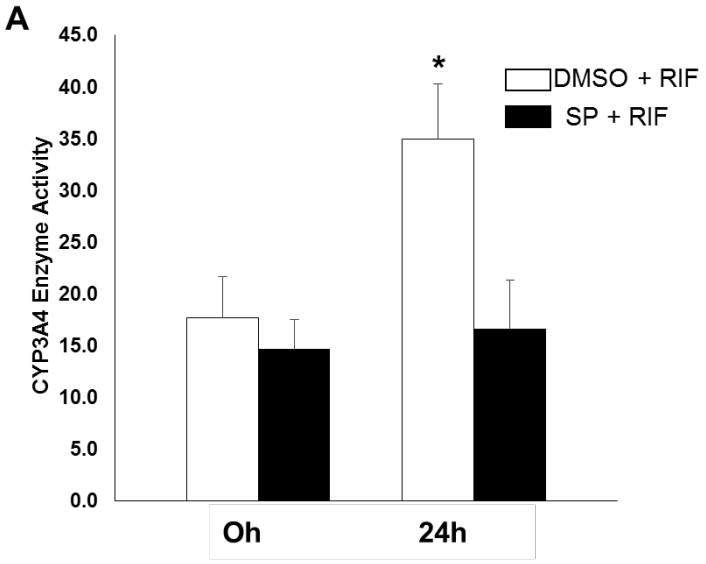

	1	2	3	4	Average	SD
DMSO/RIF 0H	22.66	15.995	18.661	13.329	17.66	3.98
SP/RIF 0H	18.661	14.662	11.996	13.329	14.66	2.88
DMSO/RIF 24H	42.654	33.323	30.657	33.323	34.99	5.26
SP/RIF 24H	21.327	13.329	19.994	11.996	16.66	4.68

Fig. 6.4.4 A) Induction of RIF-mediated CYP3A4 activity was attenuated by SP. HepG2 cells were pre-treated with vehicle (DMSO) or 30 μM SP for 30 minutes followed by 10 μM RIF for 24 hours. Following treatment, cells were incubated with specific CYP3A4 substrate, 3 μM Luciferin IPA for 60 minutes and luminescence was detected. *$p<0.05$ as compared to DMSO + RIF 2 h group. # $p<0.05$ as compared to DMSO + RIF for each time point.

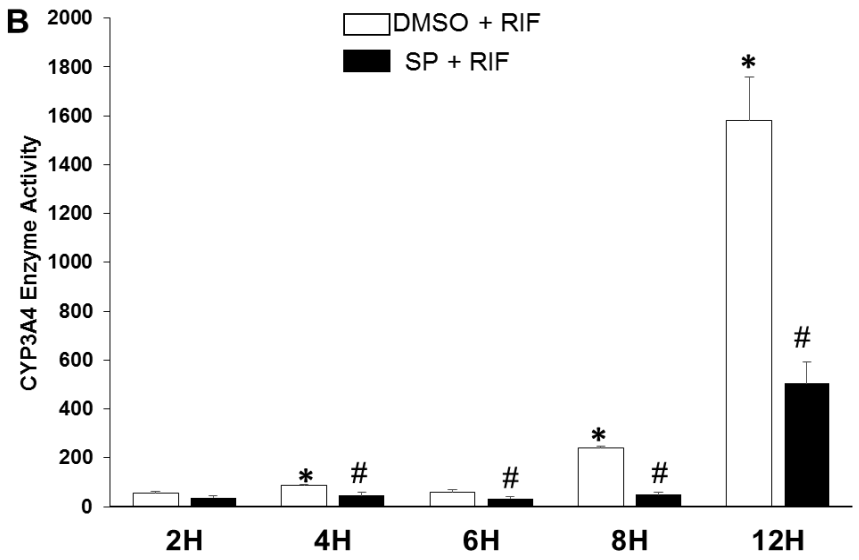

	DMSO/ RIF 2H	SP/RIF 2H	DMSO/ RIF 4H	SP/RIF 4H	DMSO/ RIF 6H	SP/RIF 6H	DMSO/ RIF 8H	SP/ RIF 8H	DMSO/ RIF 12H	SP/RIF 12H
1	61.431	42.234	-	53.752	-	28.156	236.764	38.394	1829.919	456.836
2	43.513	38.394	84.467	29.436	72.949	40.954	239.324	53.752	1769.437	447.828
3	57.591	30.715	78.068	51.192	55.032	31.995	247.003	57.591	1499.195	422.091
Average	54.18	37.11	81.27	44.79	63.99	33.70	241.03	49.91	1699.52	442.25
SD	9.43	5.87	4.52	13.36	12.67	6.57	5.33	10.16	176.10	18.03

Fig. 6.4.4 B) Induction of RIF-mediated CYP3A4 activity was attenuated by SP. HepaRG cells were pre-treated with vehicle (DMSO) or 30 μM SP for 30 mins. followed by 10 μM RIF for 2, 4, 6, 8 & 12 h. Following treatment, cells were incubated with specific CYP3A4 substrate, 3 μM Luciferin IPA for 60 minutes and luminescence was detected. *$p<0.05$ as compared to DMSO + RIF 2 h group. # $p<0.05$ as compared to DMSO + RIF for each time point.

6.4.5 RIF treatment activated JNK *in vitro*

Since treatment with JNK inhibitors resulted in attenuation of PXR-mediated CYP3A4 reporter activity, gene expression as well as enzyme activity, we determined the role of RIF in activation of JNK. Whole cells extracts were prepared from treated HepG2 cells and immunoblot analysis was carried out to determine phospho-JNK protein expression. Interestingly, we found that both phospho-JNK1 (P-JNK1) and phospho-JNK2 (P-JNK2) levels increased by RIF starting at 60 minutes (Fig. 6.4.5A and B). In the presence of JNK inhibitor, SP, P-JNK levels were significantly lower in RIF-treated cells. In agreement with these findings, we found that the JNK substrate, c-Jun was phosphorylated after RIF treatment for 4 h, and this phosphorylation was attenuated in the presence of SP (Fig. 6.4.5C and D).

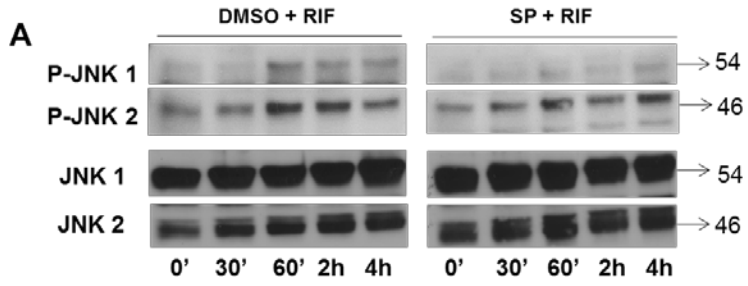

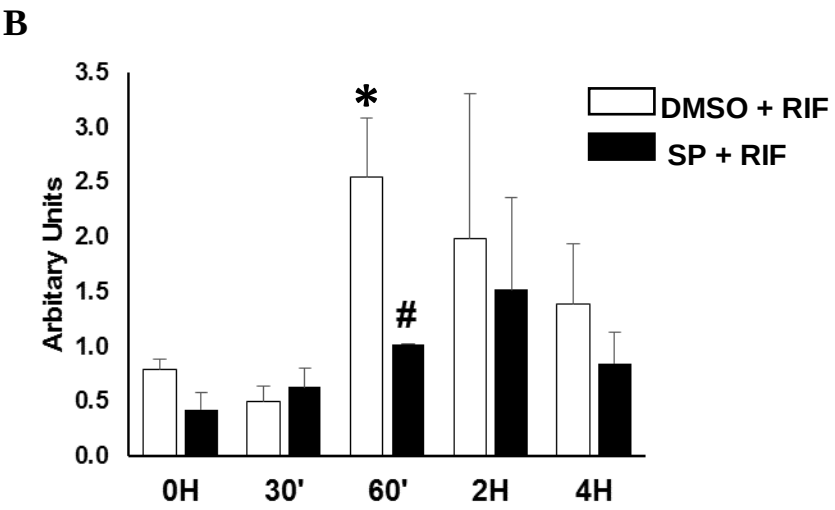

Fig. 6.4.5 A) RIF activates JNK in whole cell extracts prepared from HepG2 cells. Immunoblot of phospho (P)-JNK in whole cell extracts after treatment of HepG2 cells with vehicle (DMSO) or 30 μM SP for 30 mins. followed by 10 μM RIF for 0, 0.5, 1, 2 & 4 h. **B)** Quantification of blots by densitometry after normalizing the P-JNK levels over total JNK. Replicates from three experiments were quantified by densitometry. * $p<0.05$ as compared to untreated control (DMSO). #$p<0.05$ as compared to DMSO + RIF.

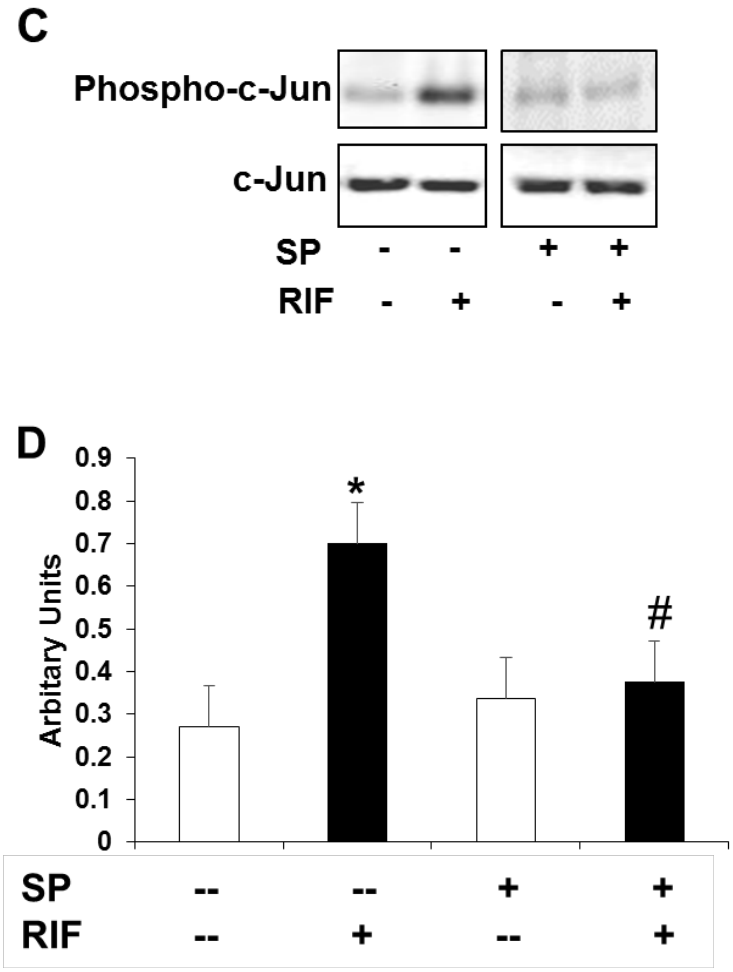

Fig. 6.4.5 C) RIF activates c-Jun in whole cell extracts prepared from HepG2 cells. C) Immunoblot of phospho-c-Jun in whole cell extracts after treatment of HepG2 cells with vehicle (DMSO) or 30 µM SP for 30 mins. followed by 10 µM RIF for 4 h. **D)** Quantification of blots by densitometry after normalizing the phospho-c-Jun levels over total c-Jun. Replicates from three experiments were quantified by densitometry. * $p<0.05$ as compared to untreated control (DMSO). #$p<0.05$ as compared to DMSO + RIF.

6.4.6 PXR nuclear levels were regulated by JNK

Our results indicate that JNK likely affects PXR function, therefore we determined the role of JNK in regulating PXR nuclear levels in RIF-treated HepG2 cells. As expected, PXR nuclear protein expression increased significantly starting 4 to 24 hours in the presence of RIF. However, SP attenuated RIF-mediated PXR accumulation in nucleus significantly at 12 and 24 hours (Fig. 6.4.6).

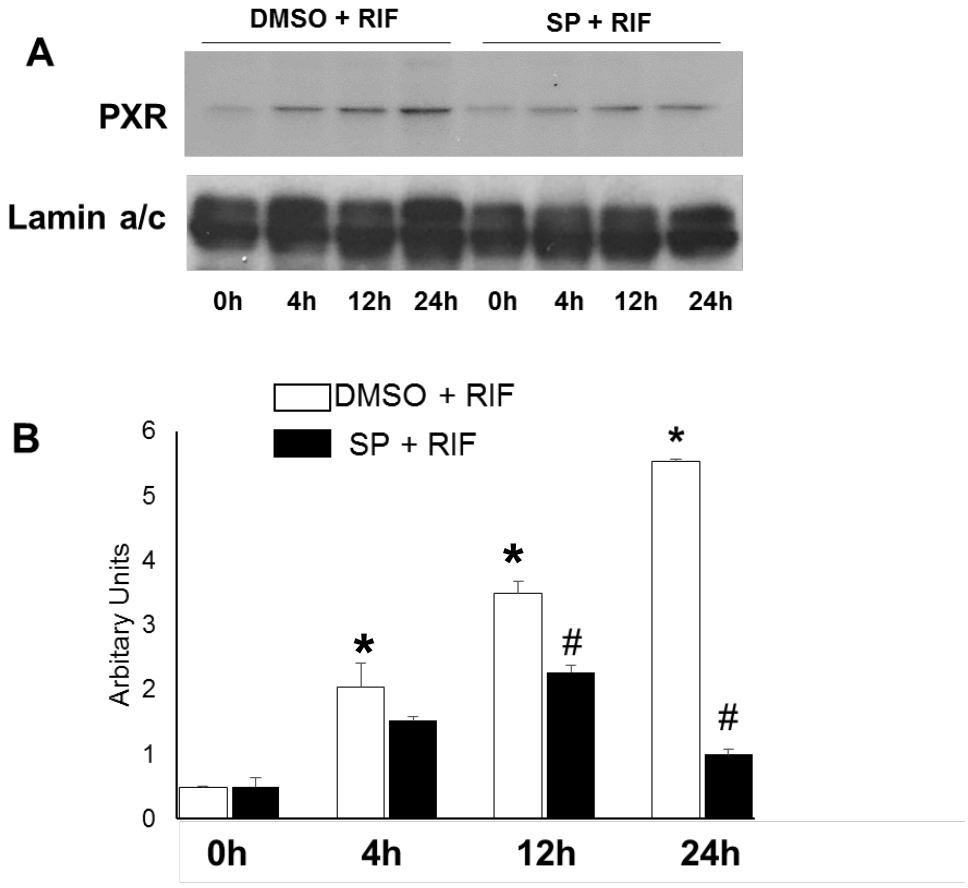

Fig.6.4.6 Attenuation of RIF-induced PXR nuclear levels by SP.

A) Immunoblot of PXR in nuclear extracts after treatment of HepG2 cells with vehicle (DMSO) or 30 μM SP for 30 mins. followed by 10 μM RIF for 0, 4, 12 & 24 h. **B)** Quantification of blots by densitometry after normalizing PXR levels over Lamin A/C nuclear housekeeping protein. Replicates from three experiments were quantified by densitometry. * $p<0.05$ as compared to DMSO + RIF 0 h group. # $p<0.05$ as compared to DMSO + RIF for each time point.

6.4.7 PXR binding to the CYP3A4 promoter was mediated by JNK

Lastly, we used *in vitro* ChIP assay to analyze whether decreased accumulation of PXR in the nucleus in the absence of JNK impacts the binding of PXR to CYP3A4 promoter. A validated ChIP grade anti-PXR antibody was used to precipitate DNA-protein complexes. RIF treatment alone significantly increased the association of PXR with the regulatory regions of CYP3A4 as compared to control. Remarkably, both our end point and qRT-PCR data showed decreased binding of PXR to CYP3A4 promoter in the absence of JNK (Fig. 6.4.7A & B), supporting the hypothesis JNK is required for optimum binding of PXR to its response elements on *CYP3A4* gene. We saw very faint bands in cell lysates precipitated without anti-PXR antibody, which might be due to non-specific binding. Input DNA from total cell lysate shows good *CYP3A4* gene expression.

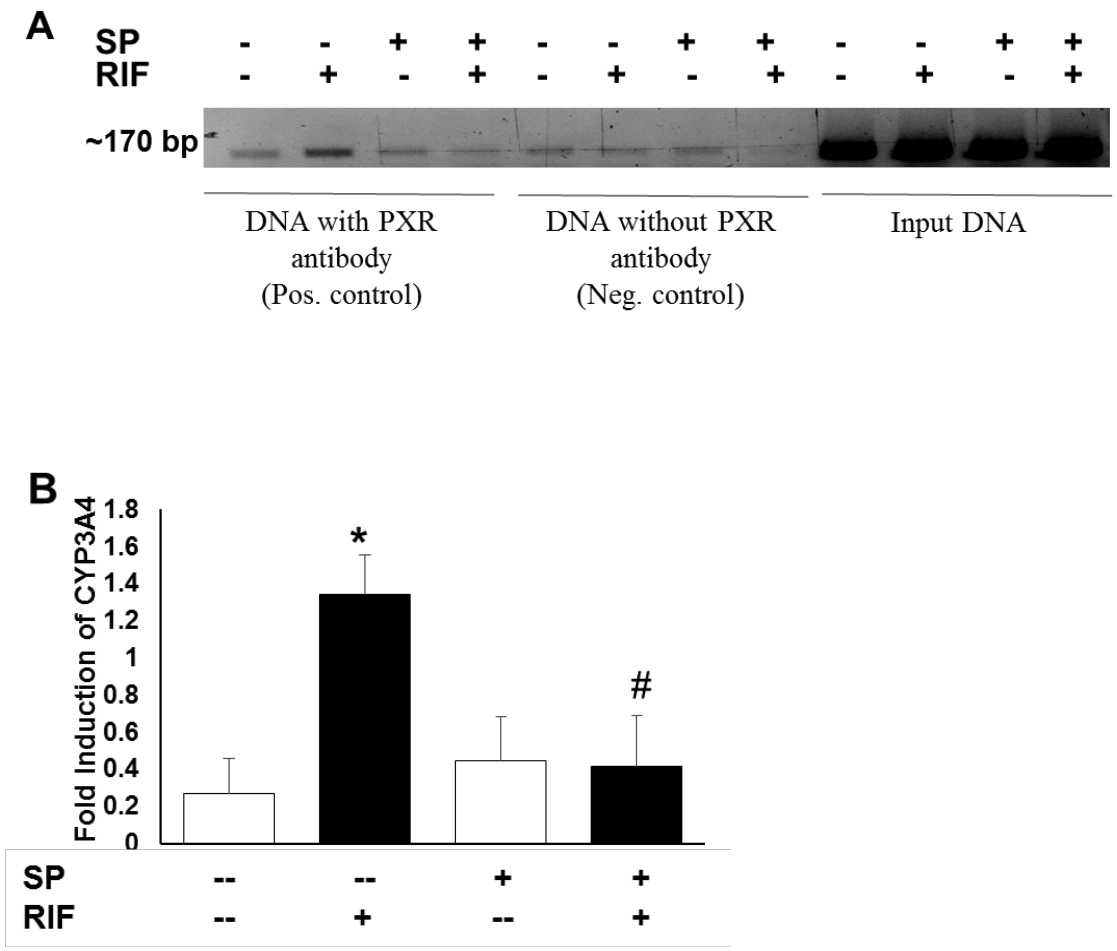

Fig. 6.4.7 Attenuation of binding of PXR to *CYP3A4* promoter region by SP. HepG2 cells were pre-treated with vehicle (DMSO) or 30 μM SP for 30 mins. followed by 10 μM RIF for 24 hours. An antibody against PXR was used to immunoprecipitate DNA-protein complexes. As a negative control, the beads were incubated with lysates without anti-PXR antibody. ChIP assays were performed as described under Material and Methods. **A)** End point PCR was performed using forward and reverse primers designed in the promoter region of CYP3A4 and analyzed on a 2% agarose gel. 10% of the total cell lysate was used

as “input”. **B)** Quantitative real time-PCR was performed using forward and reverse primers designed in the promoter region of CYP3A4. Data represents mean of triplicates ± SD. * $p<0.05$ as compared to control. # $p<0.05$ as compared to RIF treatment alone.

6.5 Discussion

In the present experiments, we show that JNK is required for induction of CYP3A4 via PXR. Research carried out in the last decade has shown that PXR target gene expression is regulated not only by xenobiotics and endobiotics (Kliewer et al., 1998; Lehmann et al., 1998; Staudinger et al., 2008; Pondugula et al., 2009), but also by cellular signaling pathways. Post-translational modifications of PXR, especially direct phosphorylation primarily led to an inhibition of its transcriptional activity (Wang YM, 2012); thereby downregulating *Cyp3a* expression. Our data, on the other hand, shows that JNK is required for optimum induction of CYP3A4 via PXR in liver cells. We provide additional evidence showing that PXR nuclear translocation as well as binding of PXR to its response elements on *CYP3A4* gene is JNK-dependent.

As reported in the results, we found that *CYP3A4* reporter gene expression increased ~8 folds in the presence of PXR ligand, RIF and this induction was attenuated ~50% by treatment with SP. Apart from RIF, we also tested the effects of hyperforin, an active component of St. John's wort & a potent activator of human PXR (Moore et al., 2000; Chen et al., 2004), on CYP3A4 reporter gene expression. Hyperforin induced CYP3A4 luciferase activity and SP attenuated this hyperforin-mediated induction significantly. The fact that SP attenuated both RIF and hyperforin-mediated induction of CYP3A4, strongly indicated that PXR is likely regulated by JNK-dependent signaling mechanism. Moreover, these ligands only activated CYP3A4 reporter expression in HepG2 cells transfected with PXR plasmid (data not shown), suggesting that this is a specific PXR-dependent effect.

To comprehensively understand the role of MAPKs in PXR-mediated CYP3A4 signaling, we investigated the role of all MAPKs by treating HepG2 cells with specific ERK 1/2 pathway inhibitor (PD098059), JNK 1/2/3 inhibitor (SP600125) and p38 inhibitor (SB203580). Specifically, SP600125, an anthrapyrazolone compound, is a potent inhibitor of all isoforms of JNK with an IC50 of 0.04 µM but exhibits greater than 300 fold selectivity against other MAPKs- ERK and p38 (IC50 > 10 µM) (Bennett et al, 2001). In our studies, while JNK and ERK 1/2 inhibition significantly attenuated PXR-mediated CYP3A4 luciferase activity by ~2 folds and ~3 folds respectively, p-38 inhibition showed no significant change (data not shown). Curcumin, both JNK (IC50: 5 µM) and ERK (IC50: 20 µM) inhibitor (Chen and Tan, 1998), also attenuated PXR-mediated CYP3A4 luciferase activity ~50%. MAPKs phosphorylate downstream kinases and nuclear factors such as c-Jun, c-Fos, c-Myc, SP1, Elk1 etc. Since different MAPKs phosphorylate varying nuclear factors, it could be possible that only nuclear factors activated by JNK and ERK might be involved in CYP3A4 regulation. However, the possibility of ERK being involved was eliminated from the results that the ERK inhibitor, PD098059 had no effect on RIF-induced *CYP3A4* mRNA expression (data not shown). A similar study by Yasunami *et. al*. reported that inhibition of JNK suppressed VDR-mediated induction of CYP3A4 mRNA and promoter activity while ERK or p-38 inhibition had no effect (Yasunami et al, 2004).

JNK exists in 3 distinct isoforms (JNK1-3). While JNKl and JNK2 genes are ubiquitously expressed including liver, the JNK3 gene is selectively expressed in the brain, heart, and testis (Ip and Davis, 1998). Hence, to confirm the role of curcumin and SP in attenuating

CYP3A4 induction by PXR, we also investigated whether simultaneous knockdown of JNK1 and JNK2 using a siRNA that targets a homologous region present in both kinases affects PXR-mediated CYP3A4 reporter activity. Knockdown of JNK1/2 expression by siRNA dramatically reduced the ability of RIF to stimulate CYP3A4 in HepG2 cells. This data confirmed that JNK is indeed required for optimal activation of CYP3A4 as pharmacological inhibition as well as genetic knock-down of JNK1 & JNK2 attenuated its promoter activity significantly at 24 hours. However, the role of individual isoforms of JNK needs to be further investigated.

Additionally, we studied the effect of SP on RIF-mediated CYP3A4 mRNA and activity in HepG2 cells. HepG2 cells, human liver carcinoma cells, are frequently used for *in vitro* biotransformation assays (Westerink & Schoonen, 2007). They are a continuous cell line, cheap and easy to use as compared to primary human hepatocytes. However, endogenous activity and expression of enzymes and NRs is relatively low in HepG2 cells (Xu et al, 2004). Therefore, as an additional approach, we performed enzyme activity studies in HepaRG cells which is a well-established model for biotransformation applications (Gripon et al. 2002; Lambert et al. 2009; Anthérieu et al. 2010). Attenuation of PXR-mediated induction of CYP3A4 enzyme activity in the presence of JNK inhibitor in HepaRG cells also confirmed that JNK is required for induction of CYP3A4.

To determine the mechanism involved in JNK-mediated regulation of CYP3A4, we studied the role of JNK in regulating PXR nuclear translocation or it's binding to CYP3A4

gene. PXR exists as a phospho-protein in cells (Litchi-Kaiser et al, 2009) and previous studies have mainly shown that kinases decrease PXR transcription by either strengthening PXR-co-repressor interaction or weakening PXR-co-activator interactions. To understand the role of JNK in PXR regulation, we first sought to understand whether RIF directly affects JNK expression. Interestingly, we found that RIF activates JNK in HepG2 cells and SP attenuates this activation, as expected. Thus we find that RIF activates PXR and increases PXR protein levels (starting at about 4 hours) while simultaneously, it activates JNK in HepG2 cells. Loss of JNK and/or p-JNK in turn decreases the binding of PXR to its response elements on *CYP3A4* gene. There could be multiple mechanisms playing a role including a) JNK is directly phosphorylating PXR and increasing its nuclear translocation/binding to the CYP3A4 gene or b) JNK is phosphorylating cytoplasmic retention proteins associated with PXR, and impacting its translocation or c) JNK is increasing PXR-co-repressor binding or d) JNK is decreasing PXR-co-activator binding. Although we did not study whether PXR is directly phosphorylated by JNK, we found that JNK is required for PXR nuclear translocation & binding to CYP3A4 promoter, ultimately affecting PXR function. Using *in silico* computer-based analysis in our lab using PhosphoSitePlus®, we found 9 serine phosphorylation sites & 7 threonine phosphorylation sites on PXR and further studies to reveal their association with JNK are ongoing. Similar to our study, seven serine/ threonine residues were also identified in human PXR protein which are good potential substrates for an array of kinases, including MAPKs (Litchi-Kaiser et al, 2009). Using mass spectrometry analysis, some of these serine-threonine

residues such as S114, T133/135, S167 and S200 in PXR were also found to be phosphorylated by cyclin-dependent kinase 2 (Elias et al, 2014).

In summary, our *in vitro* data indicates that JNK, but not ERK or p38, is required for *CYP3A4* gene activation by PXR. Further studies exploring the role of JNK on CYP3A4 induction *in vivo* will be clinically relevant in studying PXR-mediated target gene expression. JNK is activated by various extracellular stimuli and thus regulates gene expression through phosphorylation of transcription/nuclear factors. Hence, elucidation of the contribution of JNK in the xenobiotic-induced expression of P450 genes may be instrumental in understanding the mechanism of induction of P450s which can impact therapeutic outcome in patients undergoing treatment with multiple medications. JNK-mediated phosphorylation of PXR or its transcriptional co-activators/ co-repressors may also serve as a valuable surrogate marker of predicting altered plasma concentrations of CYP3A4 substrates in diseases. Ultimately, understanding the role of JNK in induction of CYP3A4 could provide novel strategies to address concerns of loss of drug safety and/or efficacy due to alteration of expression and activity of the CYP3A4 enzyme.

Appendix

7.1. Designing Primer and Probes

While designing custom primers and probes, following considerations should be kept in mind:

- Length of 18-24 bases
- 40-60% G/C content
- Start and end with 1-2 G/C pairs
- Melting temperature (Tm) of 50-60°C
- Primer pairs should have a Tm within 5°C of each other
- Primer pairs should not have complementary regions

To design custom primers for a specific gene, gene sequence was first found out using Pubmed search engine (by selecting Nucleotide in the search engine and typing the gene name). Then, using NCBI-Primer BLAST system primers were generated based on the above sequence. A total of 5 primer sequences are usually generated and among them the primer set which meets all the above criteria was selected. Finally, using NCBI blastn suite, the specificity of the primers for the particular gene was verified.

7.2. Reverse Phase Protein Array Analysis

Fig. 7.2.1 Differentially regulated genes by LPS as compared to control

Genes	Fold Change
Annexin1_R_V	9.17
SOX9_R_V	1.71
c-Jun(60A8)_R_V	0.64
FBX011_R_V	0.51
Stat3(D3Z2G)_R_V	0.46
ASH2_R_V	0.41
p-p38(D3F9) XP(T180/Y182)_R_V	-0.53
AR-441_M_V	-0.58
p27/KIP1(C-term)_R_V	-0.64
p-IkappaB-a(S32/36)_M_V	-0.78
p-Beta-Catenin(S33/37/T41)_R_V	-1.34
p-PDGFRa(23B2)(Y754)_R_V	-7.24
Integrinb1(D2E5)_R_V	-8.11
p-Rb(S807/811)_R_V	-10.01

Fig. 7.2.2 Differentially regulated genes by PCN as compared to control

Genes	Fold Change
Annexin1_R_V	7.03
SOX9_R_V	3.78
c-Fos(9F6)_R_V	0.92
FBX011_R_V	0.37
p-c-Myc(T58)_R_V	-0.34
Bak_R_V	-0.37
LRP6_R_V	-0.39
MEK6_R_V	-0.41
FoxO1(C29H4)_R_V	-0.42
MMP-9_R_V	-0.43
Bad_R_V	-0.45
LC3A(D50G8)XP_R_V	-0.48
Integrinb3(D7X3P)XP_R_V	-0.63

p-mTOR(D9C2)XP(S2448)_R_V	-0.83

7.3. CYP3A4 gene expression analysis in Huh7 cells and primary mouse hepatocytes

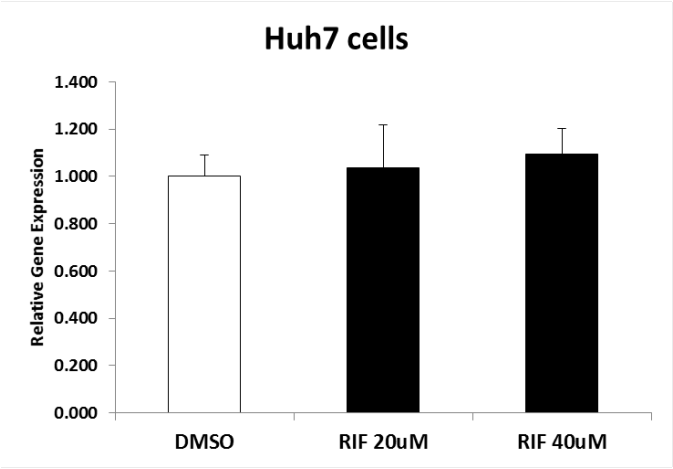

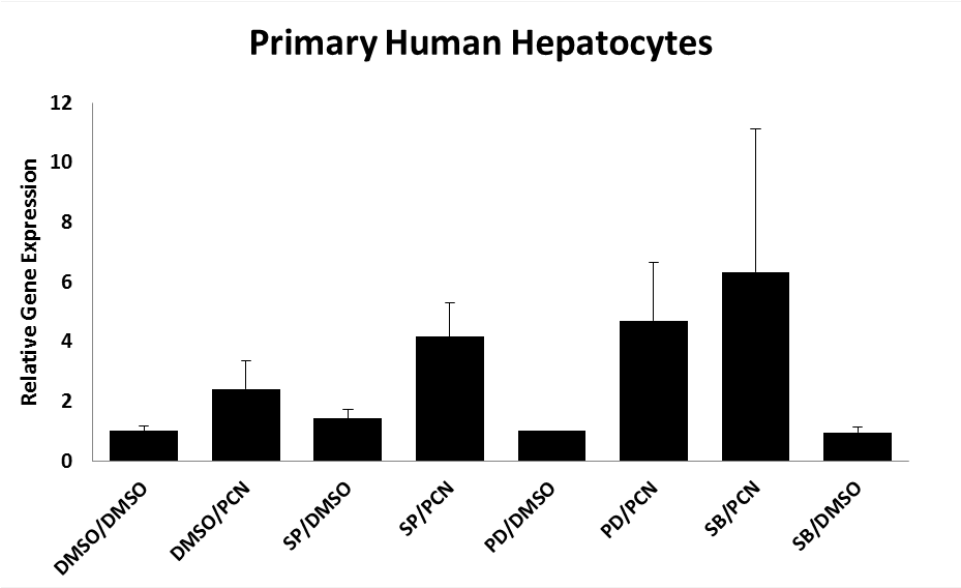

7.4. miRNA analysis from Microarray Data

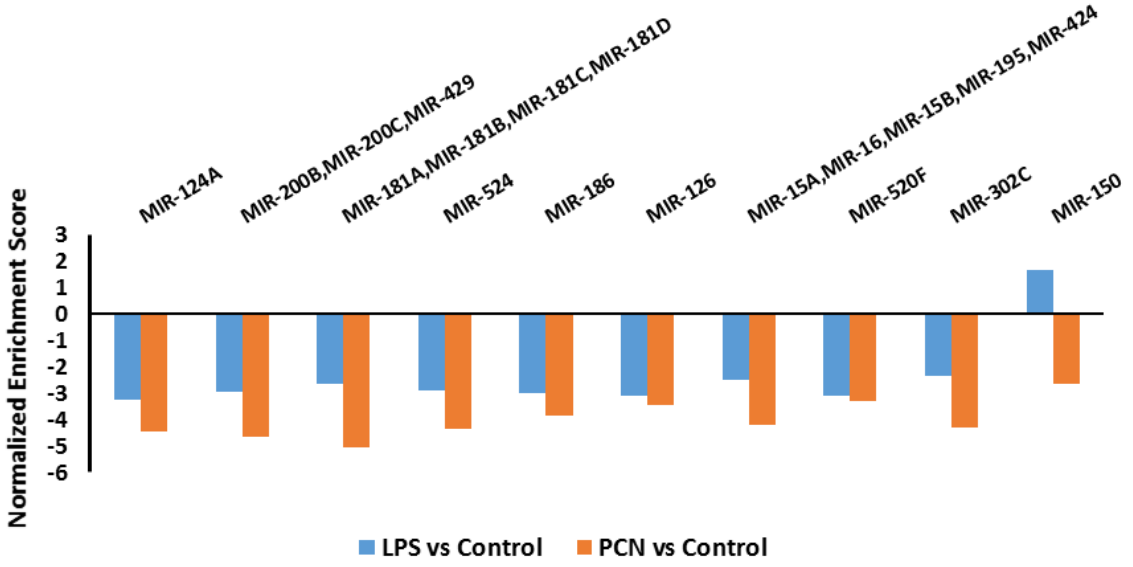

7.5. Gene expression analysis in Humanized CYP3A4/PXR/CAR mice

A.CYP3A4

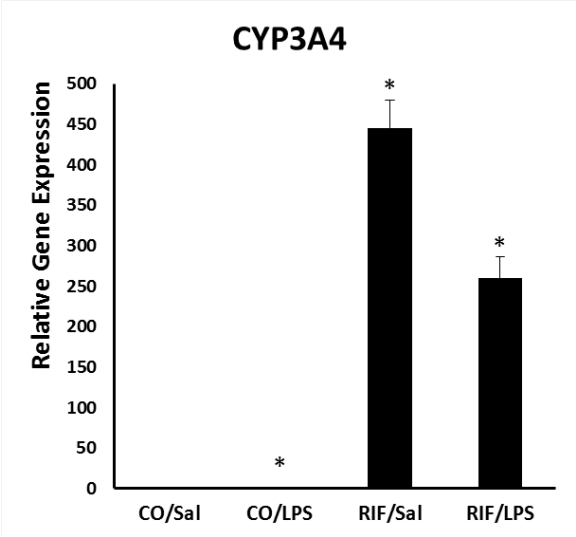

S.No	CO/Sal	CO/LPS	RIF/Sal	RIF/LPS
1	0.224	0.155	330.713	176.282
2	0.776	0.280	393.423	217.088
3	1.385	0.109	338.799	226.550
Average	0.795	0.182	354.312	206.640
SD	0.581	0.089	34.112	26.713

B. MEF2

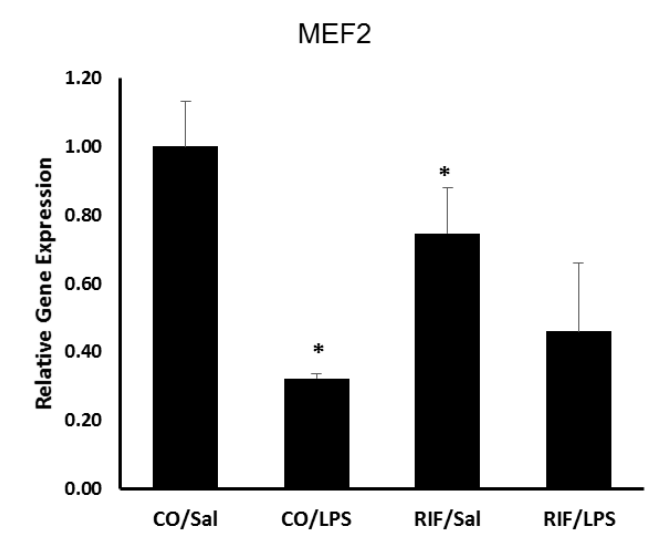

	CO/Sal	CO/LPS	RIF/Sal	RIF/LPS
1	1.057	0.318	0.761	0.237
2	1.164	0.342	0.934	0.551
3	0.863	0.312	0.677	0.373
4	0.941	-	0.631	0.690
Average	1.006	0.324	0.751	0.463
SD	0.132	0.016	0.133	0.199

C. NFE2

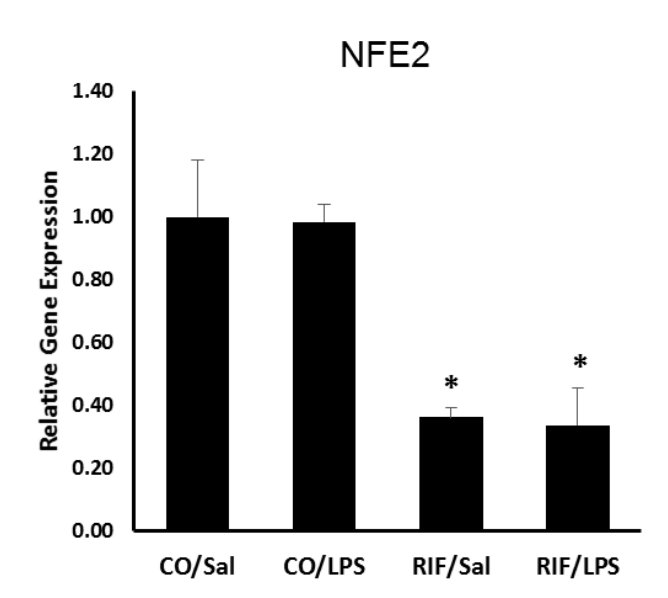

	CO/Sal	CO/LPS	RIF/Sal	RIF/LPS
1	0.832	0.997	0.376	0.453
2	0.975	0.938	-	0.356
3	0.977	-	0.392	0.214
4	1.262	1.051	0.329	-
Average	1.011	0.995	0.366	0.341
SD	0.181	0.056	0.033	0.120

7.6. List of all *in vivo* experiments

No.	Performed By	Mice	Treatments	Tissue Storage	
GT1	Pranav/Guncha (UH main campus)	Lean and DIO mice (n= 4)	Fed 10% or 60% fat diet	80 Freezer	
	Oct-13				

GT2	Guncha (UH TMC)	C57Bl6 mice (n=6 or 7)	Corn Oil + Olive Oil (n=6), Corn oil + Fish Oil (n=6), Aspirin Fish Oil + Olive Oil (n=7) Oral Gavage, 200ul for14 days	Plasma Samples shipped	
	Nov-14				
GT3	Weiwu and Guncha (At Baylor)	C57Bl6 mice (n=4)	PCN (50 mg/kg/day for 3 days IP) or Corn Oil followed by LPS (2 mg/kg for 16 hours IP) or Saline	(Collected plasma and liver samples)80 freezer	Used Zymo Kit to prepare mRNA and sent samples for Microarray analysis
	Aug-14				
GT4	Guncha (UH TMC)	C57Bl6 mice (n=4)	PCN (50 mg/kg/day for 3 days IP) or Corn Oil followed by LPS (2 mg/kg for 16 hours IP) or Saline followed by Irinotecan (10 mg/kg Oral)	(Collected whole blood from tail vein at 0h, 15', 30', 60', 2h, 3h, 4h, 5h, 6h and 24h) Also plasma, liver, kidney , intestine samples at the end)80 freezer	
	Feb-17				

R2	Weiwu and Guncha (At Baylor)	Taconic Mice (Humanized CYP3A4, PXR, CAR)	RIF (10 mg/kg/day) i.p. for 4 days, Day 4: i.p.-inject with LPS (2 mg/kg). Sacrifice after 24h on last day.	Collected Aorta, Blood, Brain, Liver, Lung, Heart, Spleen, Kidney, Intestine, Testis (80 freezer)	Mesured gene expression of CYP3A4, MEF2 and NFE2
	Sep-16				

7. List of all in vitro experiments

No.	Name	Cells	Treatments	Sample Storage
1	Luciferase Assays	HepG2 cells transfected with hCYP3A4 and PXR plasmid with Renilla vector	30 um SP600125 or 10 um Rif or 1ug/ml LPS or TNFa or Curcumin or SB or PD	Luciferase activity of CYP3A4 measured
	Started: June 2014 till Oct 2014			
2	Hepatocyte 1 and 2	Primary hepatocytes isolated by Pankajini	Pretreatment with SP/PD/SB for 30 mins followed by PCN (10 um) for 24 hours	RNA/cDNA in 80 freezer
	Sep-14			

3	HepG2_1-14	HepG2 cell culture for RT-PCR analysis	Pretreatment with SP/PD/SB for 30 mins followed by Rif (10 or 20 or 40 um)	RNA/cDNA in 80 freezer
	Sep 2014 to March 2015			
4	Huh7_1 & 2	Huh7 cell culture for RT-PCR analysis	Rif (10, 20 or 40 uM)	RNA/cDNA in 80 freezer
	Oct-14			
5	Nuclear and Cytosolic extracts_ 1-4	HepG2 cells	Pretreatment with SP for 30 mins followed by Rif (10 um)	80 degrees
	May 2015 to July 2015			
6	Whole Cells extracts_ 1-5	HepG2 cells	Pretreatment with SP for 30 mins followed by Rif (10 um)	80 degrees
	May 2015 to July 2015			
7	siRNA_1-7	HepG2 cells co-transfected with CYP3A4, PXR plasmid and JNK siRNA	Rif 10 uM	Luciferase activity of CYP3A4 measured
	Aug 2015 to Dec 2015			
8	Hyperforin 1-5	HepG2 cells transfected with hCYP3A4 and PXR plasmid with Renilla vector	Pretreatment with SP for 30 mins followed by Rif (10 um)	Luciferase activity of CYP3A4 measured

	Nov 2015 to Dec 2015			
9	P450 Glo Assay	HepG2 and HepaRG cells	Pretreatment with SP for 30 mins followed by Rif (10 um)	Glo for CYP3A4 substrate measured
	April 2015 and Feb 2016			
10	ChIP assay	HepG2 cells	Pretreatment with SP for 30 mins followed by Rif (10 um)	80 degrees
	Jan-17			

Bibliography

Abdulla D, Goralski KB, Del Busto Cano EG, and Renton KW (2005) The signal transduction pathways involved in hepatic cytochrome P450 regulation in the rat during a lipopolysaccharide-induced model of central nervous system inflammation. *Drug Metab Dispos* **33**:1521–1531.

Acevedo LG, Bieda M, Green R, and Farnham PJ (2008) Analysis of the mechanisms mediating tumor-specific changes in gene expression in human liver tumors. *Cancer Res* **68**:2641–2651.

Aitken AE, Richardson TA, and Morgan ET (2006) Regulation of Drug-Metabolizing Enzymes and Transporters in Inflammation. *Annu Rev Pharmacol Toxicol* **46**:123–49.

Aouabdi, S., Gibson, G. and Plant, N. (2006) Transcriptional regulation of the PXR gene: identification and characterization of a functional peroxisome proliferator-activated receptor alpha binding site within the proximal promoter of PXR. Drug Metab Dispos (34):138-44.

Adam, R. (2003). "Chemotherapy and surgery: new perspectives on the treatment of unresectable liver metastases." Ann Oncol 14 Suppl 2: ii13-16.

Anthérieu S, Chesné C, Li R, Camus S, Lahoz A, Picazo L, Turpeinen M, Tolonen A, Uusitalo J, Guguen-Guillouzo C, and Guillouzo A (2010) Stable expression, activity, and inducibility of cytochromes P450 in differentiated HepaRG cells. *Drug Metab Dispos* **38**:516–525.

Araya Z, and Wikvall K (1999) 6??-Hydroxylation of taurochenodeoxycholic acid and lithocholic acid by CYP3A4 in human liver microsomes. *Biochim Biophys Acta - Mol Cell Biol Lipids* **1438**:47–54.

Besnard A, Galan-Rodriguez B, Vanhoutte P, and Caboche J (2011) Elk-1 a transcription factor with multiple facets in the brain.

Bird A (2002) DNA methylation patterns and epigenetic memory.

Bruijn D, and Jonge JA De (1998) Irinotecan Metabolism and Disposition in Cancer. *Clin Cancer Res* **4**:2747–2753.

Bennett BL, Sasaki DT, Murray BW, O'Leary EC, Sakata ST, Xu W, Leisten JC, Motiwala A, Pierce S, Satoh Y, Bhagwat SS, Manning AM, and Anderson DW (2001) SP600125, an anthrapyrazolone inhibitor of Jun N-terminal kinase. *Proc Natl Acad Sci* **98**:13681–13686.

Brandi, G., J. Dabard, P. Raibaud, M. Di Battista, C. Bridonneau, A. M. Pisi, A. M. Morselli Labate, M. A. Pantaleo, A. De Vivo and G. Biasco (2006). "Intestinal microflora and digestive toxicity of irinotecan in mice." Clin Cancer Res **12**(4): 1299-1307.

Brandi, G., F. de Rosa and G. Biasco (2009). "Irinotecan toxicity: genes or intestinal microflora?" Br J Cancer **100**(6): 1017.

Burke, T. G., C. B. Munshi, Z. Mi and Y. Jiang (1995). "The important role of albumin in determining the relative human blood stabilities of the camptothecin anticancer drugs." J Pharm Sci **84**(4): 518-519.

Benson, A. B., 3rd, J. A. Ajani, R. B. Catalano, C. Engelking, S. M. Kornblau, J. A. Martenson, Jr., R. McCallum, E. P. Mitchell, T. M. O'Dorisio, E. E. Vokes and S. Wadler (2004). "Recommended guidelines for the treatment of cancer treatment-induced diarrhea." J Clin Oncol **22**(14): 2918-2926.

Bergheim, I., S. Weber, M. Vos, S. Kramer, V. Volynets, S. Kaserouni, C. J. McClain and S. C. Bischoff (2008). "Antibiotics protect against fructose-induced hepatic lipid accumulation in mice: role of endotoxin." J Hepatol **48**(6): 983-992.

Brun, P., I. Castagliuolo, V. Di Leo, A. Buda, M. Pinzani, G. Palu and D. Martines (2007). "Increased intestinal permeability in obese mice: new evidence in the pathogenesis of nonalcoholic steatohepatitis." Am J Physiol Gastrointest Liver Physiol **292**(2): G518-525.

Basseville A, Preisser L, de Carne Trecesson S, Boisdron-Celle M, Gamelin E, Coqueret O, et al. (2011). Irinotecan induces steroid and xenobiotic receptor (SXR) signaling to detoxification pathway in colon cancer cells. Mol Cancer 10: 80.

Cani, P. D., R. Bibiloni, C. Knauf, A. Waget, A. M. Neyrinck, N. M. Delzenne and R. Burcelin (2008). "Changes in gut microbiota control metabolic endotoxemia-induced inflammation in high-fat diet-induced obesity and diabetes in mice." Diabetes **57**(6): 1470-1481.

Chen Y, Ferguson SS, Negishi M, and Goldstein J a (2004) Induction of human CYP2C9 by rifampicin, hyperforin, and phenobarbital is mediated by the pregnane X receptor. *J Pharmacol Exp Ther* **308**:495–501.

Chen YR, and Tan TH (1998) Inhibition of the c-Jun N-terminal kinase (JNK) signaling pathway by curcumin. *Oncogene* **17**:173–178.

Crawford JM, and Boyer JL (1998) Clinicopathology conferences: Inflammation-induced

cholestasis. *Hepatology* **28**:253–260.

Cui JY, Choudhuri S, Knight TR, and Klaassen CD (2010) Genetic and Epigenetic Regulation and Expression Signatures of Glutathione S-Transferases in Developing Mouse Liver. *Toxicol Sci an Off J Soc Toxicol* **116**:32–43.

Cunningham D (2001) Optimizing the Use of Irinotecan in Colorectal Cancer. *Oncologist* **6**:17–23.

Di-Luoffo M, Daems C, Bergeron F, and Tremblay JJ (2015) Novel Targets for the Transcription Factors MEF2 in MA-10 Leydig Cells. *Biol Reprod* **93**:9–9.

de Wildt SN, Kearns GL, Leeder JS, & van den Anker JN (1999). Cytochrome P450 3A: ontogeny and drug disposition. Clin Pharmacokinet 37**:** 485-505.

Dresser GK, Spence JD, & Bailey DG (2000). Pharmacokinetic-pharmacodynamic consequences and clinical relevance of cytochrome P450 3A4 inhibition. Clin Pharmacokinet 38**:** 41-57.

Ding X, and Staudinger JL (2005) Induction of drug metabolism by forskolin: the role of the pregnane X receptor and the protein kinase a signal transduction pathway. *J Pharmacol Exp Ther* **312**:849–856.

Ding X, and Staudinger JL (2005) Repression of PXR-mediated induction of hepatic CYP3A gene expression by protein kinase C. *Biochem Pharmacol* **69**:867–873.

Endou H (2000) Molecular mechanisms of drug transport. *Nihon yakurigaku zasshiFolia Pharmacol Jpn* **116**:114–124.

Everett L, Hansen M, and Hannenhalli S (2010) Regulating the Regulators: Modulators of Transcription Factor Activity, in *Computational Biology of Transcritpion Factor Binding, Methods in Molecular Biology* pp 297–312.

Elias A, High AA, Mishra A, Ong SS, Wu J, Peng J, and Chen T (2014) Identification and characterization of phosphorylation sites within the pregnane X receptor protein. *Biochem Pharmacol* **87**:360–370.

Gellner K, Eiselt R, Hustert E, Arnold H, Koch I, Haberl M, Deglmann CJ, Burk O, Buntefuss D, Escher S, Bishop C, Koebe HG, Brinkmann U, Klenk HP, Kleine K, Meyer UA, Wojnowski L (2001). Genomic organization of the human CYP3A locus: identification of a new, inducible CYP3A gene. *Pharmacogenetics*

Ghose R, Guo T, Vallejo JG, and Gandh A (2011) Differential role of toll-interleukin 1 receptor domain-containing adaptor protein in toll-like receptor 2-mediated regulation of gene expression of hepatic cytokines and drug-metabolizing enzymes. *Drug Metab Dispos* **39**:874–881.

Ghose R, Mulder J, von Furstenberg RJ, Thevananther S, Kuipers F, and Karpen SJ (2007) Rosiglitazone attenuates suppression of RXR??-dependent gene expression in inflamed liver. *J Hepatol* **46**:115–123.

Ghose R, Guo T, and Haque N (2009) Regulation of gene expression of hepatic drug metabolizing enzymes and transporters by the Toll-like receptor 2 ligand, lipoteichoic acid. *Arch Biochem Biophys* **481**:123–130, Elsevier Inc.

Ghose R, Zimmerman TL, Thevananther S, and Karpen SJ (2004) Endotoxin leads to rapid subcellular re-localization of hepatic RXRα: A novel mechanism for reduced hepatic gene expression in inflammation. *Nucl Recept* **2**:4.

Goodwin B, Hodgson E, and Liddle C (1999) The orphan human pregnane X receptor mediates the transcriptional activation of CYP3A4 by rifampicin through a distal enhancer module. *Mol Pharmacol* **56**:1329–39.

Gu X, Ke S, Liu D, Sheng T, Thomas PE, Rabson AB, Gallo MA, Xie W, and Tian Y (2006) Role of NF-??B in regulation of PXR-mediated gene expression: A mechanism for the suppression of cytochrome P-450 3A4 by proinflammatory agents. *J Biol Chem* **281**:17882–17889.

Guengerich FP (2001) Common and Uncommon Cytochrome P450 Reactions Related to Metabolism and Chemical Toxicity. *Chem Res Toxicol* **14**:611–650.

Guengerich FP (1999) CYTOCHROME P-450 3A4: Regulation and Role in Drug Metabolism. *Annu Rev Pharmacol Toxicol* **39**:1–17.

Guengerich FP (2008) Cytochrome P450 and chemical toxicology.

Guzelian J, Barwick JL, Hunter L, Phang TL, Quattrochi LC, and Guzelian PS (2006) Identification of genes controlled by the pregnane X receptor by microarray analysis of mRNAs from pregnenolone 16alpha-carbonitrile-treated rats. *Toxicol Sci* **94**:379–87.

Goey AKL, Meijerman I, Rosing H, Marchetti S, Mergui-Roelvink M, Keessen M, Burgers JA, Beijnen JH, and Schellens JHM (2014) The effect of St John's Wort on the pharmacokinetics of docetaxel. *Clin Pharmacokinet* **53**:103–110.

Goodwin B, Redinbo MR, and Kliewer SA (2002) Regulation of cyp3a gene transcription by the pregnane x receptor. *Annu Rev Pharmacol Toxicol* **42**:1–23.

Gripon P, Rumin S, Urban S, Le Seyec J, Glaise D, Cannie I, Guyomard C, Lucas J, Trepo C, and Guguen-Guillouzo C (2002) Infection of a human hepatoma cell line by hepatitis B virus. *Proc Natl Acad Sci U S A* **99**:15655–15660.

Guengerich FP (1995) Human cytochrome P-450 enzymes. *Cytochrome P450 pp. 473–*

535. New York: Plenum. 2nd ed.

Gallelli L, Gioffre V, Vero G, Gallelli A, Roccia F, Naty S, et al. (2005). Clarithromycin in the Treatment of Legionella pneumophila Pneumonia Associated with Multiorgan Failure in a Previously Healthy Patient. Clin Drug Investig 25: 485-490.

Han J-Y, Lim H-S, Park YH, Lee SY, and Lee JS (2009) Integrated pharmacogenetic prediction of irinotecan pharmacokinetics and toxicity in patients with advanced non-small cell lung cancer. *Lung Cancer* **63**:115–20.

Hart SN, Cui Y, Klaassen CD, and Zhong X (2009) Three patterns of cytochrome P450 gene expression during liver maturation in mice. *Drug Metab Dispos* **37**:116–21.

Hakkola J, Raunio H, Purkunen R, Saarikoski S, Vähäkangas K, Pelkonen O, Edwards R, J, Boobis A, R, Pasanen M (2001) Cytochrome P450 3A Expression in the Human Fetal Liver: Evidence that CYP3A5 Is Expressed in Only a Limited Number of Fetal Livers. Biol Neonate;80:193-201

Harmsen S, Meijerman I, Beijnen JH, and Schellens JHM (2007) The role of nuclear receptors in pharmacokinetic drug-drug interactions in oncology. *Cancer Treat Rev* **33**:369–380.

Houliston R a, Pearson JD, and Wheeler-Jones CP (2001) Agonist-specific cross talk between ERKs and p38(mapk) regulates PGI(2) synthesis in endothelium. *Am J Physiol Cell Physiol* **281**:C1266-76.

Hoskins, J. M., R. M. Goldberg, P. Qu, J. G. Ibrahim and H. L. McLeod (2007). "UGT1A1*28 genotype and irinotecan-induced neutropenia: dose matters." J Natl Cancer Inst **99**(17): 1290-1295.

Ip YT, and Davis RJ (1998) Signal transduction by the c-Jun N-terminal kinase (JNK)--from inflammation to development. *Curr Opin Cell Biol* **10**:205–19.

Ingelman-Sundberg M, and Gomez A (2010) The past, present and future of pharmacoepigenomics. *Pharmacogenomics* **11**:625–627.

Ingelman-Sundberg M, Zhong X, Hankinson O, Beedanagari S, Yu A, Peng L, and Osawa Y (2013) Potential role of epigenetic mechanisms in the regulation of drug metabolism and transport. *Drug Metab Dispos* **41**:1725–31.

Ikegami T, Ha L, Arimori K, Latham P, Kobayashi K, Ceryak S (2002) Intestinal alkalization as a possible preventive mechanism in irinotecan (CPT-11)-induced diarrhoea. Cancer Res 62(1):179–87.

Inoue K, and Negishi M (2009) Early growth response 1 loops the CYP2B6 promoter for synergistic activation by the distal and proximal nuclear receptors CAR and HNF4α.

FEBS Lett **583**:2126–2130.

Inoue K, and Negishi M (2008) Nuclear receptor CAR requires early growth response 1 to activate the human cytochrome P450 2B6 gene. *J Biol Chem* **283**:10425–32.

Ito K, Suzuki H, Horie T, and Sugiyama Y (2005) Apical/basolateral surface expression of drug transporters and its role in vectorial drug transport.

Kawato Y, Aonuma M, Hirota Y, Kuga H, and Sato K (1991) Intracellular Roles of SN-38, a Metabolite of the Camptothecin Derivative CPT-11, in the Antitumor Effect of CPT-11. *Cancer Res* **51**:4187–4191.

Kojima K, Nagata K, Matsubara T, and Yamazoe Y (2007) Broad but distinct role of pregnane x receptor on the expression of individual cytochrome p450s in human hepatocytes. *Drug Metab Pharmacokinet* **22**:276–286.

Krishna DR, and Klotz U (1994) Extrahepatic Metabolism of Drugs in Humans.

Kroetz DL (2006) Role for drug transporters beyond tumor resistance: Hepatic functional imaging and genotyping of multidrug resistance transporters for the prediction of irinotecan toxicity. *J Clin Oncol* **24**:4225–4227.

Kim SW, Hasanuzzaman M, Cho M, Heo YR, Ryu MJ, Ha NY, Park HJ, Park HY, and Shin JG (2015) Casein kinase 2 (CK2)-mediated phosphorylation of Hsp90β as a novel mechanism of rifampin-induced MDR1 expression. *J Biol Chem* **290**:17029–17040.

Kliewer S a, Moore JT, Wade L, Staudinger JL, Watson M a, Jones S a, McKee DD, Oliver BB, Willson TM, Zetterström RH, Perlmann T, and Lehmann JM (1998) An orphan nuclear receptor activated by pregnanes defines a novel steroid signaling pathway. *Cell* **92**:73–82.

Kast HR, Goodwin B, Tarr PT, Jones SA, Anisfeld AM, Stoltz CM, et al. (2002). Regulation of multidrug resistance-associated protein 2 (ABCC2) by the nuclear receptors pregnane X receptor, farnesoid X-activated receptor, and constitutive androstane receptor. J Biol Chem 277: 2908-2915.

Kwatra D, Venugopal A, Standing D, Ponnurangam S, Dhar A, Mitra A, et al. (2013). Bitter melon extracts enhance the activity of chemotherapeutic agents through the modulation of multiple drug resistance. J Pharm Sci 102: 4444-4454.

Kehrer DFS, Sparreboom A, Verweij J, De Bruijn P, Nierop CA, van de Schraaf J (2001) Modulation of Irinotecan-induced Diahrrea by cotreatment with Neomycin in Cancer Patients. Clinical Cancer Research 1136–41.

Lambert CB, Spire C, Claude N, and Guillouzo A (2009) Dose- and time-dependent effects of phenobarbital on gene expression profiling in human hepatoma HepaRG cells. *Toxicol Appl Pharmacol* **234**:345–360.

Leeder JS, and Okey AB (1996) Cytochromes P-450 and liver injury. *In Drug Induced Hepatotoxicity pp. 119–53.*

Laille E, Patel M, Jones SF, Burris HA, Infante J, Lemech C, Liu L, and Arkenau HT (2015) Evaluation of CYP3A-mediated drug-drug interactions with romidepsin in patients with advanced cancer. *J Clin Pharmacol* **55**:1378–1385.

Lan F, Bayliss PE, Rinn JL, Whetstine JR, Wang JK, Chen S, Iwase S, Alpatov R, Issaeva I, Canaani E, Roberts TM, Chang HY, and Shi Y (2007) A histone H3 lysine 27 demethylase regulates animal posterior development. *Nature* **449**:689–694.

Lichti-Kaiser K, Xu C, and Staudinger JL (2009) Cyclic AMP-dependent protein kinase signaling modulates pregnane x receptor activity in a species-specific manner. *J Biol Chem* **284**:6639–49.

Leslie M. Tompkins and Hongbing Wang (2011). LIVER DRUG METABOLISM in Oral Bioavailability: Basic Principles, Advanced Concepts, and Applications.

Liu F-J, Song X, Yang D, Deng R, and Yan B (2008) The far and distal enhancers in the *CYP3A4* gene co-ordinate the proximal promoter in responding similarly to the pregnane X receptor but differentially to hepatocyte nuclear factor-4α. *Biochem J* **409**:243–250.

Lu C, Han HD, Mangala LS, Ali-Fehmi R, Newton CS, Ozbun L, Armaiz-Pena GN, Hu W, Stone RL, Munkarah A, Ravoori MK, Shahzad MMK, Lee JW, Mora E, Langley RR, Carroll AR, Matsuo K, Spannuth WA, Schmandt R, Jennings NB, Goodman BW, Jaffe RB, Nick AM, Kim HS, Guven EO, Chen YH, Li LY, Hsu MC, Coleman RL, Calin GA, Denkbas EB, Lim JY, Lee JS, Kundra V, Birrer MJ, Hung MC, Lopez-Berestein G, and Sood AK (2010) Regulation of tumor angiogenesis by EZH2. *Cancer Cell* **18**:185–197.

Luo G, Guenthner T, Gan L-S, and Humphreys WG (2004) CYP3A4 induction by xenobiotics: biochemistry, experimental methods and impact on drug discovery and development. *Curr Drug Metab* **5**:483–505.

Lynch T, and Price A (2007) The effect of cytochrome P450 metabolism on drug response, interactions, and adverse effects. *Am Fam Physician* **76**:391–396.

Lehmann JM, McKee DD, Watson MA, Willson TM, Moore JT, and Kliewer SA (1998) The human orphan nuclear receptor PXR is activated by compounds that regulate CYP3A4 gene expression and cause drug interactions. *J Clin Invest* **102**:1016–1023.

Lichti-Kaiser K, Brobst D, Xu C, and Staudinger JL (2009) A systematic analysis of predicted phosphorylation sites within the human pregnane X receptor protein. *J Pharmacol Exp Ther* **331**:65–76.

Lin W, Wu J, Dong H, Bouck D, Zeng FY, and Chen T (2008) Cyclin-dependent kinase 2 negatively regulates human pregnane X receptor-mediated CYP3A4 gene expression in HepG2 liver carcinoma cells. *J Biol Chem* **283**:30650–30657.

Lillibridge JH, Liang BH, Kerr BM, Webber S, Quart B, Shetty BV, *et al.* (1998). Characterization of the selectivity and mechanism of human cytochrome P450 inhibition by the human immunodeficiency virus-protease inhibitor nelfinavir mesylate. Drug Metab Dispos 26**:** 609-616.

Lockhart DJ, Dong H, Byrne MC, Follettie MT, Gallo MV, Chee MS, *et al.* (1996). Expression monitoring by hybridization to high-density oligonucleotide arrays. Nat Biotechnol 14**:** 1675-1680.

Maglich JM (2002) Nuclear Pregnane X Receptor and Constitutive Androstane Receptor Regulate Overlapping but Distinct Sets of Genes Involved in Xenobiotic Detoxification. *Mol Pharmacol* **62**:638–646.

Mannel M (2004) Drug interactions with St John's Wort: Mechanisms and clinical implications. *Drug Saf* **27 (11)**:773–797.

Marsh S, and Hoskins JM (2010) Irinotecan pharmacogenomics. *Pharmacogenomics* **11**:1003–10.

Mullins ME, Horowitz BZ, Linden DH, Smith GW, Norton RL, Stump J. (1998) Life-threatening interaction of mibe-fradil and beta-blockers with dihydropyridine calcium channel blockers. JAMA;280:157–8.

Markowitz JS, Wells BG, Carson WH. (1995) Interactions between antipsychotic and antihypertensive drugs. Ann Pharmacother Jun; 29(6):603-9.

Muirhead GJ, Wulff MB, Fielding A, Kleinermans D, Buss N. (2000) Pharmacokinetic interactions between sildenafil and saquinavir/ritonavir. Br J Clin Pharmacol. Aug; 50(2):99-107.

Martínez-Jiménez CP, Gómez-Lechón MJ, Castell J V, and Jover R (2005) Transcriptional regulation of the human hepatic CYP3A4: identification of a new distal enhancer region responsive to CCAAT/enhancer-binding protein beta isoforms (liver activating protein and liver inhibitory protein). *Mol Pharmacol* **67**:2088–2101.

Matsumura K, Saito T, Takahashi Y, Ozeki T, Kiyotani K, Fujieda M, Yamazaki H, Kunitoh H, and Kamataki T (2004) Identification of a novel polymorphic enhancer of

the human CYP3A4 gene. *Mol Pharmacol* **65**:326–34.

Monshouwer M, Witkamp RF, Nijmeijer SM, Van Leengoed LA, Vernooy HC, Verheijden JH, and Van Miert AS (1996) A lipopolysaccharide-induced acute phase response in the pig is associated with a decrease in hepatic cytochrome P450-mediated drug metabolism. *J Vet Pharmacol Ther* **19**:382–388.

Morgan ET (1989) Suppression of constitutive cytochrome P-450 gene expression in livers of rats undergoing an acute phase response to endotoxin. *Mol Pharmacol* **36**:699–707.

Moore LB, Goodwin B, Jones S a, Wisely GB, Serabjit-Singh CJ, Willson TM, Collins JL, and Kliewer S a (2000) St. John's wort induces hepatic drug metabolism through activation of the pregnane X receptor. *Proc Natl Acad Sci U S A* **97**:7500–7502.

Mao Z, Li Y, Peng Y, Luan X, Gui H, Feng X, et al. (2011). Lipopolysaccharide down-regulates carbolesterases 1 and 2 and reduces hydrolysis activity in vitro and in vivo via p38MAPK-NF-kappaB pathway. Toxicol Lett 201: 213-220.

Mayer, R. J. (2000). "Moving beyond fluorouracil for colorectal cancer." N Engl J Med **343**(13): 963-964.

Murray M (1992). P450 enzymes. Inhibition mechanisms, genetic regulation and effects of liver disease. Clin Pharmacokinet 23**:** 132-146.

Murray M (1997). Drug-mediated inactivation of cytochrome P450. Clin Exp Pharmacol Physiol 24**:** 465-470.

NEBERT DW, NELSON DR, ADESNIK M, COON MJ, ESTABROOK RW, GONZALEZ FJ, GUENGERICH FP, GUNSALUS IC, JOHNSON EF, KEMPER B, LEVIN W, PHILLIPS IR, SATO R, and WATERMAN MR (1989) The P450 Superfamily: Updated Listing of All Genes and Recommended Nomenclature for the Chromosomal Loci. *DNA* **8**:1–13.

Nebert DW, and Russell DW (2002) Clinical importance of the cytochromes P450. *Lancet* **360**:1155–1162.

Nelson DR, Kamataki T, Waxman DJ, Guengerich FP, Estabrook RW, Feyereisen R, Gonzalez FJ, Coon MJ, Gunsalus IC, Gotoh O, Okuda K, and Nebert DW (1993) The P450 Superfamily : Update on new sequences, gene-mapping, accession numbers, early trivial names of enzymes, and nomenclature. *DNA Cell Biol* **12**:1–51.

Nelson SD, and Gordon WP (1983) Mammalian Drug Metabolism1. *J Nat Prod* **46**:71–78.

Nordlinger B, Van Cutsem E, Rougier P, Köhne CH, Ychou M, Sobrero A, Adam R, Arvidsson D, Carrato A, Georgoulias V, Giuliante F, Glimelius B, Golling M, Gruenberger T, Tabernero J, Wasan H, and Poston G (2007) Does chemotherapy prior

to liver resection increase the potential for cure in patients with metastatic colorectal cancer? A report from the European Colorectal Metastases Treatment Group. *Eur J Cancer* **43**:2037–2045.

Nordlinger, B., H. Sorbye, B. Glimelius, G. J. Poston, P. M. Schlag, P. Rougier, W. O. Bechstein, J. N. Primrose, E. T. Walpole, M. Finch-Jones, D. Jaeck, D. Mirza, R. W. Parks, L. Collette, M. Praet, U. Bethe, E. Van Cutsem, W. Scheithauer, T. Gruenberger, E. G.-I. T. C. Group, U. K. Cancer Research, O. Arbeitsgruppe Lebermetastasen undtumoren in der Chirurgischen Arbeitsgemeinschaft, G. Australasian Gastro-Intestinal Trials and D. Federation Francophone de Cancerologie (2008). "Perioperative chemotherapy with FOLFOX4 and surgery versus surgery alone for resectable liver metastases from colorectal cancer (EORTC Intergroup trial 40983): a randomised controlled trial." Lancet **371**(9617): 1007-1016.

Niederhuber JE, Ensminger WD (1993) Treatment of metastatic cancer to the liver. In: DeVita VT, Hellman S, Rosenberg SA (eds) Cancer – principles and practice of oncology. Lippincott, Philadelphia, pp 2201–2225

Oh A (1972) Progress report Hepatic metabolism of drugs. 579–585.

Palleria C, Di Paolo A, Giofrè C, Caglioti C, Leuzzi G, Siniscalchi A, De Sarro G, and Gallelli L (2013) Pharmacokinetic drug-drug interaction and their implication in clinical management.

Paine MF, Khalighi M, Fisher JM, Shen DD, Kunze KL, Marsh CL, *et al.* (1997). Characterization of interintestinal and intraintestinal variations in human CYP3A-dependent metabolism. J Pharmacol Exp Ther 283**:** 1552-1562.

Paine MF, Hart HL, Ludington SS, Haining RL, Rettie AE, & Zeldin DC (2006). The human intestinal cytochrome P450 "pie". Drug Metab Dispos 34: 880-886.

Pan YZ, Gao W, and Yu AM (2009) MicroRNAs regulate CYP3A4 expression via direct and indirect targeting. *Drug Metab Dispos* **37**:2112–2117.

Park SH, Liu X, Hennighausen L, Davey HW, and Waxman DJ (1999) Distinctive roles of STAT5a and STAT5b in sexual dimorphism of hepatic P450 gene expression: Impact of Stat5a gene disruption. *J Biol Chem* **274**:7421–7430.

Parent R, Marion MJ, Furio L, Trépo C, and Petit MA (2004) Origin and Characterization of a Human Bipotent Liver Progenitor Cell Line. *Gastroenterology* **126**:1147–1156.

Parkinson A, Klaasen CD, and Watkins JB (2001) *Biotransformation of xenobiotics.*

Pascussi JM, Gerbal-Chaloin S, Drocourt L, Maurel P, and Vilarem MJ (2003) The expression of CYP2B6, CYP2C9 and CYP3A4 genes: A tangle of networks of nuclear

and steroid receptors, in *Biochimica et Biophysica Acta - General Subjects* pp 243–253.

Potthoff MJ, and Olson EN (2007) MEF2: a central regulator of diverse developmental programs. *Development* **134**:4131–4140.

Pondugula SR, Brimer-Cline C, Wu J, Schuetz EG, Tyagi RK, and Chen T (2009) A phosphomimetic mutation at threonine-57 abolishes transactivation activity and alters nuclear localization pattern of human pregnane X receptor. *Drug Metab Dispos* **37**:719–730.

Pondugula SR, Dong H, and Chen T (2009) Phosphorylation and protein–protein interactions in PXR-mediated CYP3A repression. *Expert Opin Drug Metab Toxicol* **5**:861–873.

Randolph Hecht J (1998) Gastrointestinal Toxicity of Irinotecan. *Oncology* **12**:72–78.

Reik W (2007) Stability and flexibility of epigenetic gene regulation in mammalian development. *Nature* **447**:425–432.

Renton KW (2004) Cytochrome p450 regulation and drug biotransformation during inflammation and infection. *CurrDrug Metab* **5**:235–243.

Renton KW (2000) Hepatic drug metabolism and immunostimulation. *Toxicology* **142**:173–178.

Rim SH, Seeff L, Ahmed F, King JB, and Coughlin SS (2009) Colorectal cancer incidence in the United states, 1999-2004. *Cancer* **115**:1967–1976.

Rivera CA, Adegboyega P, van Rooijen N, Tagalicud A, Allman M, and Wallace M (2007) Toll-like receptor-4 signaling and Kupffer cells play pivotal roles in the pathogenesis of non-alcoholic steatohepatitis. *J Hepatol* **47**:571–579.

Rodriguez-Antona C (2003) Transcriptional Regulation of Human CYP3A4 Basal Expression by CCAAT Enhancer-Binding Protein alpha and Hepatocyte Nuclear Factor-3gamma. *Mol Pharmacol* **63**:1180–1189.

Rudolf E, Kralova V, Rudolf K, and John S (2013) The role of p38 in irinotecan-induced DNA damage and apoptosis of colon cancer cells. *Mutat Res* **741**–**742**:27–34.

Raynal C, Pascussi JM, Leguelinel G, Breuker C, Kantar J, Lallemant B, et al. (2010). Pregnane X Receptor (PXR) expression in colorectal cancer cells restricts irinotecan chemosensitivity through enhanced SN-38 glucuronidation. Mol Cancer 9: 46.

Saltz, L. B., J. V. Cox, C. Blanke, L. S. Rosen, L. Fehrenbacher, M. J. Moore, J. A. Maroun, S. P. Ackland, P. K. Locker, N. Pirotta, G. L. Elfring and L. L. Miller (2000).

"Irinotecan plus fluorouracil and leucovorin for metastatic colorectal cancer. Irinotecan Study Group." N Engl J Med **343**(13): 905-914.

Santos, A., S. Zanetta, T. Cresteil, A. Deroussent, F. Pein, E. Raymond, L. Vernillet, M. L. Risse, V. Boige, A. Gouyette and G. Vassal (2000). "Metabolism of irinotecan (CPT-11) by CYP3A4 and CYP3A5 in humans." Clin Cancer Res **6**(5): 2012-2020.

Saito M, Hirata-Koizumi M, Matsumoto M, Urano T, & Hasegawa R (2005). Undesirable effects of citrus juice on the pharmacokinetics of drugs: focus on recent studies. Drug Saf 28: 677-694.

Synold TW, Dussault I, & Forman BM (2001). The orphan nuclear receptor SXR coordinately regulates drug metabolism and efflux. Nat Med 7: 584-590.

Sabo JP, Kort J, Ballow C, Haschke M, Battegay M, Fuhr R, Girlich B, Schobelock M, Feifel U, Lang B, Li Y, and Elgadi M (2014) Clinical assessment of potential drug interactions of faldaprevir, a hepatitis C virus protease inhibitor, with darunavir/ritonavir, efavirenz and tenofovir. *Clin Infect Dis*, doi: 10.1093/cid/ciu616.

Sargent DJ, Niedzwiecki D, O'Connell MJ, Schilsky RL. (2001) Reccomendation for caution with irinotecan, fluorouracil, and leucovorin for colorectal cancer. N Engl J Med;345:144–5.

Saliba F, Hagipantelli R, Misset JL, Bastian G, Vassal G, Bonnay M, Herait P, Cote C, Mahjoubi M, Mignard D, and Cvitkovic E (1998) Pathophysiology and therapy of irinotecan-induced delayed-onset diarrhea in patients with advanced colorectal cancer: a prospective assessment. *J Clin Oncol* **16**:2745–51.

Schena M, Shalon D, Davis RW, and Brown PO (1995) Quantitative Monitoring of Gene Expression Patterns with a Complementary DNA Microarray. *Science (80-)* **270**:467–470.

Subramanian A, Tamayo P, Mootha VK, Mukherjee S, Ebert BL, Gillette MA, Paulovich A, Pomeroy SL, Golub TR, Lander ES, and Mesirov JP (2005) Gene set enrichment analysis: a knowledge-based approach for interpreting genome-wide expression profiles. *Proc Natl Acad Sci U S A* **102**:15545–50.

Suzuki MM, and Bird A (2008) DNA methylation landscapes: provocative insights from epigenomics. *Nat Rev Genet* **9**:465–476.

Swigut T, and Wysocka J (2007) H3K27 Demethylases, at Long Last.

Shah P, Guo T, Moore DD, and Ghose R (2014) Role of constitutive androstane receptor in toll-like receptor-mediated regulation of gene expression of hepatic drug-metabolizing enzymes and transporters. *Drug Metab Dispos* **42**:172–181.

Squires EJ, Sueyoshi T, Negishi M (2004) Cytoplasmic localization of pregnane X receptor and ligand-dependent nuclear translocation in mouse liver. *J. Biol. Chem.* 279, 49307–49314

Staudinger JL, and Lichti K (2007) Cell Signaling and Nuclear Receptors : New Opportunities for Molecular Pharmaceuticals in Liver Disease. *Mol Pharm* **5**:17–34.

Staudinger JL, Xu C, Biswas A, and Mani S (2011) Post-translational modification of pregnane x receptor. *Pharmacol Res* **64**:4–10.

Sutton D, Butler AM, Nadin L, & Murray M (1997). Role of CYP3A4 in human hepatic diltiazem N-demethylation: inhibition of CYP3A4 activity by oxidized diltiazem metabolites. J Pharmacol Exp Ther 282**:** 294-300.

Sansone-Parsons A, Krishna G, Martinho M, Kantesaria B, Gelone S, Mant TG. Pharmacotherapy. 2007 Effect of oral posaconazole on the pharmacokinetics of cyclosporine and tacrolimus. Jun; 27(6):825-34.

Tateishi, T, Watanabe, M, Moriya H, Yamaguchi S, Sato T and Kobayashi S (1999). No ethnic difference between Caucasian and Japanese hepatic samples in the expression frequency of CYP3A5 and CYP3A7 proteins. Biochem. Pharmacol., 57(8), 935-939.

Thummel KE, and Wilkinson GR (1998) In vitro and in vivo drug interactions involving human CYP3A. *Annu Rev Pharmacol Toxicol* **38**:389–430.

Takasuna K, Hagiwara T, Watanabe K, Onose S, Yoshida S, Kumazawa E, Nagai E, and Kamataki T (2006) Optimal antidiarrhea treatment for antitumor agent irinotecan hydrochloride (CPT-11)-induced delayed diarrhea. *Cancer Chemother Pharmacol* **58**:494–503.

Tan Z, Huang M, Puga A, and Xia Y (2004) A critical role for MAP kinases in the control of Ah receptor complex activity. *Toxicol Sci* **82**:80–87.

Vanhoefer U, Harstrick A, Achterrath W, Cao S, Seeber S, and Rustum YM (2001) Irinotecan in the treatment of colorectal cancer: clinical overview. *J Clin Oncol* **19**:1501–18.

Veith H, Southall N, Huang R, James T, Fayne D, Artemenko N, Shen M, Inglese J, Austin CP, Lloyd DG, and Auld DS (2009) Comprehensive characterization of cytochrome P450 isozyme selectivity across chemical libraries. *Nat Biotechnol* **27**:1050–1055.

Wakelee HA, Takimoto CH, Lopez-Anaya A, Chu Q, Middleton G, Dunlop D, Ramlau R, Leighl N, Rowinsky EK, Hao D, Zatloukal P, Jacobs CD, and Rodon J (2012) The effect of bexarotene on atorvastatin pharmacokinetics: Results from a phase i trial of bexarotene plus chemotherapy in patients with advanced non-small cell lung cancer.

Cancer Chemother Pharmacol **69**:563–571.

Wang Y-M, Ong SS, Chai SC, and Chen T (2012) Role of CAR and PXR in xenobiotic sensing and metabolism. *Expert Opin Drug Metab Toxicol* **8**:803–817.

Watanabe M, Homma M, Momo K, Okoshi Y, Wada T, Hara A, *et al.* (2011). Effects of voriconazole co-administration on oxycodone-induced adverse events: a case in the retrospective survey. Eur J Clin Pharmacol 67**:** 859-861.

Waxman DJ, Lapenson DP, Aoyama T, Gelboin H V., Gonzalez FJ, and Korzekwa K (1991) Steroid hormone hydroxylase specificities of eleven cDNA-expressed human cytochrome P450s. *Arch Biochem Biophys* **290**:160–166.

Westerink WMA, and Schoonen WGEJ (2007) Phase II enzyme levels in HepG2 cells and cryopreserved primary human hepatocytes and their induction in HepG2 cells. *Toxicol Vitr* **21**:1592–1602.

Weekes J, Lam AKY, Sebesan S, and Ho YH (2009) Irinotecan therapy and molecular targets in colorectal cancer: A systemic review.

Weir HK (2003) Annual Report to the Nation on the Status of Cancer, 1975-2000, Featuring the Uses of Surveillance Data for Cancer Prevention and Control. *CancerSpectrum Knowl Environ* **95**:1276–1299.

Wheeler JB, Stourman N V., Thier R, Dommermuth A, Vuilleumier S, Rose JA, Armstrong RN, and Guengerich FP (2001) Conjugation of haloalkanes by bacterial and mammalian glutathione transferases: Mono- and dihalomethanes. *Chem Res Toxicol* **14**:1118–1127.

Wigg AJ, Roberts-Thomson IC, Dymock RB, McCarthy PJ, Grose RH, and Cummins AG (2001) The role of small intestinal bacterial overgrowth, intestinal permeability, endotoxaemia, and tumour necrosis factor alpha in the pathogenesis of non-alcoholic steatohepatitis. *Gut* **48**:206–11.

Wilkinson GR (2005) Drug metabolism and variability among patients in drug response. *N Engl J Med* **352**:2211–2221.

Wrighton SA, Brian WR, Sari MA, Iwasaki M, Guengerich FP, Raucy JL, *et al.* (1990). Studies on the expression and metabolic capabilities of human liver cytochrome P450IIIA5 (HLp3). Mol Pharmacol 38**:** 207-213.

Xie W, Uppal H, Saini SPS, Mu Y, Little JM, Radominska-Pandya A, and Zemaitis MA (2004) Orphan nuclear receptor-mediated xenobiotic regulation in drug metabolism.

Xie, W., M. F. Yeuh (2003) Control of steroid, heme, and carcinogen metabolism by nuclear pregnane X receptor and constitutive androstane receptor. Proc Natl Acad Sci U S A 100(7): 4150-4155.

Xu JJ, Diaz D, and O'Brien PJ (2004) Applications of cytotoxicity assays and pre-lethal mechanistic assays for assessment of human hepatotoxicity potential.

Yasunami Y, Hara H, Iwamura T, Kataoka T, and Adachi T (2004) C-jun N-terminal kinase modulates 1,25-dihydroxyvitamin D3-induced cytochrome P450 3A4 gene expression. *Drug Metab Dispos* **32**:685–8.

Yonemori K, Takeda Y, Toyota E, Kobayashi N, and Kudo K (2004) Potential interactions between irinotecan and rifampin in a patient with small-cell lung cancer. *Int J Clin Oncol* **9**.

Yu AM, Tian Y, Tu MJ, Ho PY, and Jilek JL (2016) MicroRNA Pharmacoepigenetics: Posttranscriptional Regulation Mechanisms behind Variable Drug Disposition and Strategy to Develop More Effective Therapy.

Yu R, Lei W, Mandlekar S, Weber MJ, Der CJ, Wu J, and Kong ANT (1999) Role of a mitogen-activated protein kinase pathway in the induction of phase II detoxifying enzymes by chemicals. *J Biol Chem* **274**:27545–27552.

Yueh, M. F., Y. H. Huang (2003) Involvement of the xenobiotic response element (XRE) in Ah receptor-mediated induction of human UDP-glucuronosyltransferase 1A1. J Biol Chem 278(17): 15001-15006

Zanger UM, and Schwab M (2013) Cytochrome P450 enzymes in drug metabolism: Regulation of gene expression, enzyme activities, and impact of genetic variation. *Pharmacol Ther* **138**:103–141, Elsevier Inc.

Zhang L, Zhang Y (Derek), Zhao P, and Huang S-M (2009) Predicting Drug–Drug Interactions: An FDA Perspective. *AAPS J* **11**:300–306.

Zhou H, Lu N, Chen ZQ, Song QL, Yu HM, and Li XJ (2009) Osteopontin mediates dense culture-induced proliferation and adhesion of prostate tumour cells: Role of protein kinase C, p38 mitogen-activated protein kinase and calcium. *Basic Clin Pharmacol Toxicol* **104**:164–170.